

1. Report No. FHWA/TX-10/0-5627-2		2. Government Accession No.		3. Recipient's Catalog No.	
4. Title and Subtitle FIELD EVALUATION OF ASPHALT MIXTURE SKID RESISTANCE AND ITS RELATIONSHIP TO AGGREGATE CHARACTERISTICS				5. Report Date August 2009 Published: December 2010	
				6. Performing Organization Code	
7. Author(s) Eyad Masad, Arash Rezaei, Arif Chowdhury, and Tom Freeman				8. Performing Organization Report No. Report 0-5627-2	
9. Performing Organization Name and Address Texas Transportation Institute The Texas A&M University System College Station, Texas 77843-3135				10. Work Unit No. (TRAIS)	
				11. Contract or Grant No. Project 0-5627	
12. Sponsoring Agency Name and Address Texas Department of Transportation Research and Technology Implementation Office P.O. Box 5080 Austin, Texas 78763-5080				13. Type of Report and Period Covered Technical Report: September 2006–August 2008	
				14. Sponsoring Agency Code	
15. Supplementary Notes Project performed in cooperation with the Texas Department of Transportation and the Federal Highway Administration. Project Title: Aggregate Resistance to Polishing and Its Relationship to Skid Resistance URL: <a href="http://tti.tamu.edu/documents/0-5627-2.pdf">http://tti.tamu.edu/documents/0-5627-2.pdf</a>					
16. Abstract This report documents the findings from the research that was carried out as part of Phase II of Texas Department of Transportation (TxDOT) Project 0-5627. The research included measuring and analyzing the mechanical and physical properties of aggregates used in surface mixes in the state of Texas. These properties were aggregate shape characteristics measured by the Aggregate Imaging System (AIMS), British pendulum value, coarse-aggregate acid insolubility, Los Angeles weight loss, Micro-Deval weight loss, and magnesium-sulfate weight loss. In addition, a database of field skid-number measurements that were obtained over a number of years using the skid trailer was established. Field measurements of selected sections were conducted using the dynamic friction tester (DFT) and circular texture meter (CTMeter). These data and measurements were used to carry out comprehensive statistical analyses of the influence of aggregate properties and mixture design on the skid-resistance value and its variability. Consequently, a system was developed for predicting asphalt-pavement skid resistance based on aggregate characteristics and aggregate gradation.					
17. Key Words Skid Resistance, Asphalt Mixture, Aggregate Characteristics			18. Distribution Statement No restrictions. This document is available to the public through NTIS: National Technical Information Service Springfield, Virginia 22161 <a href="http://www.ntis.gov">http://www.ntis.gov</a>		
19. Security Classif.(of this report) Unclassified		20. Security Classif.(of this page) Unclassified		21. No. of Pages 128	22. Price



**FIELD EVALUATION OF ASPHALT MIXTURE  
SKID RESISTANCE AND ITS RELATIONSHIP TO  
AGGREGATE CHARACTERISTICS**

by

Eyad Masad, Ph.D., P.E.  
Halliburton Associate Professor  
Zachry Department of Civil Engineering  
Texas A&M University

Arash Rezaei  
Graduate Research Assistant  
Zachry Department of Civil Engineering  
Texas A&M University

Arif Chowdhury, P.E.  
Assistant Research Engineer  
Texas Transportation Institute

and

Tom Freeman, P.E.  
Associate Research Scientist  
Texas Transportation Institute

Report 0-5627-2

Project 0-5627

Project Title: Aggregate Resistance to Polishing and Its Relationship to Skid Resistance

Performed in cooperation with the  
Texas Department of Transportation  
and the  
Federal Highway Administration

August 2009

Published: December 2010

TEXAS TRANSPORTATION INSTITUTE  
The Texas A&M University System  
College Station, Texas 77843-3135



## **DISCLAIMER**

The contents of this report reflect the views of the authors, who are responsible for the facts and accuracy of the data presented herein. The contents do not necessarily reflect the official view or policies of the Texas Department of Transportation (TxDOT) or Federal Highway Administration (FHWA). This report does not constitute a standard, specification, or regulation. The engineer in charge was Eyad Masad, P.E. #96368.

## **ACKNOWLEDGMENTS**

This project was made possible by the Texas Department of Transportation. Many people made possible the coordination and accomplishment of the work presented herein. German Claros, P.E., is the research engineer, and Caroline Herrera, P.E., is the project director for this project; their guidance and direction are greatly appreciated. Engineers, laboratory supervisors, and inspectors at the Texas Department of Transportation and several districts assisted in providing information, taking samples, and completing tests. Special thanks go to Edward Morgan for his time, effort, assistance, and guidance in this project.

# TABLE OF CONTENTS

	Page
List of Figures .....	ix
List of Tables .....	xi
Chapter I – Introduction.....	1
Problem Statement .....	2
Objectives .....	2
Scope of the Study .....	3
Organization of the Report.....	3
Chapter II – Summary of Phase I.....	5
Introduction.....	5
Relationship between Aggregate Characteristics and Skid Resistance .....	5
Chapter III – Relationship of Field Skid Measurements to Aggregate Characteristics.....	9
Introduction.....	9
Selection of the Field Sections and Data Mining.....	10
Analysis of the Collected Field Data .....	14
Traffic Load .....	18
Mix Design.....	20
Aggregate Type.....	24
Summary of the Results of the Field-Data Analysis.....	38
Chapter IV – Analysis of the Measured Field Data.....	41
Introduction.....	41
Selection of the Field Sections.....	41
Testing Program.....	42
Analysis of Field Measurements.....	44
Relationship of Field Measurements to Aggregate Properties .....	55
Relationship between Field Measurements and Laboratory Measurements.....	58
Summary of the Results of the Field Measurement.....	60
Chapter V – A System for Predicting Skid Number of Asphalt Pavements.....	63
Introduction.....	63
Development of System for Predicting Skid Number .....	63
Sensitivity Analysis of Prediction System.....	68
Recommended System for Predicting Skid Number .....	73
Chapter VI – Conclusions and Recommendations .....	75
Summary of the Results of the Field-Data Analysis.....	75
Recommendations.....	77

References.....	79
Appendix.....	83



## LIST OF FIGURES

	Page
Figure 1. International Friction Index (IFI) Model Input Parameters.....	6
Figure 2. Mixture Types Used in the Selected Road Segments.....	12
Figure 3. Data Availability for the Different TxDOT Districts.....	13
Figure 4. Coefficient of Variation of Measured Skid Resistance for Different Sections.....	14
Figure 5. Measured SN Values versus Traffic Level.....	18
Figure 6. Median SN Values versus Traffic Level.....	19
Figure 7. Standard Deviation of Measured SN Values versus Traffic Level.....	20
Figure 8. Measured SN Values for Different Mix Types.....	21
Figure 9. Median of Measured SN Values for Different Mix Types.....	22
Figure 10. Standard Deviation of Measured SN Values for Different Mixes.....	22
Figure 11. Standard Deviation of the Measured SN Values for Low TMF Level.....	23
Figure 12. Standard Deviation of the Measured SN Values for Medium and High TMF Level.....	24
Figure 13. Values of Measured SN for Different Aggregate Types.....	25
Figure 14. Median of Measured SN Values for Different Aggregate and Mix Types.....	27
Figure 15. Median of Measured SN Values for Type C Mix Design.....	31
Figure 16. Median of Measured SN Values for PFC Mix Design.....	34
Figure 17. Median of Measured SN Values for Surface Treatment Grade 3. (a) Aggregate H (SAC A). (b) Aggregate K (SAC B). (c) Aggregate L (SAC A). (d) Aggregate M (SAC B). (e) Aggregate N (SAC B).....	36
Figure 18. Median of Measured SN Values for Surface Treatment Grade 4. (a) Aggregate Q (SAC B). (b) Aggregate J (SAC B). (c) Aggregate K (SAC B). (d) Aggregate M (SAC B). (e) Aggregate N (SAC B). (f) Aggregate O (SAC A).....	37
Figure 19. Layout of the Measurement Section.....	43
Figure 20. Measured MPD Values for Different Mix Types.....	45
Figure 21. Mean Dynamic Friction at 12.4 mph.....	47
Figure 22. Mean Profile Depth versus Measured Skid Number.....	49
Figure 23. Mean Profile Depth versus Measured Skid Number for Different Mix Types (Continued).....	51
Figure 24. Dynamic Friction at 12.4 mph versus Measured Skid Number.....	51
Figure 25. Dynamic Friction at 12.4 mph versus Measured Skid Number for Different Mix Types.....	52
Figure 26. Dynamic Friction at 50 mph versus Measured Skid Number for Different Mix Types.....	53
Figure 27. Measured Skid Number versus Calculated Skid Number Using PIARC Equation.....	59
Figure 28. Measured Skid Number versus Calculated Skid Number Using Modified PIARC Equation.....	60
Figure 29. TMF versus Number of Polishing Cycles.....	67

Figure 30. Relationship between Measured and Calculated MPD Values.....	68
Figure 31. Terminal Friction Values for Different Aggregates and Mix Designs.....	70
Figure 32. Polishing Rate for Different Aggregates.....	71
Figure 33. IFI Values as a Function of TMF for Sample 1.....	71
Figure 34. IFI Values as a Function of TMF for Sample 8.....	72
Figure 35. SN Values as a Function of TMF for Sample 1.....	72
Figure 36. SN Values as a Function of TMF for Sample 8.....	73

## LIST OF TABLES

	Page
Table 1. Number of Road Sections in Each District.....	11
Table 2. Aggregate Sources Used in Pavement Sections. ....	11
Table 3. Mixture Types Used in Road Segments. ....	12
Table 4. Traffic Clusters in Terms of Traffic Multiplication Factor. ....	15
Table 5. Summary of Skid Resistance Measurements.....	16
Table 6. Aggregate Ranking Based on Measured Skid Resistance for Surface Treatment Grade 3 in Low Traffic Level.....	28
Table 7. Aggregate Ranking Based on Measured Skid Resistance for Surface Treatment Grade 4 in Medium and Low Traffic Level. ....	28
Table 8. Aggregate Ranking Based on Measured Skid Resistance for Type C Mixture in High, Medium, and Low Traffic Level.....	29
Table 9. Aggregate Ranking Based on Measured Skid Resistance for PFC Mixture in High, Medium, and Low Traffic Level.....	29
Table 10. Measured Field Sections.....	42
Table 11. Lane Distribution Factor.....	44
Table 12. Percent Change in MPD Values in Terms of TMF. ....	46
Table 13. Percent Change in DFT <sub>20</sub> Values in Terms of 1000 TMF.....	47
Table 14. R-Square and Significance of Different Aggregate Properties for Different Mixes.....	57
Table 15. R-Square and Significance of Different Aggregate Properties for Different Traffic Level.....	57
Table 16. R-Square and Significance of Different Aggregate Properties to Explain SN Change. ....	57
Table 17. Calculated Scale and Shape Factors for Different Mixes.....	66
Table 18. Selected Aggregates Based on Terminal Texture.....	69
Table 19. Selected Aggregates Based on Polishing Rate. ....	69



## CHAPTER I – INTRODUCTION

In 2005, 6.1 million traffic crashes, 43,443 traffic fatalities, and approximately 2.7 million traffic-related injuries were reported in the United States by the National Highway Traffic Safety Administration (NHTSA) throughout the United States (Noyce et al., 2005).

Nationwide studies show that between 15 to 18 percent of crashes occur on wet pavements (Smith, 1976; Davis et al., 2002; Federal Highway Administration [FHWA], 1990). According to the National Transportation Safety Board and FHWA reports, approximately 13.5 percent of fatal accidents occur when pavements are wet (Chelliah et al., 2003; Kuemmel et al., 2000). Research studies have demonstrated that a relationship exists between wet-weather accidents and pavement friction (Rizenbergs et al., 1972; Giles et al., 1964; McCullough and Hankins, 1966; Wallman and Astron, 2001; Gandhi et al., 1991). The accident rate can be reduced greatly by implementing corrective measures in hazardous areas. Safety evaluation of roads and analysis of the different factors affecting pavement friction are necessary for future safety improvements. Research has shown that an increase in average pavement surface friction from 0.40 to 0.55 would result in a 63 percent decrease in wet-pavement crashes (Hall et al., 2006; Miller and Johnson, 1973). Research by Kamel and Gartshore also showed that by improving the skid resistance, the wet-weather crashes decreased by 71 percent on intersections and 54 percent on freeways (Kamel and Gartshore, 1982; Hall et al., 2006).

Pavement friction is primarily a function of the surface texture, which includes both microtexture and macrotexture. Pavement microtexture is defined as “a deviation of a pavement surface from a true planar surface with characteristic dimensions along the surface of less than 0.5 mm,” while the pavement macrotexture is defined as “a deviation of 0.5 mm - 50 mm from a true planar surface” (Henry, 1996; Wambold et al., 1995).

Microtexture, which is primarily a function of aggregate surface characteristics, is needed to provide a rough surface that disrupts the continuity of the water film and produces frictional resistance between the tire and pavement by creating intermolecular bonds. Macrotexture, which primarily depends on aggregate gradation and method of

construction, provides surface drainage paths for water to drain faster from the contact area between the tire and pavement. Macrotexture helps to prevent hydroplaning and improve wet frictional resistance particularly at high speed (Fulop et al., 2000; Hanson and Prowell, 2004; Kowalski, 2007).

While there have been many research studies about increasing the life span of pavement materials, there is no direct specification for the selection and use of aggregate and mixture design to ensure satisfactory frictional performance. In addition, current methods of evaluating aggregates for use in asphalt mixtures are mainly based on the historical background of the aggregate performance and chemical examination (West et al., 2001; Goodman et al., 2006).

The high correlation between pavement skid resistance and rate of crashes demands a comprehensive system for predicting asphalt-pavement skid resistance based on material characteristics and mixture design. This report documents the results of comprehensive measurements of aggregate properties and field skid resistance. It also outlines a system for predicting asphalt-pavement skid resistance based on aggregate characteristics and mixture design.

## **PROBLEM STATEMENT**

The selection of aggregates such that their frictional properties contribute to maintaining acceptable asphalt-pavement skid resistance has always been a question for mix designers. There is a need for developing a comprehensive system for selecting aggregates based on quantitative measurement of their properties that influence skid resistance in order to improve safety and reduce the cost of maintenance and rehabilitation.

## **OBJECTIVES**

The objectives of this project were to (1) study the influence of aggregate properties and mix types on asphalt-pavement skid resistance and (2) develop a system for predicting asphalt-pavement skid resistance. These objectives were achieved based on measuring and analyzing skid-trailer data over a number of years, measuring friction

and pavement texture of asphalt pavements using a dynamic friction tester (DFT) and circular texture meter (CTMeter), and measuring aggregate characteristics.

## **SCOPE OF THE STUDY**

The literature survey shows that aggregate characteristics affect frictional properties of flexible pavements to a high degree. The hypothesis behind this study is that it is possible to measure the frictional characteristics of different aggregate types and improve the frictional performance of the pavement surface by the selection of polish-resistant aggregates with certain shape characteristics.

The scope of this project included measuring and analyzing the various properties of aggregates used in the surface mixes in the state of Texas. These properties were aggregate shape characteristics measured using the Aggregate Imaging System (AIMS), British pendulum value, coarse-aggregate acid insolubility, Los Angeles weight loss, Micro-Deval weight loss, and magnesium-sulfate weight loss. In addition, this project included developing a database of the annual field skid-resistance data, conducting field measurements of the selected sites, and developing a relationship to predict skid resistance as a function of aggregate characteristics and mixture design.

## **ORGANIZATION OF THE REPORT**

[Chapter II](#) of this report includes a summary of the results of Phase I of Texas Department of Transportation (TxDOT) Project 0-5627. [Chapter III](#) includes a description of the Phase II part of the project and the results of the office data analysis. This is followed by the results of measuring asphalt-pavement frictional properties, documented in [Chapter IV](#). The system for predicting the asphalt-pavement skid number as a function of aggregate properties and mixture design is presented in [Chapter V](#). The last chapter ([Chapter VI](#)) includes conclusions and recommendations.





## **CHAPTER II – SUMMARY OF PHASE I**

### **INTRODUCTION**

TxDOT Project 5-1707 developed an effective method to measure aggregate shape, angularity, and texture, and the changes of these characteristics as a function of polishing time. Project 0-5627 was developed to produce a new aggregate classification system based on relating the results of the new test method developed in Project 5-1707 for measuring aggregate characteristics to real-life field pavement skid resistance. The following tasks were completed in the first phase of this study and are summarized in Report 0-5627-1:

- A comprehensive literature survey was completed to determine available tests for measuring aggregate characteristics related to asphalt-pavement skid resistance.
- Researchers conducted laboratory and field tests for directly or indirectly measuring asphalt-pavement skid resistance.
- Models for predicting skid resistance as a function of material properties, speed, and environmental conditions were developed.

### **RELATIONSHIP BETWEEN AGGREGATE CHARACTERISTICS AND SKID RESISTANCE**

During the laboratory part of the project, three different asphalt mixture types, namely porous friction course (PFC), Type C, and Type D, with different aggregate types were fabricated and tested using slabs produced from these mixes. Researchers intermittently performed friction and surface-texture measurements after sample compaction and during polishing by using different testing methods.

In summary, the results of the research indicated that it is possible to control and predict frictional properties of the pavement by selecting the aggregate type and asphalt mixture design. Researchers developed a new laboratory testing methodology to evaluate the rate of decrease in friction and the terminal value of friction. The terminal value refers to the condition in which skid resistance does not change with an increase in traffic. The

influence of the aggregate type on asphalt-pavement skid properties was investigated through preparing and testing laboratory slabs. The results of the analysis confirmed the strong relationship between mixture frictional properties and aggregate properties. The main aggregate properties affecting the mix skid resistance were found to be the British pendulum value, texture change before and after Micro-Deval measured by AIMS, terminal texture after Micro-Deval measured by AIMS, and coarse-aggregate acid insolubility value. Based on the findings, a model that is able to predict the initial F60, terminal F60, and rate of polishing was developed using the parameters in the aggregate-polishing relationship developed by Mahmoud (2005). Figure 1 and Equations 1 to 5 present the model developed in Phase I of this research project.

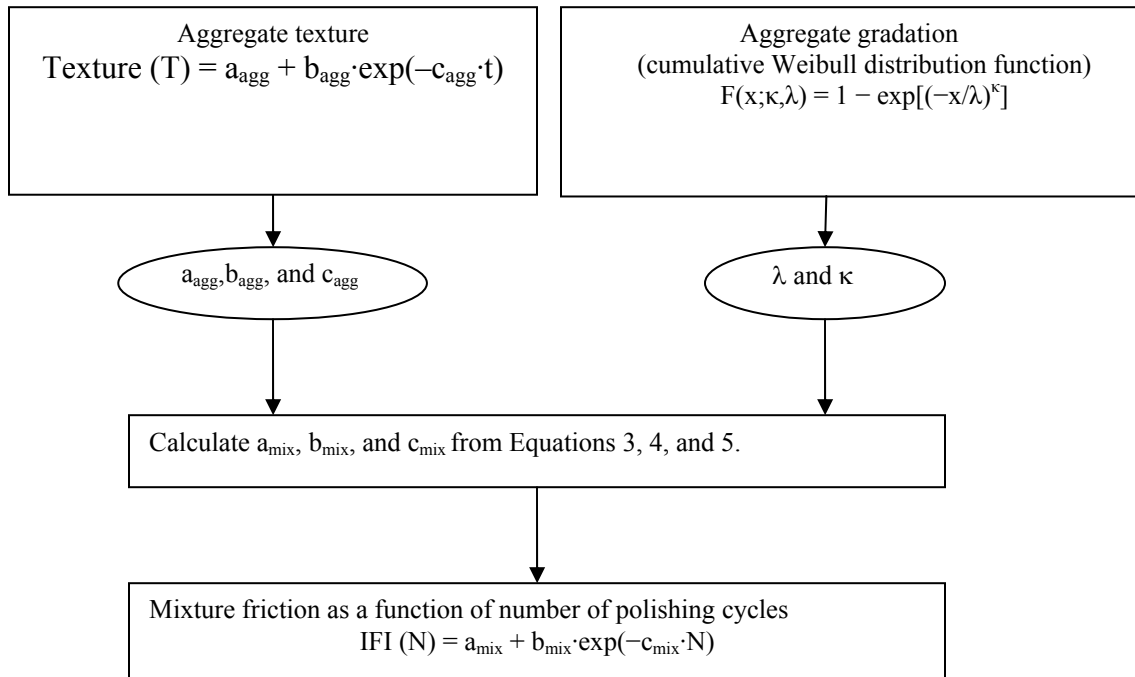


**Figure 1. International Friction Index (IFI) Model Input Parameters.**

$$IFI (N) = a_{mix} + b_{mix} \cdot \exp(-c_{mix} \cdot N) \quad (1)$$

$$F(x; \kappa, \lambda) = 1 - \exp\left[-\left(\frac{x}{\lambda}\right)^\kappa\right] \quad (2)$$

$$a_{mix} = \frac{18.422 + \lambda}{118.936 - 0.0013 \times (AMD)^2} \quad (3)$$

$$a_{mix} + b_{mix} = 0.4984 \ln(5.656 \times 10^{-4} (a_{agg} + b_{agg}) + 5.846 \times 10^{-2} \lambda - 4.985 \times 10^{-2} \kappa) + 0.8619 \quad (4)$$

$$c_{mix} = 0.765 \cdot e^{\left( \frac{-7.297 \cdot 10^{-2}}{c_{agg}} \right)} \quad (5)$$

where:

$a_{mix}$ : terminal IFI value for the mix,

$a_{mix} + b_{mix}$ : initial IFI value for the mix,

$c_{mix}$ : rate of change in IFI for the mix,

AMD: aggregate texture after Micro-Deval,

$a_{agg} + b_{agg}$ : aggregate initial texture using texture model,

$c_{agg}$ : aggregate texture rate of change using texture model,

k-value: shape factor of Weibull distribution used to describe aggregate gradation,

and

$\lambda$ -value: scale factor of Weibull distribution used to describe aggregate gradation.

This model can be used to predict mix friction based on gradation and aggregate resistance to polishing. This model also facilitates selecting the appropriate aggregate type for desired mixture friction, and it can be used as a starting point to classify aggregates based on their frictional properties.



## **CHAPTER III – RELATIONSHIP OF FIELD SKID MEASUREMENTS TO AGGREGATE CHARACTERISTICS**

### **INTRODUCTION**

The objective of Phase II is to correlate laboratory measurements of the asphalt-pavement skid resistance and aggregate resistance to polishing to field skid-resistance measurements. This objective was achieved by developing and executing an experiment of field-test sections incorporating different surface mixes.

Skid resistance is typically measured using the friction trailer, which is towed at a constant speed over the tested pavement. When the test is initiated, water is sprayed ahead of the tire so the wet pavement friction can be tested. The wheel is fully locked, and the resulting torque is recorded. Based on the measured torque (converted to a horizontal force) and dynamic vertical load on the test wheel, the wet coefficient of friction between the test tire and pavement surface is calculated. The skid number (SN) is then reported as the coefficient of friction multiplied by 100 (Hall et al., 2006). The same speed should be maintained before the test and when the wheel is locked. The friction trailer is typically equipped with two types of tires: a rib tire on the right side according to American Society for Testing and Materials (ASTM) E501 and a smooth tire on the left side according to ASTM E524 (ASTM, 2008). Following the recommendation of the ASTM E-274 specification, the test speed (48, 64, or 80 km/h) (30, 40 or 50 mph and type of tire (R for rib tire and S for smooth tire) should be cited when the skid number is reported (ASTM, 2008). For example, SN(64)S indicates that the test was performed at a speed of 64 km/h (40 mph) with the smooth type of tire (SN40S is used if speed is reported in miles per hour). The friction trailer used by TxDOT is equipped with smooth tires and travels at a speed of 80 km/h (50 mph).

Researchers conducted extensive work in this project to create a database of sections with different friction characteristics. The initial selection of sections was intended to include the mixes and aggregates that were already tested in the laboratory phase of this research study and to include sections for which the skid performance was available. TTI researchers and TxDOT revised the initial experimental design several times to agree on a sound and inclusive experimental design. Moreover, the availability

of the skid data, availability of the traffic data, variety of the aggregate lithologies, variety of mix types, and availability of construction and maintenance records were the main factors considered in the selection of sections. The experimental design was then finalized and implemented in Phase II of this project.

Researchers performed intensive office work to collect all the data required to fulfill the experimental design. A huge amount of data was studied to choose and extract the most reliable data. Several meetings with TxDOT research groups were held to decide on the desired sections. Since the skid data and construction record of each project are kept in two different databases, a comparative study was done to select the sections with a wide range of construction history and a long record of skid data. Any discrepancies between the data and field observations were thoroughly investigated. TTI researchers contacted each TxDOT district office to confirm the data integrity and accuracy. Many meetings and conference calls were held with data providers to obtain details about the data collection (e.g., the exact location of the tested field, date and time, etc.). Afterward, the data were analyzed using statistical analysis methods.

## **SELECTION OF THE FIELD SECTIONS AND DATA MINING**

After researchers reviewed all the data, 65 roads including 1527 Pavement Management Information System (PMIS) sections that cover a wide range of skid performance were identified. Each PMIS section is a particular stretch of roadway with predefined boundaries defined by reference markers. These sections are distributed across nine TxDOT districts.

[Table 1](#) shows the number of sections in each district. The majority of PMIS sections are located within the Corpus Christi, Brownwood, San Antonio, and Yoakum Districts. These 1527 PMIS sections contain 4068 data records including different aggregate types and different mix types in different years. As can be seen from [Table 2](#), 21 different aggregate sources in Texas were used in these sections. These aggregates were classified in different categories according to the TxDOT surface aggregate classification (SAC) system.

**Table 1. Number of Road Sections in Each District.**

<i>District</i>	<i>Number of Sections</i>
Beaumont	12
Brownwood	285
Bryan	6
Corpus Christi	862
El Paso	46
Houston	116
Lubbock	24
San Antonio	182
Yoakum	148
Total	1527

**Table 2. Aggregate Sources Used in Pavement Sections.**

<i>No.</i>	<i>Aggregate</i>	<i>Material Type</i>	<i>TxDOT Classification</i>
1	A	Crushed Siliceous Gravel	SAC A
2	B	Crushed Limestone-Dolomite	SAC B
3	C	Crushed Limestone-Dolomite	SAC B
4	D	Crushed Granite	SAC A
5	E	Crushed Limestone-Dolomite	SAC B
6	F	Crushed Limestone-Dolomite	SAC B
7	G	Crushed Limestone-Dolomite	SAC B
8	H	Sandstone	SAC A
9	I	Crushed Siliceous & Limestone Gravel	SAC A
10	J	Crushed Limestone Rock Asphalt	SAC B
11	K	Crushed Limestone-Dolomite	SAC B
12	L	Lightweight Aggregate	SAC A
13	M	Crushed Limestone-Dolomite	SAC B
14	N	Crushed Limestone-Dolomite	SAC B
15	O	Crushed Traprock	SAC A
16	P	Crushed Traprock	SAC A
17	Q	Crushed Limestone	SAC B
18	R	50 Percent Aggregate H + 50 Percent Aggregate K	SAC B
19	S	Crushed Rhyolite	SAC A
20	T	Crushed Granite	SAC A
21	U	Crushed Limestone	SAC B

Four different mixture designs were used in the selected PMIS sections. These four mixture designs are surface treatment with grade 4 (GR-4) aggregate, surface treatment with grade 3 (GR-3) aggregate, porous friction course, and Type C mixture design. [Table 3](#) shows the number of roads within each mixture group (PFC and Type C are combined in the last column). [Figure 2](#) shows the number of road segments with the specified mixture design. Although it is desirable to have a full

record of the skid data for several years, some data were missing for some sections. Figure 3 shows the data coverage for each district.

**Table 3. Mixture Types Used in Road Segments.**

District	Surface Treatment GR-4	Surface Treatment GR-3	Hot-Mix Asphalt Concrete (PFC and Type C Mixes)
Beaumont	1		
Brownwood	17	12	
Bryan			1
Corpus Christi	33		2
El Paso			7
Houston	3		5
Lubbock			4
San Antonio	7		14
Yoakum		1	1
<b>Total</b>	<b>61</b>	<b>13</b>	<b>34</b>

Note: Any combination of size 4 aggregates – according to TxDOT specification – including Type PE, Type PB, and Type B aggregate and AC-15P, AC-20-5TR, AC 20XP, CRS-2P, and HFRS-2P asphalt types was considered as surface treatment grade 4. Any combination of size 3 aggregate including Type PB and Type L aggregate with AC-20-5TR or SFHM ACP or AC-20-XP, and CRS-2P asphalt type was considered as surface treatment grade 3.

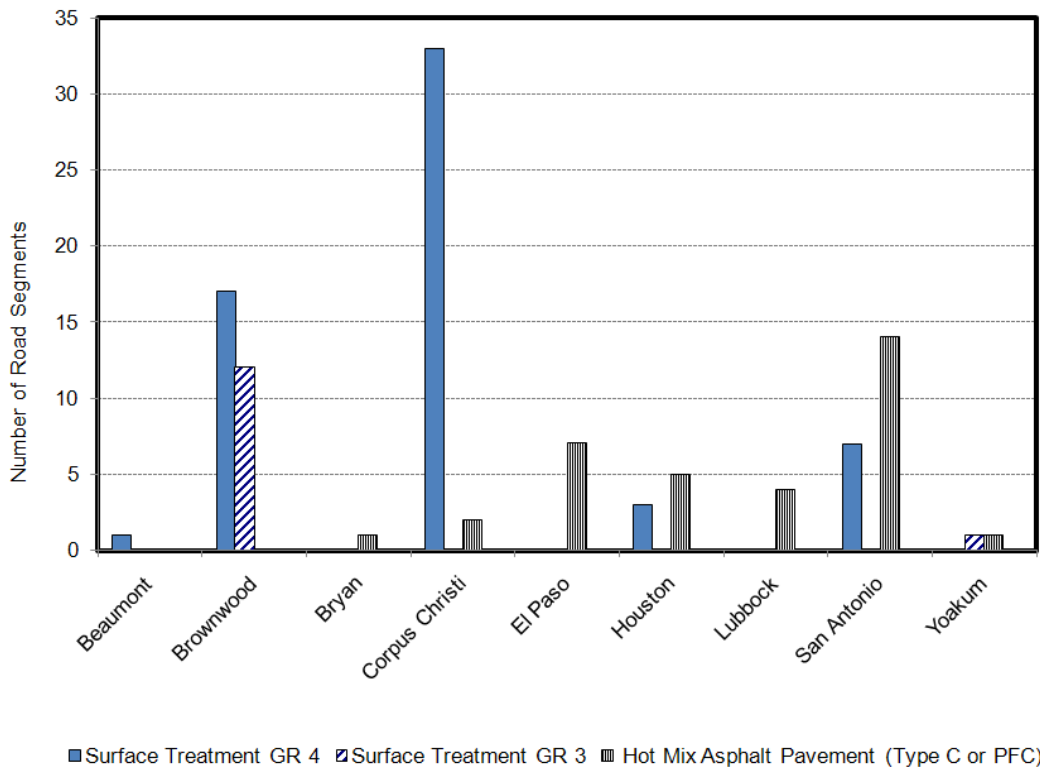


**Figure 2. Mixture Types Used in the Selected Road Segments.**



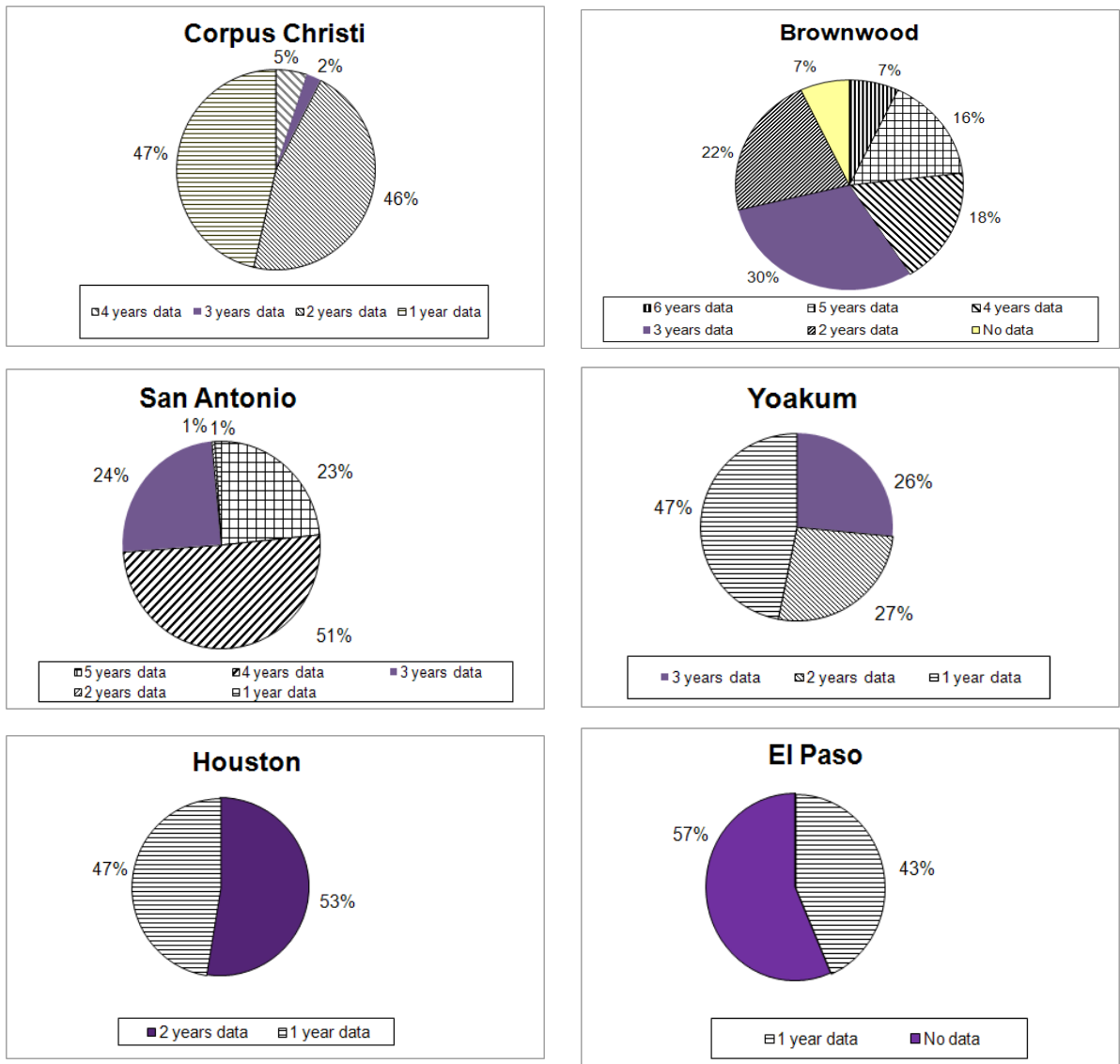


**Figure 3. Data Availability for the Different TxDOT Districts.**

To have better understanding of the data variation, plots were produced that show the variation of the skid number versus PMIS section for each road segment. These graphs were the basis for the next step of the data analysis. These figures are given in the appendix. It was found that road segments had a wide range of variation in the measured skid resistance. This variation can be due to different factors such as aggregate type, mix type, traffic, environmental condition, etc. The effects of different factors in the variation of the skid resistance are discussed in the analysis section of this report.

## ANALYSIS OF THE COLLECTED FIELD DATA

Careful evaluation of the figures in the appendix reveals that the data have high variability. Figure 4 shows the coefficient of variation of the measured skid resistance for different road segments for each year. For instance, it can be seen that in year 2005, about 30 percent of the data have a coefficient of variation between 30 to 40 percent.

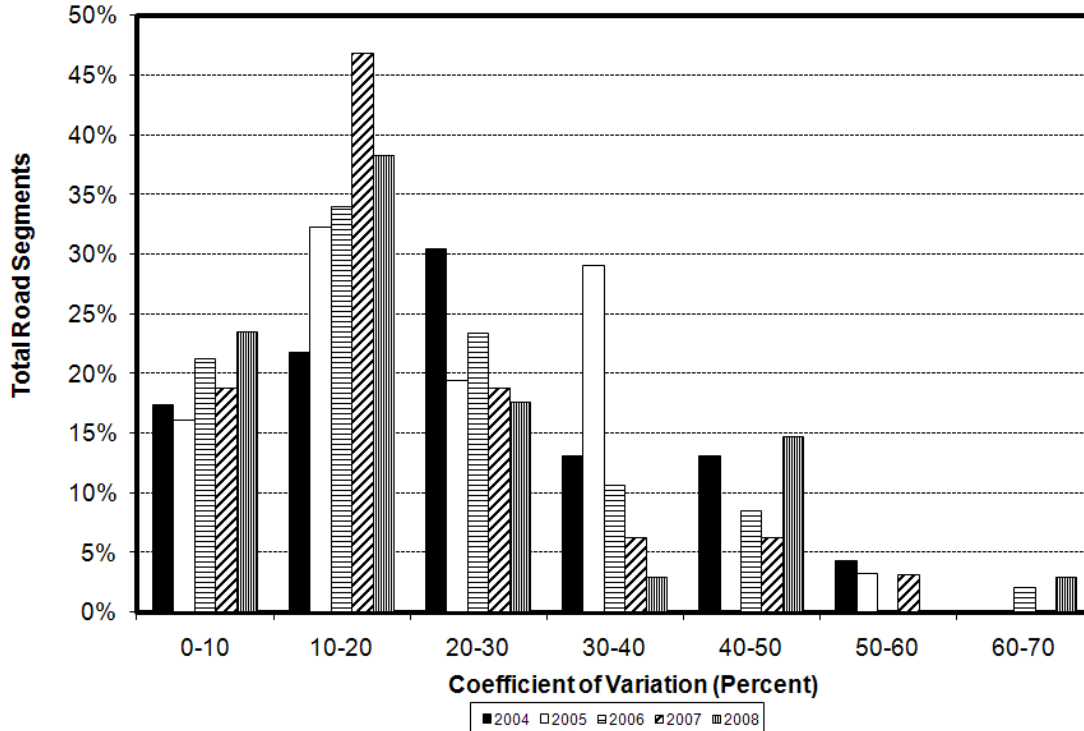


**Figure 4. Coefficient of Variation of Measured Skid Resistance for Different Sections.**

Due to the high variability of the data, analysis should consider the separate effects of different factors influencing skid resistance in order to be conclusive. In this section, the effects of different factors on the measured skid resistance are analyzed and discussed after making the following simplifications:

- As long as gradation remains the same, regardless of asphalt type, the surface treatment was assumed to be identical; e.g., surface treatment grade 4 is a combination of size 4 aggregates with AC-15P, AC-20-5TR, AC 20XP, and CRS-2P asphalt types. Furthermore, only two types of surface treatment were

considered in the analysis, and the effect of binder type on frictional characteristics was not considered.

- In order to compare different road categories in different service years, a parameter called the traffic multiplication factor (TMF) was defined. As shown in Equation 6, TMF is the multiplication of the annual average daily traffic (AADT) and number of years in service.

$$TMF = \frac{AADT \times YEARS\ IN\ SERVICE}{1000} \quad (6)$$

This factor reflects the effect of both years in service and AADT for the most critical lane in the highway, i.e., the outer lane.

In order to study the variation of measured skid numbers as a function of traffic, it was decided to identify homogeneous subgroups of road sections in which the variation of skid number as a function of traffic is more consistent. A cluster analysis algorithm included in the SPSS statistical software package known as the two-step cluster method was implemented for this purpose (SPSS, 2009). In this algorithm, the number of groups is established so that within-group variation is minimized and between-group variation is maximized. All the data in the database were classified in terms of their TMF for further analysis. Refer to the SPSS manual for additional information about the details of this clustering analysis (SPSS, 2009). Table 4 shows the TMF range for each cluster. A summary of the records based on the TMF class, aggregate type, and mix type is tabulated in Table 5.

**Table 4. Traffic Clusters in Terms of Traffic Multiplication Factor.**

<i>Level</i>	<i>Traffic Multiplication Factor</i>
Low	0-5499
Medium	5500-13,499
High	13,500-24,999
Very High	25,000-40,000

**Table 5. Summary of Skid Resistance Measurements.**

TMF Cluster	Mixture Design	Aggregate Type	N	Mean	Median	Min.	Max.	Std. Dev.
0-5500	Type C	Aggregate R	30	30.87	31.50	21	42	6.96
		Aggregate I	25	37.36	38.00	24	43	3.47
		Aggregate K	374	28.22	32.00	5	52	11.35
		Aggregate M	9	29.11	33.00	15	41	9.29
		Aggregate R	16	35.88	37.00	31	40	3.01
		Aggregate F	550	33.16	34.00	8	47	4.13
	PFC	Aggregate I	163	33.64	34.00	13	41	2.79
		Aggregate H	6	42.50	45.50	25	53	9.52
		Aggregate K	19	47.00	48.00	33	61	7.81
		Aggregate L	197	55.66	62.00	6	80	17.32
		Aggregate M	30	36.50	35.50	20	51	8.79
		Aggregate N	474	30.88	30.00	13	54	6.74
		Aggregate B	26	40.42	40.00	38	42	1.17
		Aggregate H	1	24.00	24.00	24	24	.
		Aggregate J	13	51.92	53.00	31	61	10.03
	Surface Treatment GR-4	Aggregate K	198	27.95	28.00	13	74	7.77
		Aggregate L	8	54.38	54.00	27	78	18.84
		Aggregate M	172	41.47	33.00	12	77	17.88
		Aggregate N	51	36.22	34.00	16	56	7.97
		Aggregate O	452	32.18	33.00	6	68	14.64
		Aggregate P	46	29.17	28.00	16	65	8.42
		Aggregate Q	55	30.05	29.00	12	53	8.84

**Table 5. Summary of Skid Resistance Measurements (Continued).**

TMF Cluster	Mixture Design	Producer Name	N	Mean	Median	Min.	Max.	Std. Dev.
5500-13,500	Type C	Aggregate R	114	26.82	25.50	14	55	6.54
		Aggregate F	12	22.17	22.00	17	27	3.19
		Aggregate I	37	32.46	35.00	21	39	5.32
		Aggregate K	127	13.28	12.00	7	45	5.00
		Aggregate R	16	34.50	34.50	30	38	2.42
	PFC	Aggregate F	126	31.92	31.00	27	38	2.61
		Aggregate I	185	30.78	29.00	9	42	4.92
		Aggregate M	46	29.37	30.50	14	33	4.52
		Aggregate L	9	39.89	27.00	14	73	25.00
		Aggregate H	1	25.00	25.00	25	25	.
13,500-25,000	Type C	Aggregate J	2	61.50	61.50	61	62	0.71
		Aggregate K	58	26.76	29.00	11	42	8.00
		Aggregate M	60	31.17	27.50	12	71	12.52
		Aggregate N	5	30.20	32.00	24	36	5.02
		Aggregate O	95	24.53	27.00	6	36	8.35
	PFC	Aggregate Q	7	25.14	23.00	18	40	6.99
		Aggregate R	62	22.53	21.50	14	38	4.57
		Aggregate K	2	17.00	17.00	15	19	2.83
		Aggregate R	16	29.94	30.50	26	32	2.08
		Aggregate I	72	24.78	24.50	13	36	2.96
25,000-40,000	Surface Treatment GR-4	Aggregate M	19	28.32	28.00	26	35	2.36
		Aggregate K	12	14.33	14.00	11	20	2.64
		Aggregate M	9	23.33	23.00	11	34	7.66
		Aggregate Q	3	18.33	17.00	17	21	2.31
		Aggregate R	32	18.34	18.50	12	27	3.15
	Surface Treatment GR-4	Type C	16	29.94	29.50	26	36	2.54
		PFC	10	18.10	14.00	11	59	14.43

## Traffic Load

Figure 5 shows the values of different skid numbers in terms of traffic level. Although the values of SN have high variability, a decreasing trend of SN values as a function of traffic level is identifiable. Due to high standard-error-of-mean values, a plot of median values was produced in Figure 6 to extract the possible trend of SN values. This figure clearly shows that the SN value decreases when the traffic level increases. Figure 7 shows the standard deviation of measured SN values versus traffic level. Moreover, the mixes with very high or high traffic level have lower variability compared to mixes at low traffic level.

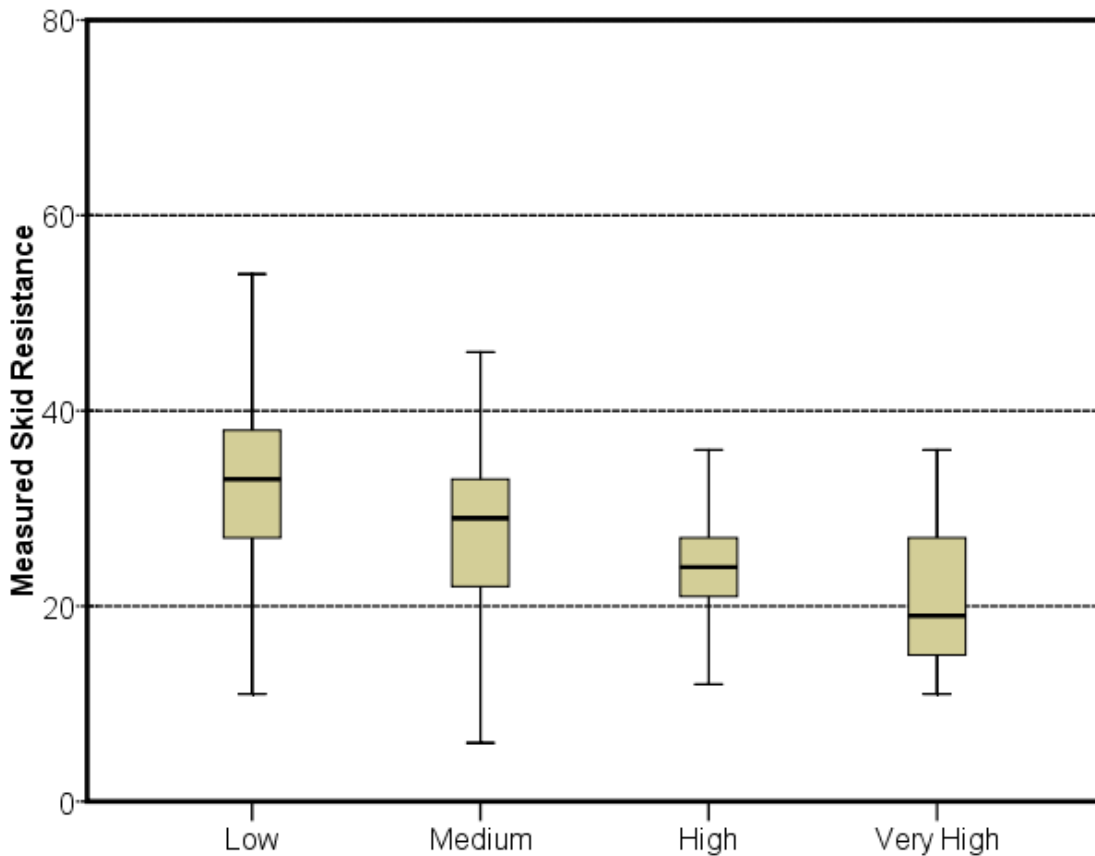
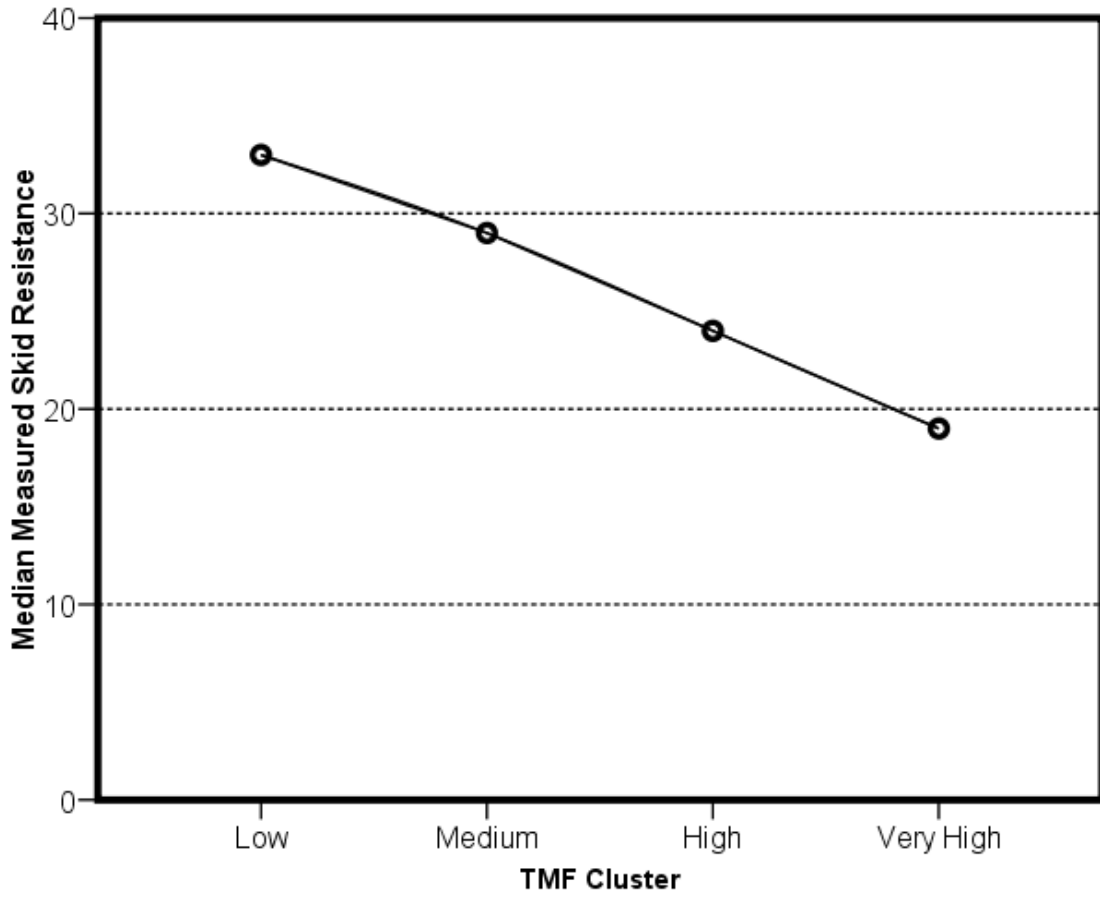
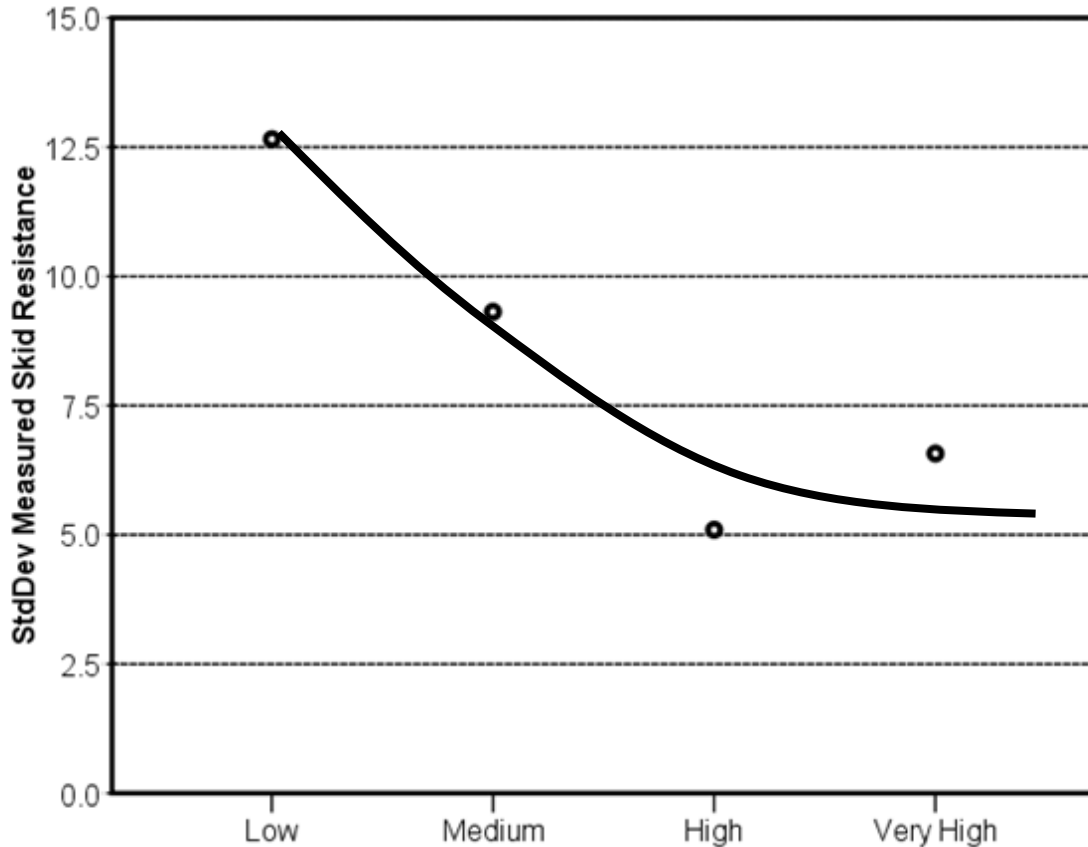


Figure 5. Measured SN Values versus Traffic Level.



**Figure 6. Median SN Values versus Traffic Level.**



**Figure 7. Standard Deviation of Measured SN Values versus Traffic Level.**

### Mix Design

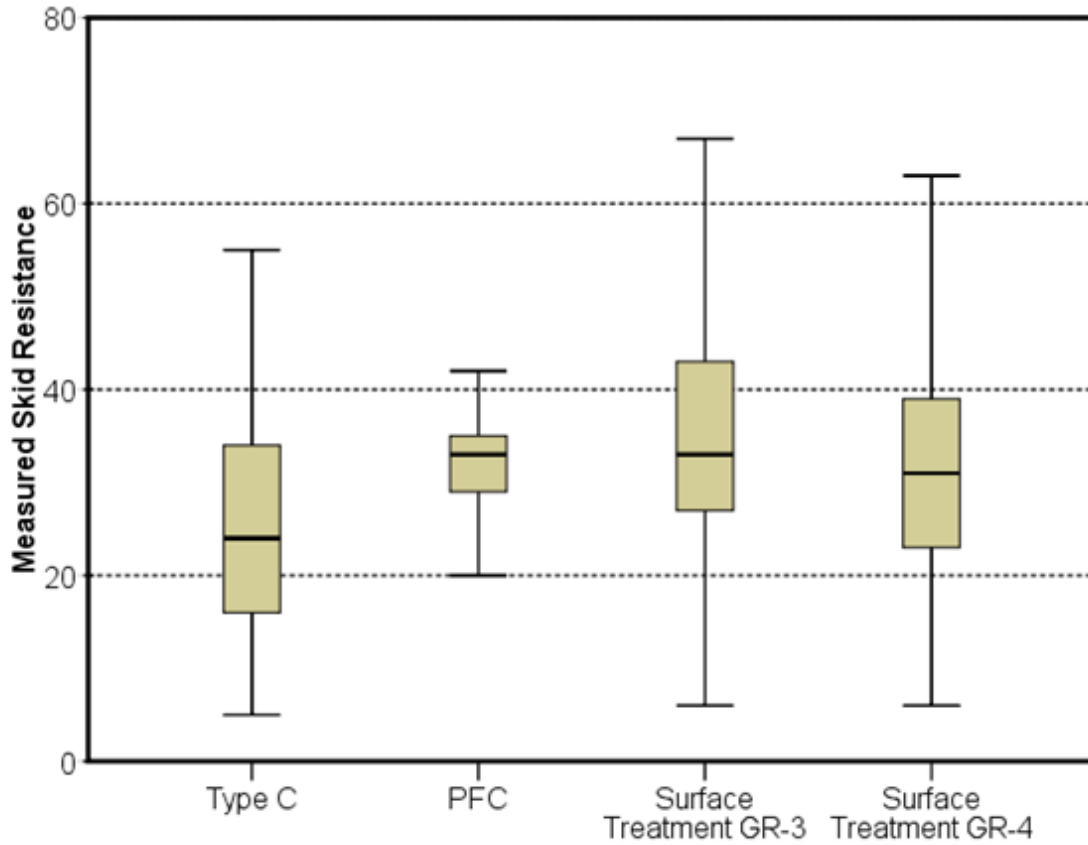
Figure 8 shows the measured SN values for different mix designs. This figure clearly shows that the results of skid measurements are highly variable and depend on the mix type. A plot of median values as shown in Figure 9 gives a better understanding of the behavior of different mixes. These results confirm the findings from Phase I of this project since it was shown that PFC mixes had higher skid resistance than Type C mixes.

Figure 10 shows the standard deviation of measured skid number for different mixes; the standard deviation for PFC mixes is less than five in all cases. This result demonstrates the low variability and consistency in frictional performance of PFC mixes. Type C mixes have more variability than PFC mixes. Surface-treatment mixes have more variation than Type C and PFC mixes.

Figures 11 and 12 show the variability of measured SN values for different mixes in low and medium/high traffic-level categories, respectively. These figures show the variability of skid resistance decreased significantly from low traffic levels to high traffic



levels. Moreover, the variability of skid measurement for surface treatment is high, and the variability of PFC mixes is the lowest among all mixes. The variability of Type C mixes is generally higher than PFC mixes. These results confirm that the PFC is the most consistent and has the lowest variability among all mixes. One reason for this might be the requirement for using aggregate SAC A or SAC B in preparing the PFC mixes.



**Figure 8. Measured SN Values for Different Mix Types.**

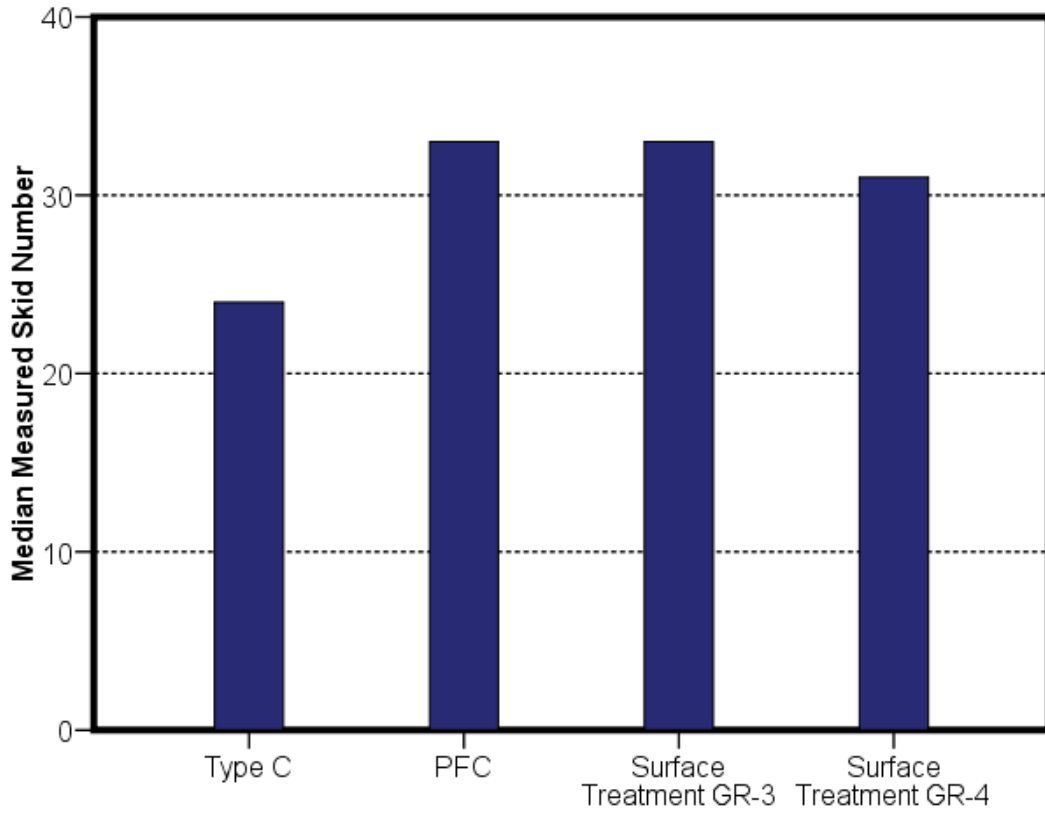


**Figure 9. Median of Measured SN Values for Different Mix Types.**

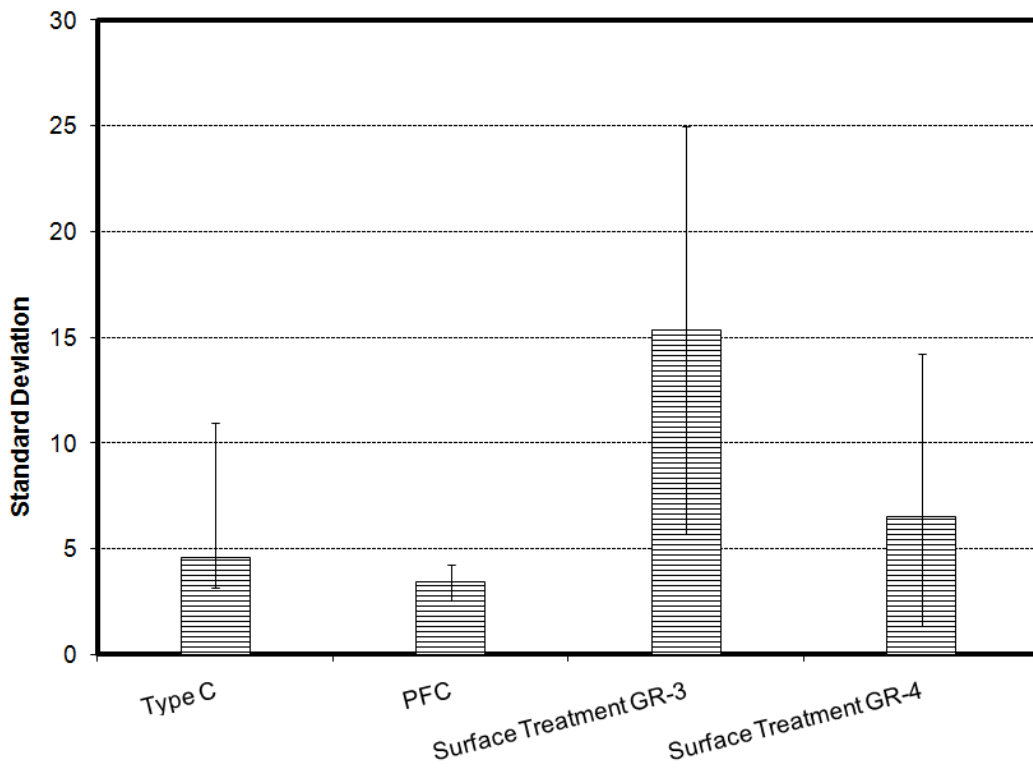


**Figure 10. Standard Deviation of Measured SN Values for Different Mixes.**

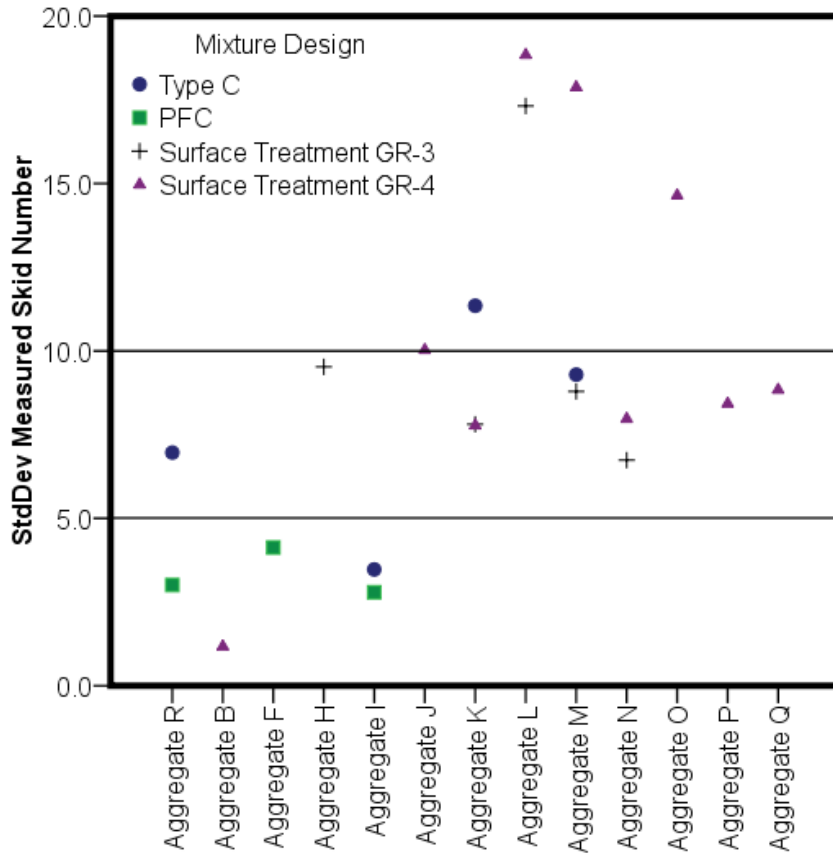


**Figure 11. Standard Deviation of the Measured SN Values for Low TMF Level.**

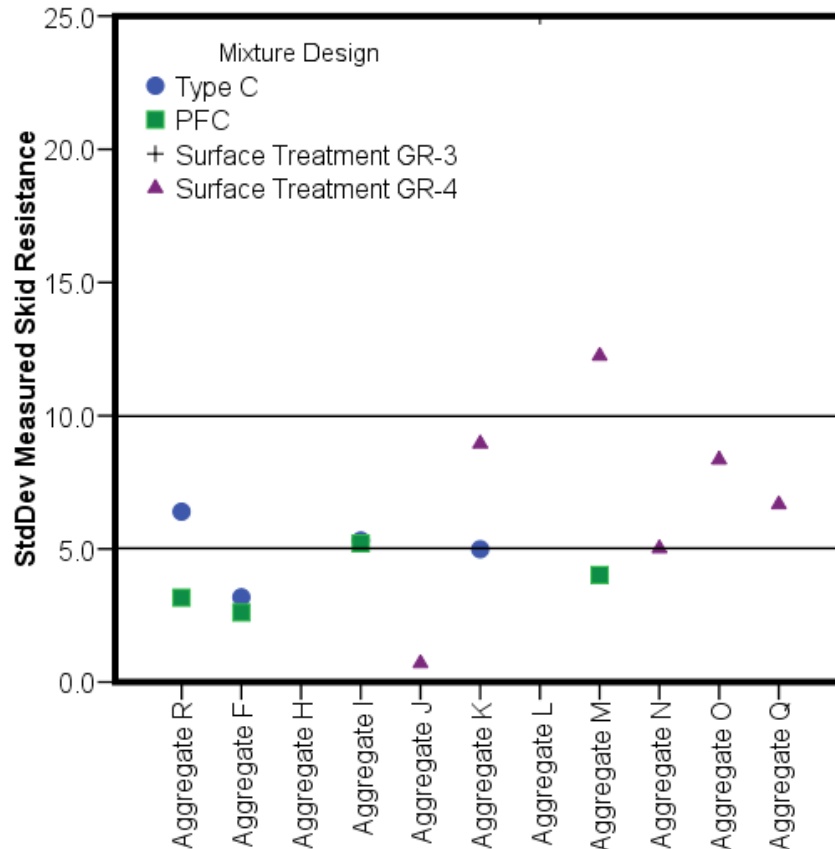


**Figure 12. Standard Deviation of the Measured SN Values for Medium and High TMF Level.**

### Aggregate Type

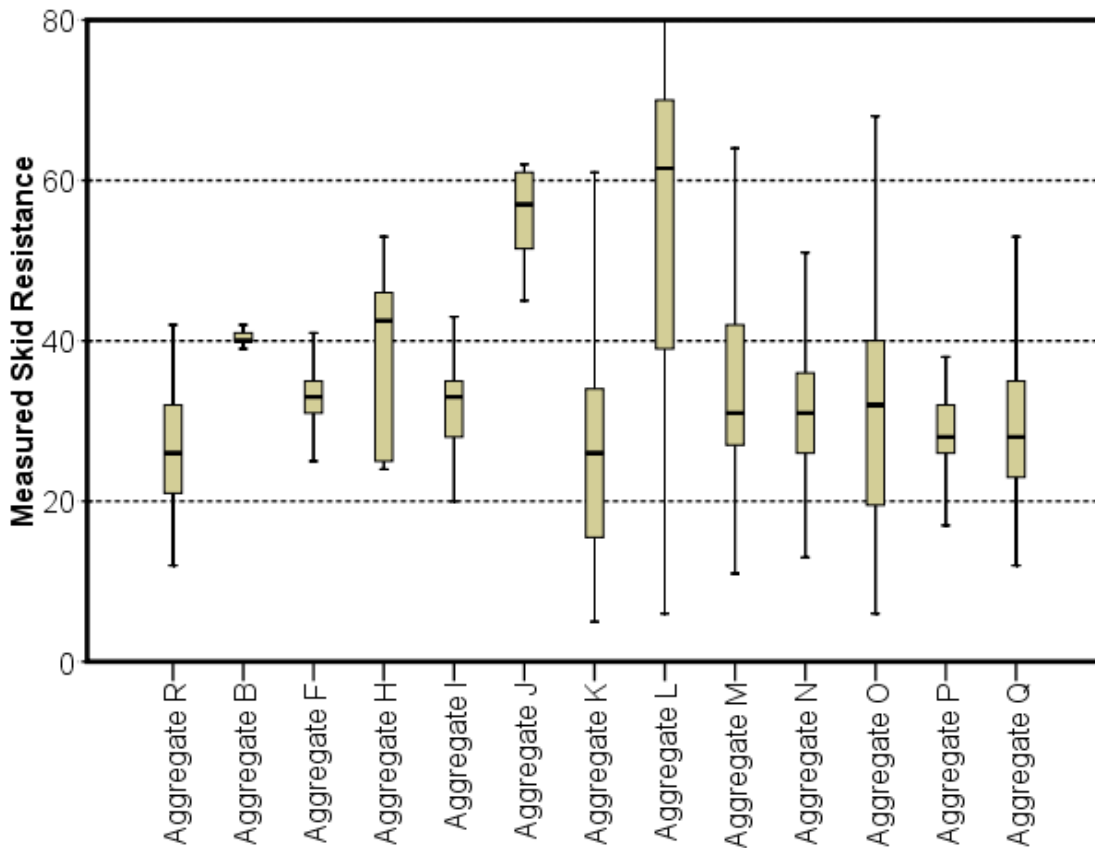
Figure 13 shows the values of measured SN for different aggregate types. The influence of aggregate type on the skid resistance cannot be studied in isolation from the effect of mix design and traffic level. Therefore, a detailed analysis of the measured skid values for different mix types and traffic level was performed.

Figure 14 shows that in almost all aggregate types, surface treatment grade 3 has the highest SN value, and among dense-graded mixes, PFC mixes have the highest skid number. Table 6 shows the median value for measured skid resistance and aggregate ranking for surface treatment grade 3. In this mix design, aggregate L has the highest skid value. Furthermore, aggregate K (classified as SAC B in the TxDOT classification system) shows satisfactory skid characteristics and lies in second place. Aggregate H, which is classified as SAC A in the TxDOT classification system, is the third in the

group. Both M and N aggregate types, classified as SAC B, sit in the fourth and fifth place, respectively.

The results of skid number values measured for surface treatment grade 4 are tabulated in

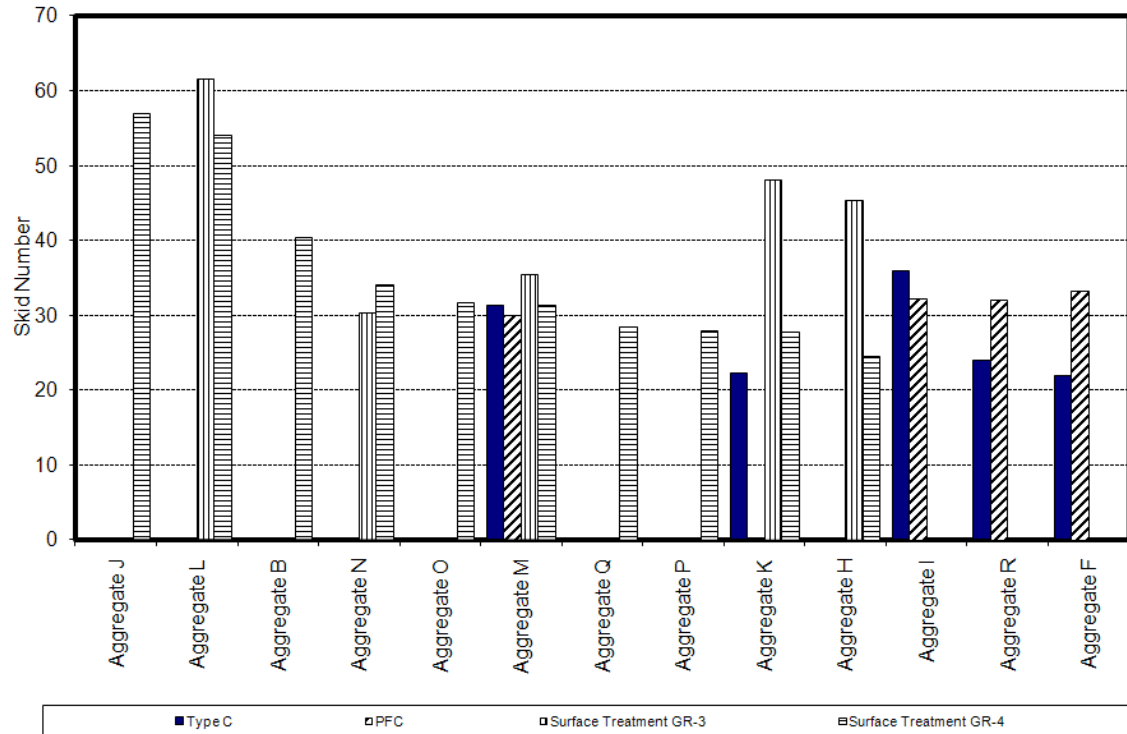
[Table 7](#). The results indicate that both aggregate L and aggregate J have satisfactory skid properties and sit in the first and second place, respectively.



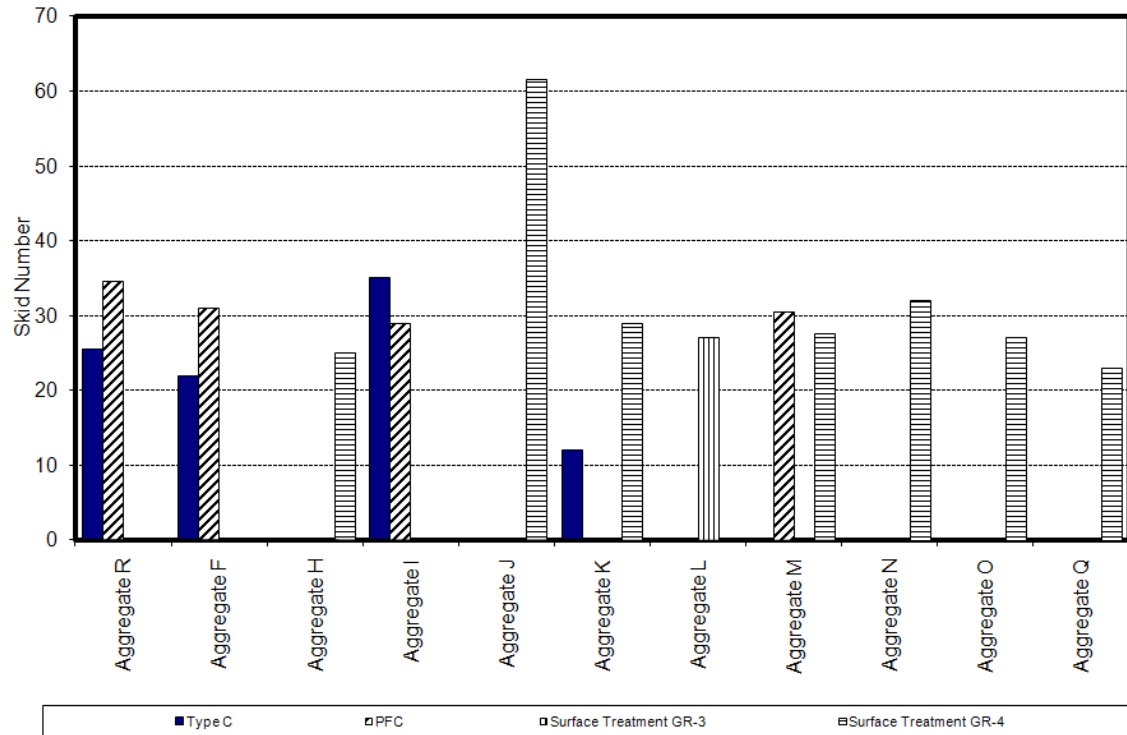
**Figure 13. Values of Measured SN for Different Aggregate Types.**

[Table 8](#) shows the median skid resistance values and aggregate ranking for the Type C mixture. In this mixture type, aggregate I provides the highest friction level. The results of the analysis of field data confirmed the findings from Phase I of this project showing aggregate R to have superior skid properties compared with aggregates K and M individually. Furthermore, data in [Table 8](#) show that mixtures containing aggregate K lose the initial texture faster than other aggregate types. The skid number of mixtures

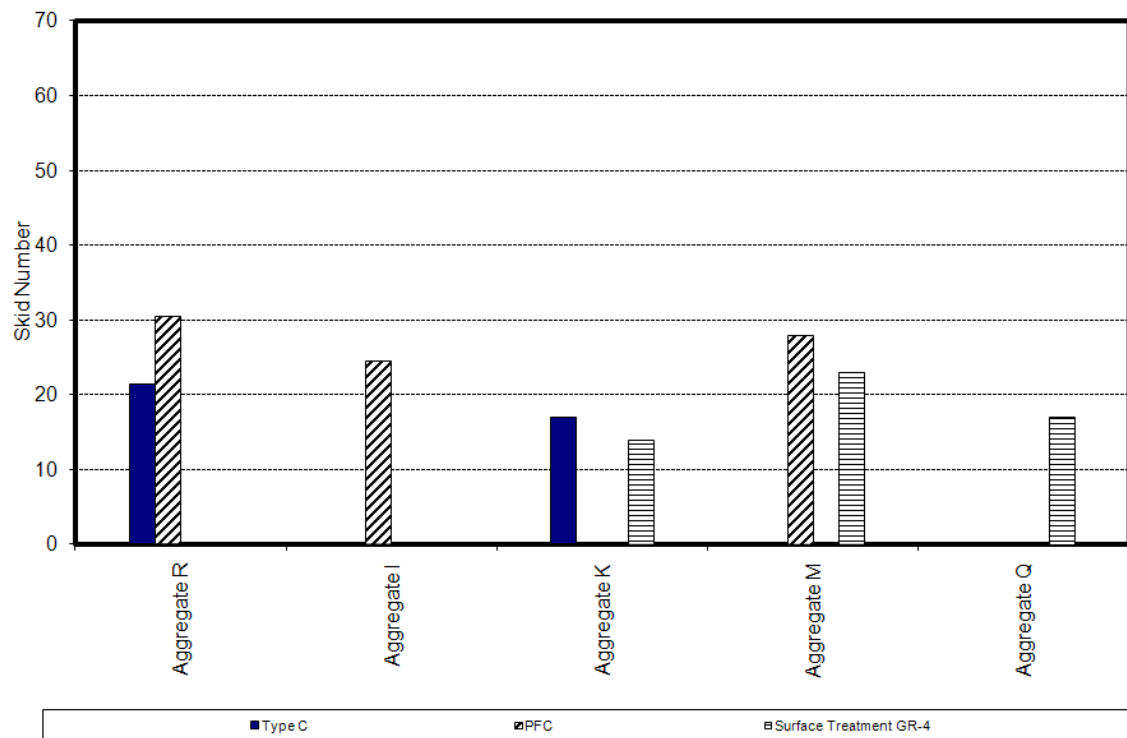
containing aggregate K dropped below 20 at higher traffic levels. Table 9 shows the results for PFC mixes. It appears that aggregate R has the highest skid value. Again, this finding is in accordance with the results of Phase I of this project. Aggregates F and I function well, and their skid values are close to or above 30.



(a) Low TMF Level



(b) Medium TMF Level



(c) High TMF Level

Figure 14. Median of Measured SN Values for Different Aggregate and Mix Types

**Table 6. Aggregate Ranking Based on Measured Skid Resistance for Surface Treatment Grade 3 in Low Traffic Level.**

Aggregate Type	Skid Number Median	Rank	TxDOT Classification
Aggregate L	62	1	SAC A
Aggregate K	48	2	SAC B
Aggregate H	45	3	SAC A
Aggregate M	36	4	SAC B
Aggregate N	30	5	SAC B

**Table 7. Aggregate Ranking Based on Measured Skid Resistance for Surface Treatment Grade 4 in Medium and Low Traffic Level.**

Cluster Number of Case	Producer Name	Measured Skid Resistance	Rank	TxDOT Classification
Low (0-5500)	Aggregate L	54	1	SAC A
	Aggregate J	54	2	SAC B
	Aggregate B	40	3	SAC B
	Aggregate N	35	4	SAC B
	Aggregate O	33	5	SAC A
	Aggregate M	33	6	SAC B
	Aggregate Q	30	7	SAC B
	Aggregate K	29	8	SAC B
	Aggregate P	28	9	SAC A
	Aggregate H	25	10	SAC A
Medium (5500-13,500)	Aggregate J	62	1	SAC B
	Aggregate N	32	2	SAC B
	Aggregate K	29	3	SAC B
	Aggregate M	28	4	SAC B
	Aggregate O	27	5	SAC A
	Aggregate H	25	6	SAC A
	Aggregate Q	23	7	SAC B



**Table 8. Aggregate Ranking Based on Measured Skid Resistance for Type C Mixture in High, Medium, and Low Traffic Level.**

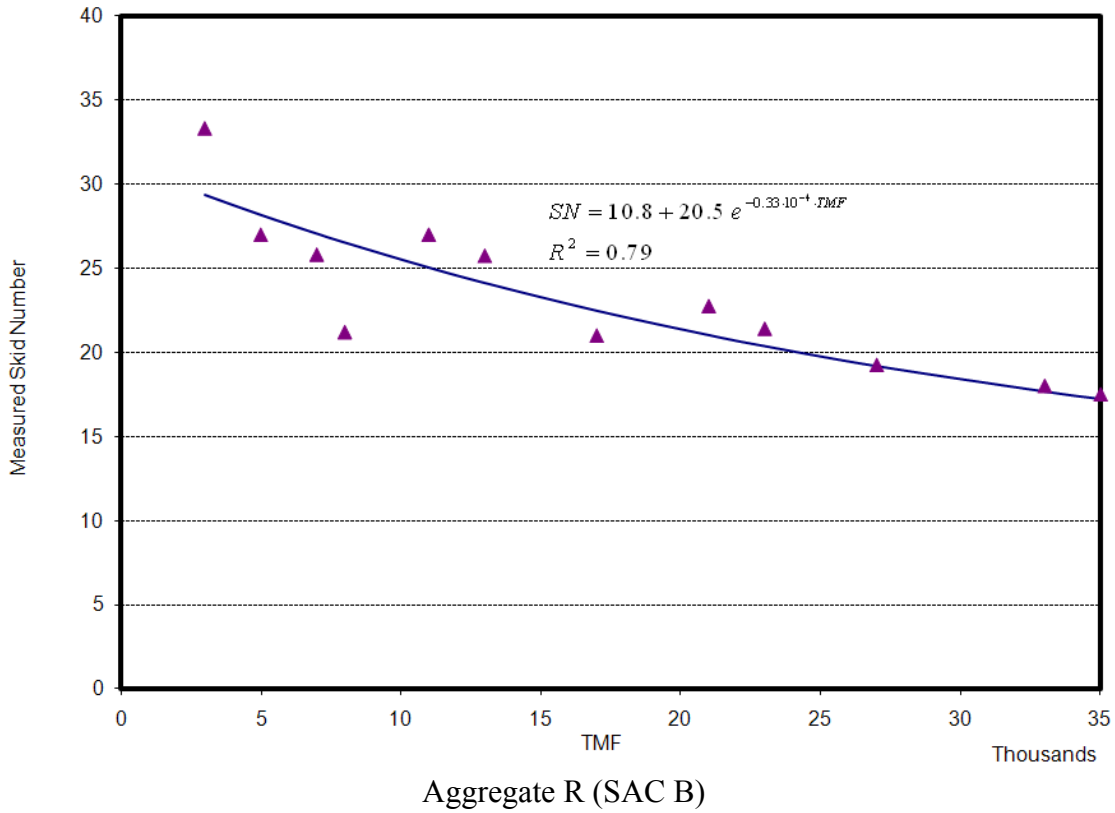
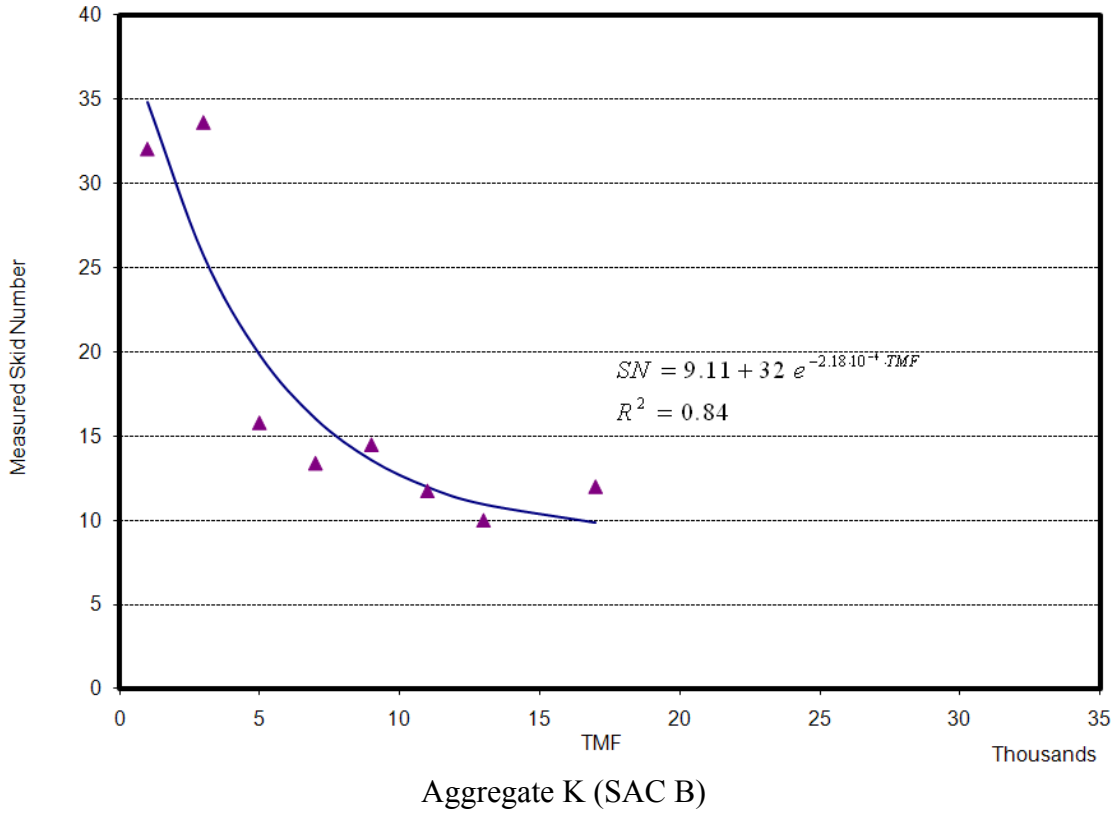
Cluster Number of Case	Producer Name	Measured Skid Resistance	Rank	TxDOT Classification
Low (0-5499)	Aggregate I	38	1	SAC A
	Aggregate R	32	2	SAC B
	Aggregate K	31	3	SAC B
	Aggregate M	31	4	SAC B
Medium (5500-13,499)	Aggregate I	35	1	SAC A
	Aggregate R	26	2	SAC B
	Aggregate F	22	3	SAC B
	Aggregate K	12	4	SAC B
High (13,500-24,999)	Aggregate R	22	1	SAC B
	Aggregate K	17	2	SAC B

**Table 9. Aggregate Ranking Based on Measured Skid Resistance for PFC Mixture in High, Medium, and Low Traffic Level.**

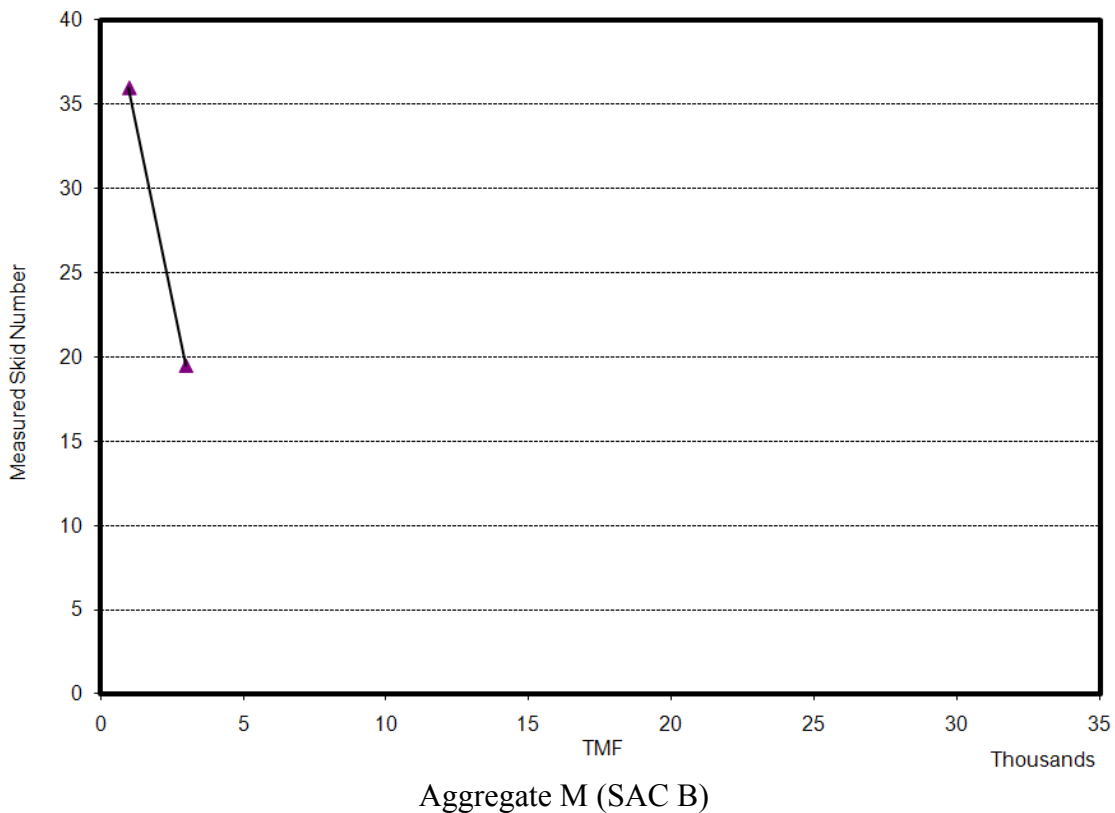
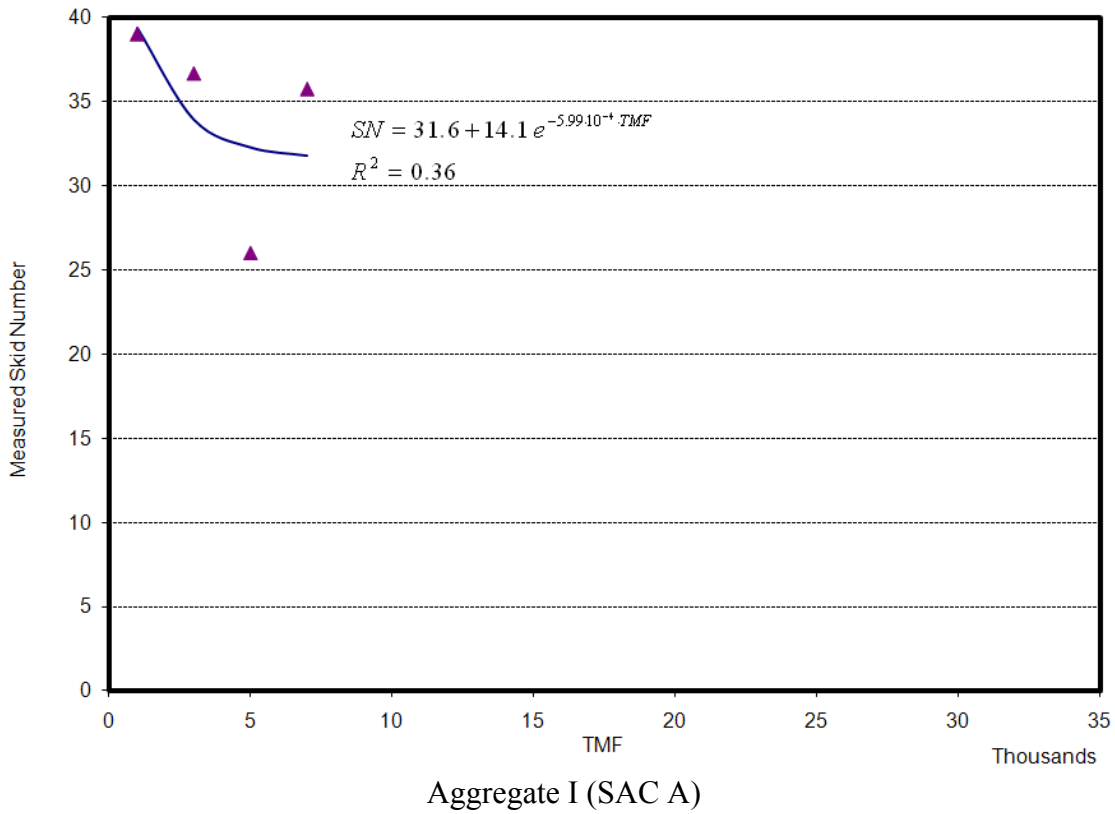
Cluster Number of Case	Producer Name	Measured Skid Resistance	Rank	TxDOT Classification
Low (0-5499)	Aggregate R	37	1	SAC B
	Aggregate F	34	2	SAC B
	Aggregate I	34	3	SAC A
Medium (5500-13,499)	Aggregate R	35	1	SAC B
	Aggregate F	31	2	SAC B
	Aggregate M	31	3	SAC B
	Aggregate I	30	4	SAC A
High (13,500-24,999)	Aggregate R	31	1	SAC B
	Aggregate M	28	2	SAC B
	Aggregate I	25	3	SAC A

Figure 11 presented earlier shows the standard deviation of the measured values of the skid number for different aggregate types at low traffic levels. Aggregates used in surface treatment grade 3 and grade 4 such as aggregates L, O, and M have high variability (a standard deviation higher than 20). On the other hand, aggregates used in PFC mixes such as aggregates M, F, and I have a standard deviation less than 5.

Since the majority of the collected data lie in low and medium categories, a new classification was used to capture the variation of each aggregate source against TMF level. Figure 15 shows the median of measured SN values for Type C mix design. This figure clearly shows that aggregate K was polished rapidly and loses its frictional characteristics in early stages of its service life. The terminal SN value for this aggregate (about 9) seems to be less than other aggregates. This observation conforms very well with lab findings about the rapid polishing of this aggregate type. Aggregate R seems to modify the skid characteristics compared with aggregate K alone since this combination has a terminal value of about 11. These graphs show that an exponential equation with the form presented in Equation 1 in Chapter II can fit the data. Moreover, the rate of change in aggregate R is lower than that of aggregate K individually. Aggregate I has the highest skid number in this mix and can maintain its initial texture. The collected data for aggregate M do not extend over a number of years to allow making a conclusion. This aggregate, however, shows a high rate of decrease in friction compared to other aggregate sources.



**Figure 15. Median of Measured SN Values for Type C Mix Design.**

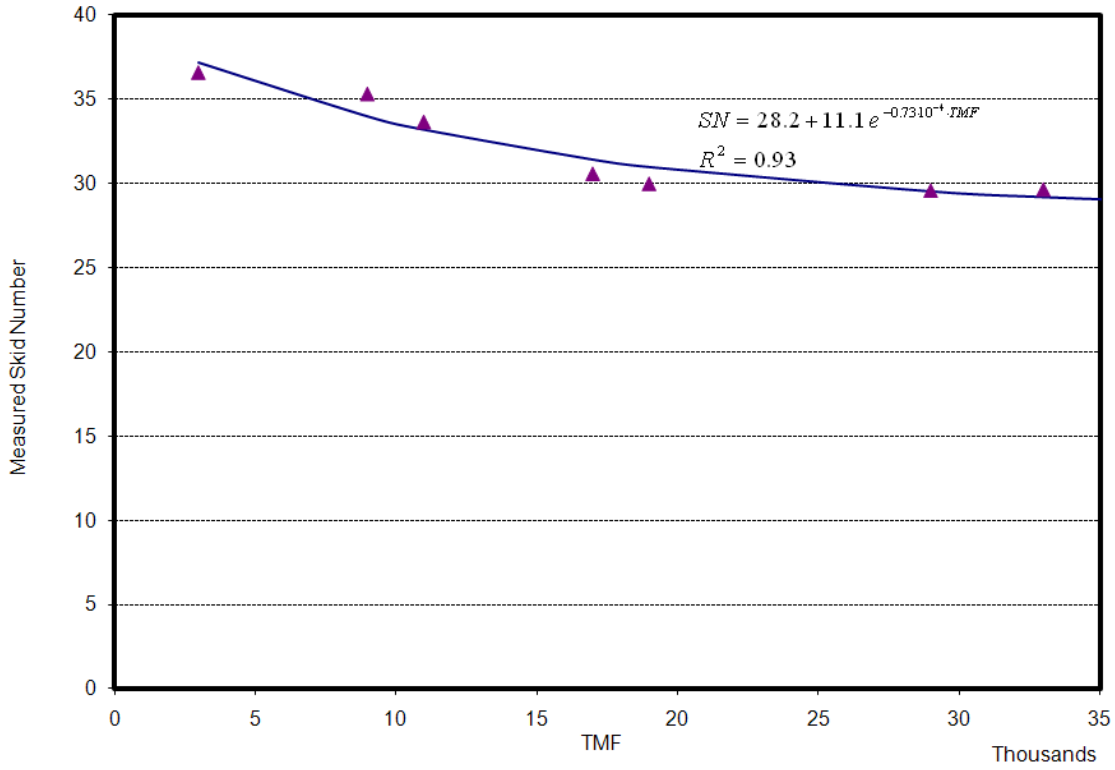


**Figure 15. Median of Measured SN Values for Type C Mix Design (Continued).**

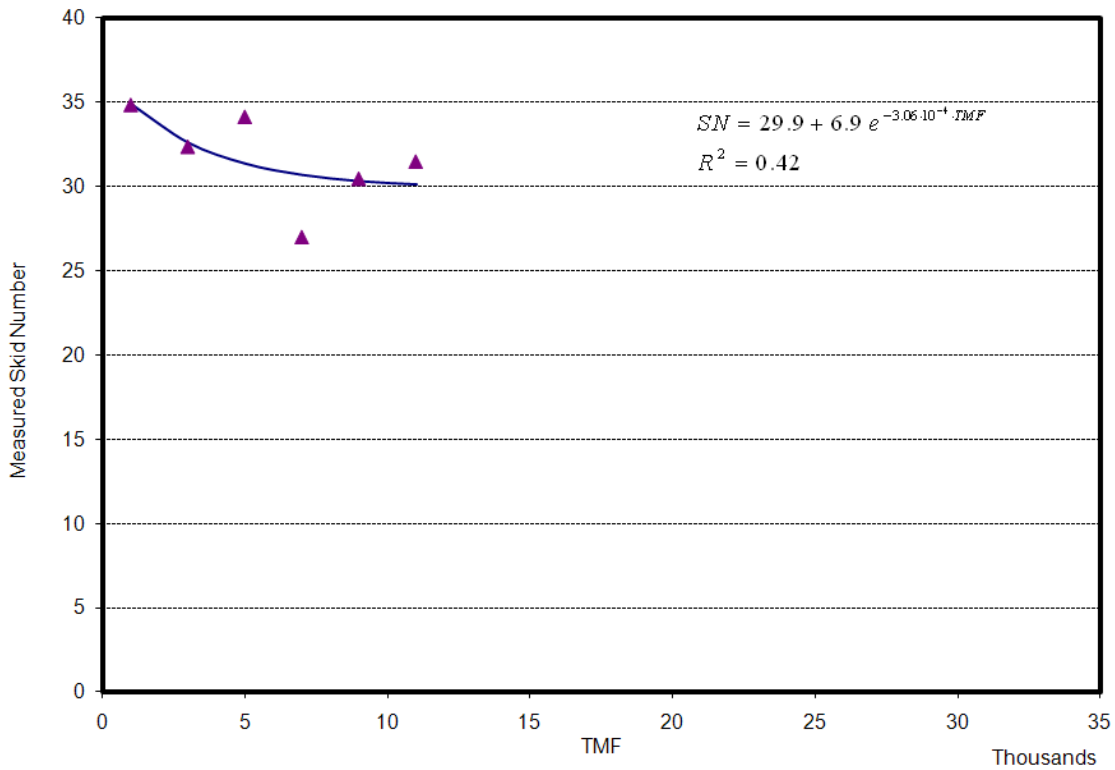
Figure 16 shows the median of measured SN values for PFC mix design. Equation 1 could fit to the data reasonably well. This figure shows that aggregates I and R have low polishing rates compared to aggregates F and N. The terminal values of aggregates I and M are less than 30. Aggregates R and F can maintain their initial texture over 30. The duration of collected skid data for aggregate M is not long enough to make a conclusive statement, but it seems this aggregate loses its initial texture rapidly and falls below 30 in its initial stages of service life. This observation confirms the finding of Phase I of this project.

Figure 17 shows the median of measured SN values for surface treatment grade 3. The collected data shown in this figure do not cover the complete range of traffic levels. This figure shows that aggregate L provides high initial skid resistance. A longer traffic range is needed to estimate the frictional performance of this aggregate in the field. Moreover, aggregates M and N have the lowest skid values in this mixture type. Aggregate K provides a fairly high level of friction ( $SN > 40$ ) although in other mix types it does not provide acceptable friction levels. Surface treatment grade 3 has an almost uniform skid number value throughout the range of TMF levels, and all aggregates are able to provide acceptable friction levels. These results suggest that the skid values for this mix are affected by gradation more than aggregate type.

Figure 18 shows the median of measured SN values for surface treatment grade 4. Aggregate J provides considerably high skid resistance, which is over 40. Aggregate K has the lowest terminal skid value at around 10. There is no significant difference between the median values of skid values for other aggregates. Similar to the performance in Type C mixes, aggregate K has the lowest terminal skid values. Aggregates M, O, and N have a fair terminal skid number between 25 and 30. Aggregate Q shows a decreasing rate of polishing, and a wider range of traffic data is needed to analyze the characteristics of this aggregate.

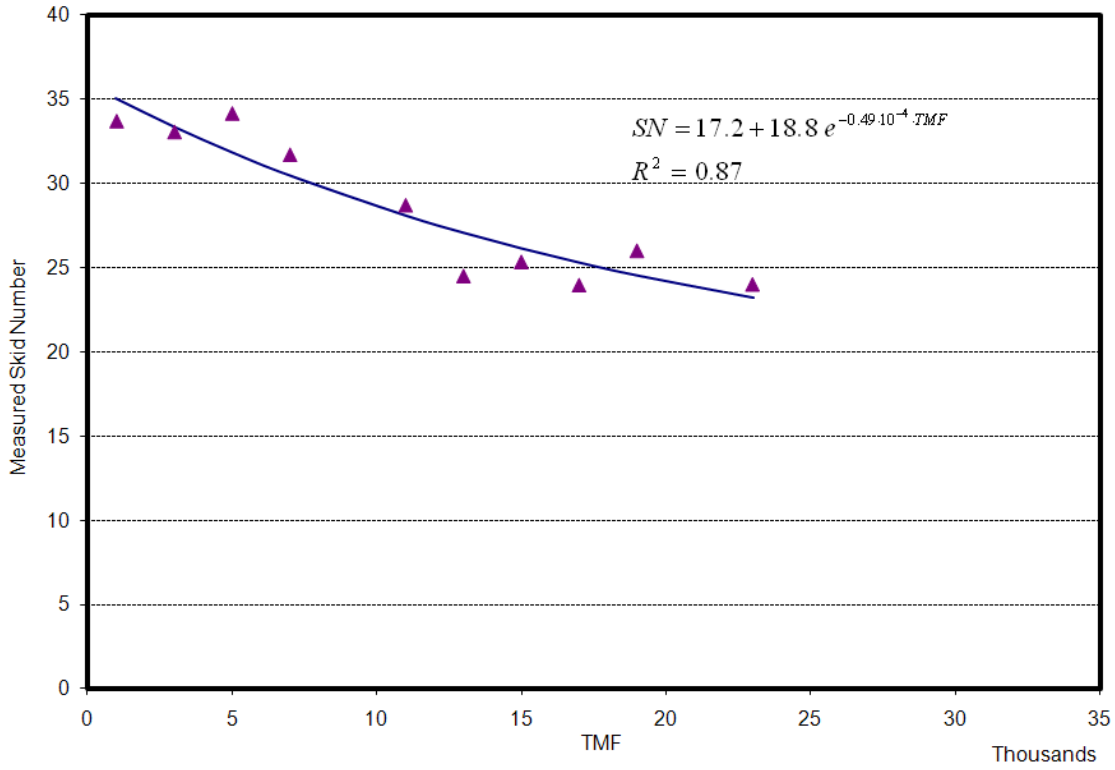


(a) Aggregate R (SAC B)

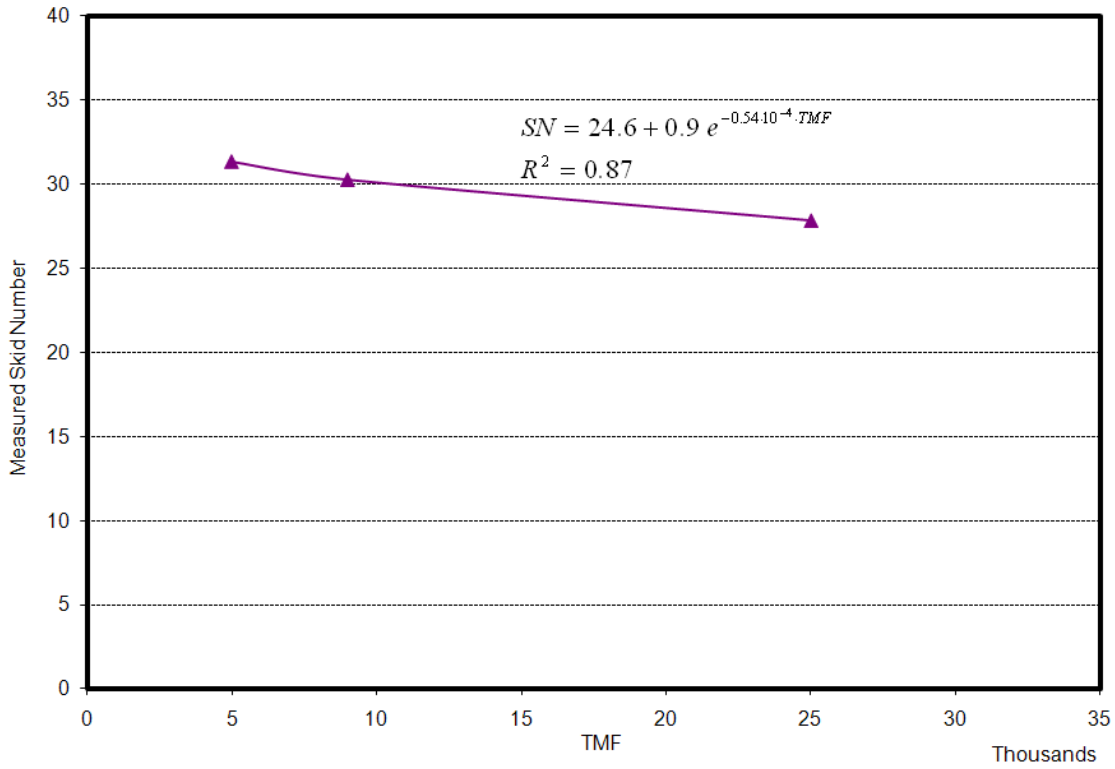


(b) Aggregate F (SAC B)

**Figure 16. Median of Measured SN Values for PFC Mix Design.**



(c) Aggregate I (SAC A)



(d) Aggregate M (SAC B)

**Figure16. Median of Measured SN Values for PFC Mix Design (Continued).**

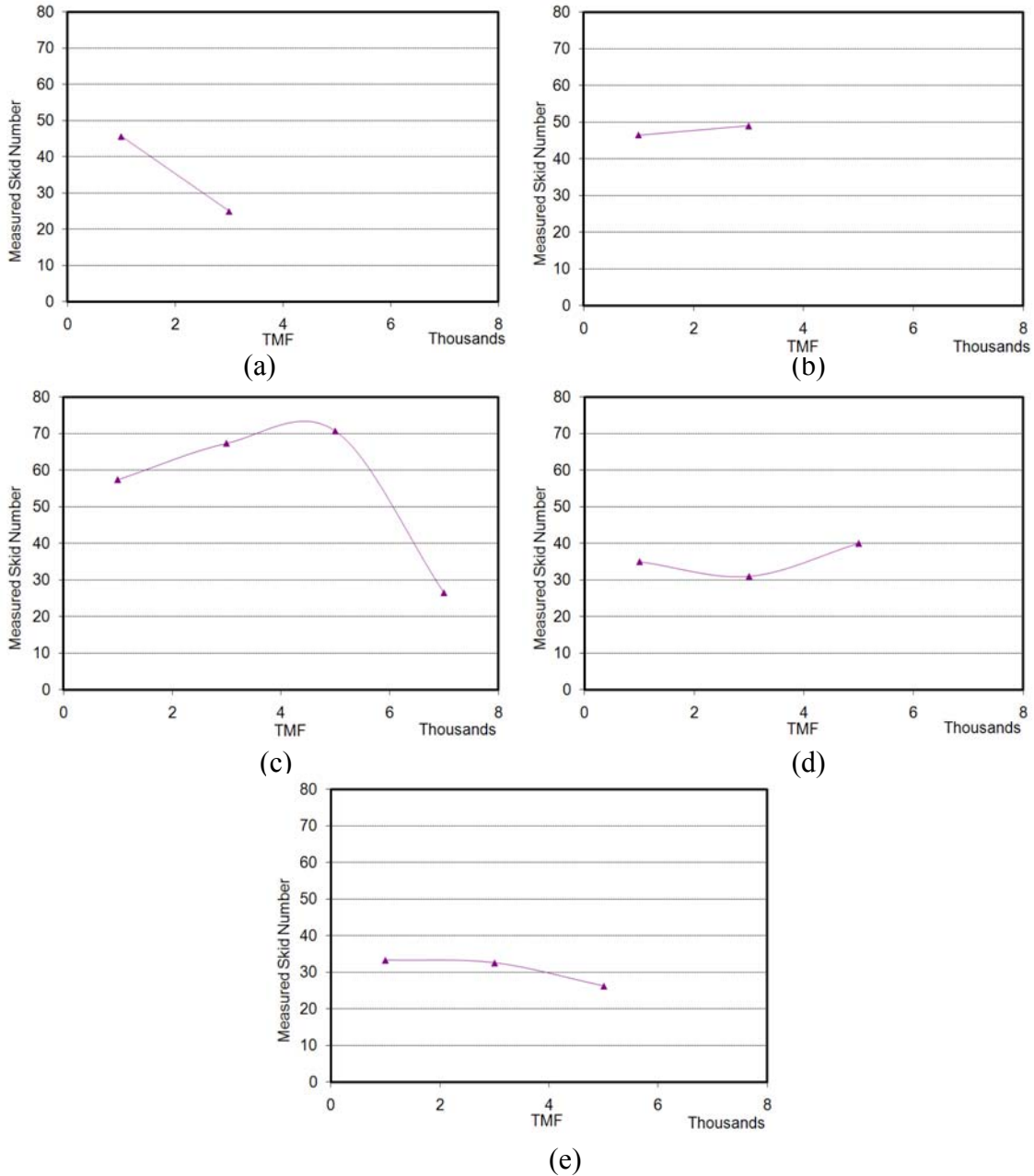
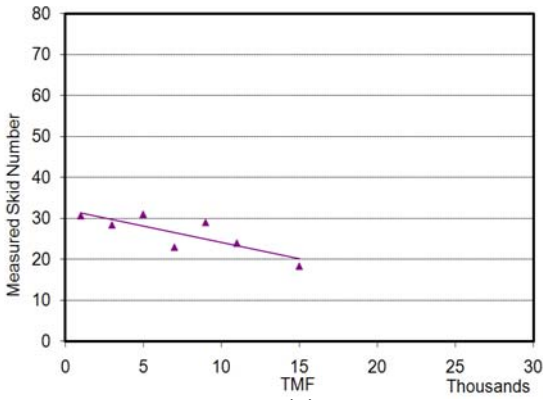
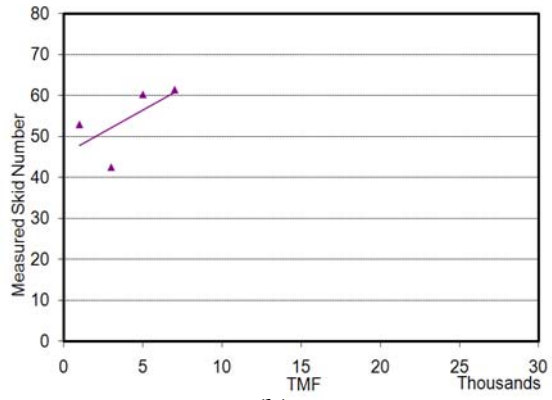


**Figure 17. Median of Measured SN Values for Surface Treatment Grade 3.**  
**(a) Aggregate H (SAC A). (b) Aggregate K (SAC B). (c) Aggregate L (SAC A).**  
**(d) Aggregate M (SAC B). (e) Aggregate N (SAC B).**

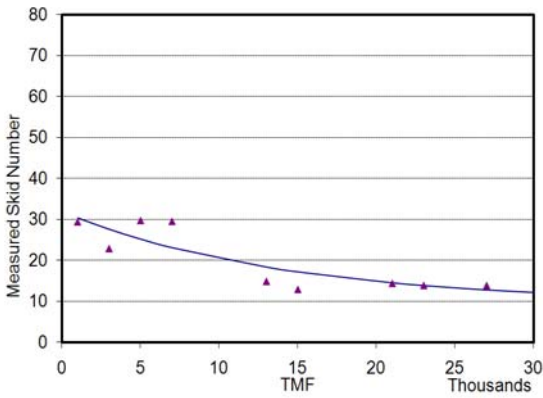




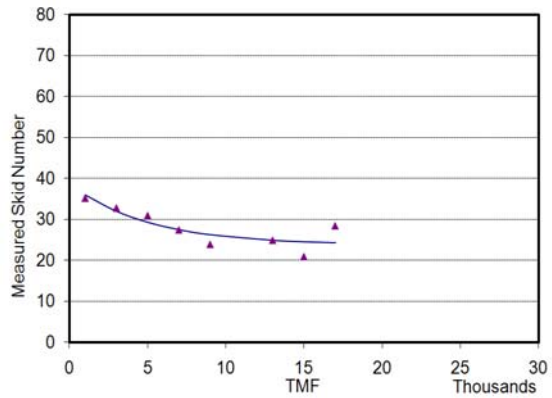
(a)



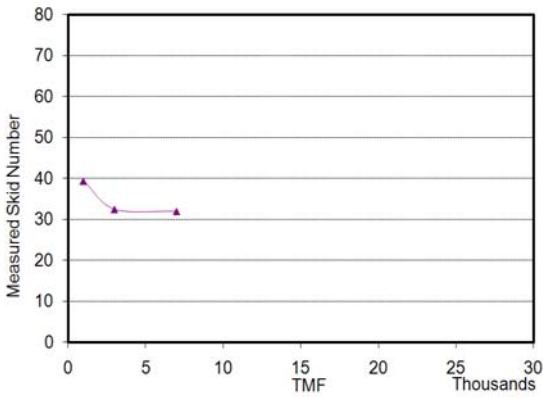
(b)



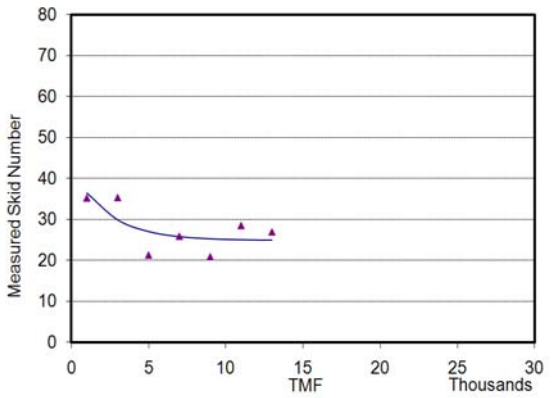
(c)



(d)



(e)



(f)

**Figure 18. Median of Measured SN Values for Surface Treatment Grade 4.**  
**(a) Aggregate Q (SAC B). (b) Aggregate J (SAC B). (c) Aggregate K (SAC B).**  
**(d) Aggregate M (SAC B). (e) Aggregate N (SAC B). (f) Aggregate O (SAC A).**

## **SUMMARY OF THE RESULTS OF THE FIELD-DATA ANALYSIS**

In Phase II of the project, skid data from different road sections with different material and mix types were collected. Traffic, mix type, and aggregate type were the main factors that were considered in the analysis of the measured skid numbers.

To facilitate comparing different road categories in their current service life, a single factor denoted TMF was defined. This factor is the multiplication of AADT in the design lane and years in service divided by 1000. This factor considers both traffic level and years of operation.

As expected, the results of the data analysis showed the measured skid number decreased as TMF increased. The measured skid numbers had less variation at higher TMF levels. This phenomenon could be attributed to mixtures reaching close to terminal skid condition, which is associated with aggregates approaching their equilibrium (or terminal) state of texture after a high number of polishing or loading cycles.

Four mix types (surface treatment grade 3, surface treatment grade 4, PFC, and Type C) were included in the field measurements. The results showed that surface treatments generally had higher skid numbers than Type C, which is a conventional dense-graded mix. Additionally, PFC mixes exhibited better skid resistance than Type C mixes and surface-treatment mixes. The results showed the PFC mixes had the lowest variation in skid number, while surface-treatment mixes had the highest variability.

The effect of aggregate type was studied, and the results showed that there was high interaction between aggregate performance, mix type in which aggregate is used, and traffic level. In general, it is hard to classify aggregates without specifying mixture type and traffic levels. For instance, aggregate K provided good skid resistance in surface treatment grade 3 at a low TMF, whereas dense-graded mixtures (Type C) with this aggregate showed low skid performance. This poor performance could be attributed to the high polishing rate of aggregate K as was found in the laboratory measurements conducted in Phase I of this project. The good performance of aggregate K in surface treatment grade 3 can be attributed to the high macrotexture of the pavement surface. It is worthwhile to note that the macrotexture of surface treatment dominates the skid resistance.

Aggregate K, which is classified as SAC B in the TxDOT classification system, and aggregate O, which is classified as SAC A, functions similarly in surface treatment grade 4. Aggregate J, classified as SAC B, provides a very high skid-resistance level in surface treatment grade 4 at a low and medium TMF. On the other hand, aggregate P, which is classified as SAC A, provides only good skid resistance in surface treatment grade 4. It is interesting to note that the current classification system places aggregate K with a measured skid number of 29 and aggregate J with a measured skid number of 54 in surface treatment grade 4 in the same class (SAC B).

For the most part, the results of the field-data analysis are in agreement with the laboratory findings in Phase I. It was interesting to find that the same equation form (i.e., [Equation 1](#)) that was used to describe the aggregate rate of polishing can be used to describe skid number versus TMF values in the field and to describe skid number versus polishing cycles in the laboratory.



## **CHAPTER IV – ANALYSIS OF THE MEASURED FIELD DATA**

### **INTRODUCTION**

This chapter presents the analysis and results of field measurements using a CTMeter and DFT and development of a theoretical relationship between lab and field data. During the field-testing, efforts were made to test the same part of the pavement section that was already tested by the TxDOT towed friction trailer.

Friction and macrotexture tests using a DFT and CTMeter, respectively, were conducted in the selected sections in such a way that the total number of tests was distributed uniformly within the length of the tested section (section length was about 0.5 miles for the highway).

### **SELECTION OF THE FIELD SECTIONS**

In this study, researchers selected 25 sections for friction and macrotexture evaluation. The sections were selected to cover a wide range of material types and traffic levels, and represent different road types (i.e., interstates, state highways, U.S. highways, and farm-to-market roads). Also, sections were selected that had a complete record of the construction and skid measurement in the TxDOT database. The pavement age of these sections was between two and seven years. These sections were distributed across different TxDOT districts. [Table 10](#) shows a list of the sections.

**Table 10. Measured Field Sections.**

District	County	Highway	Texas Reference Marker (TRM)	Direction	Mix Type	
Brownwood	Brown	FM 2524	TRM 340+0.4	SB	Type D	
		FM 3064	TRM 458+0.9	WB	Type D	
		SH 153	TRM 372+0.7	WB	Type D	
		US 67	TRM 570+0.4	WB	Type D	
	Eastland	IH 20	TRM 362+0.6	WB	Type D	
		SH 36	TRM 346+1.6	WB	PFC	
Houston	Conroe	IH 45	TRM 92+0.5	SB	PFC	
			TRM 93+0.1	SB		
			TRM 93-0.5	SB		
	Waller	SH 6	TRM 628+0.5	NB	PFC	
			TRM 628+1	NB		
San Antonio	Atascosa	SH 16	TRM 632+1	SB	Type C	
	Bexar	IH 35	TRM 168+0.8	NB	PFC	
			SH 16	TRM 614+0	SB	Type C
			US 90	TRM 560+1.75	EB	Type C
				TRM 570+0.4	WB	
	Wilson	US 181	TRM 518+0	SB	Novachip Type C	
	Yoakum	Victoria	US 59	TRM 632+0.5	SB	PFC
TRM 632+0.5				NB	Type C	
TRM 634+0				SB	PFC	
TRM 634+0				NB	Type C	
Wharton		US 59	TRM 560+1	SB	PFC	
			TRM 562+0	NB	Type C	
Gonzales		IH 10	TRM 636+0	WB	PFC	
			TRM 642+0	EB		

**TESTING PROGRAM**

Since DFT and CTMeter devices require traffic-control arrangements and lane closure, only the outer lane was tested. The outer lane experiences the most polishing because most truck traffic uses this lane. During tests the CTMeter and DFT devices were positioned in the left wheel path in all test sections. Six locations were tested in each section. Two locations were at the shoulder, and four locations were at the outer lane. Two DFT and six CTMeter readings were performed at each location. The DFT and CTMeter measurements were conducted at the exact same locations according to ASTM E 2157 and ASTM E 1911 procedures, respectively (ASTM, 2008). Figure 19 shows the

layout of the measurement locations. The testing was conducted between June and the end of November, when temperatures were above the water freezing temperature (above 41°F). Pavements were tested at air temperatures between 50°F and 98°F and on cloudy and sunny days. Information about construction, traffic, and skid-trailer measurements data was also collected. Since no traffic was on the shoulder, skid-resistance measurements were assumed to represent the initial skid measurements.

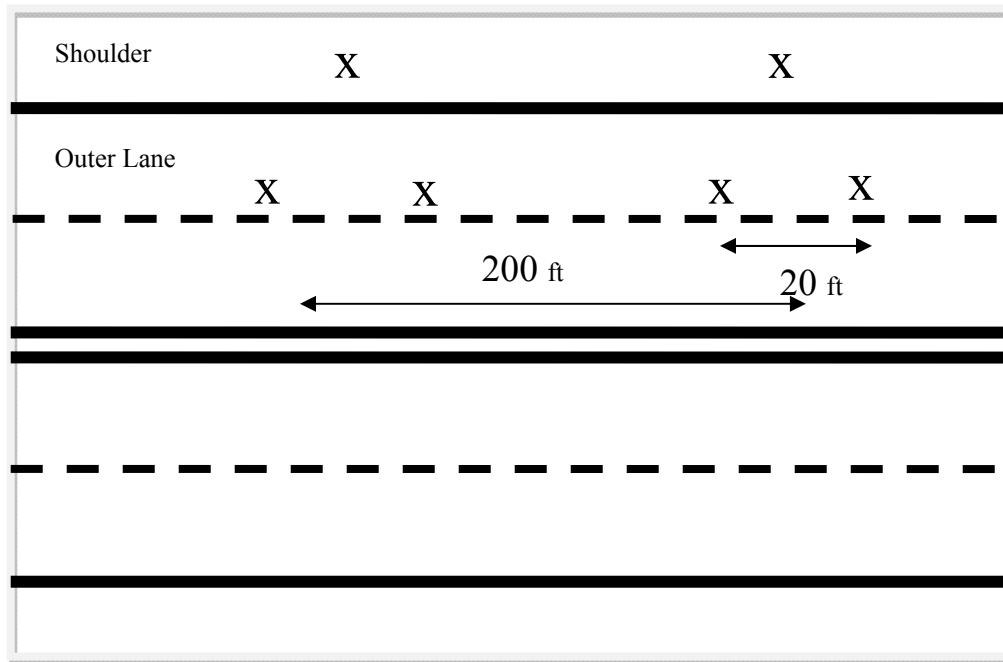


**Figure 19. Layout of the Measurement Section.**

Based on the AADT traffic information, the TMF on the test section was calculated. The following assumptions were made in calculating the TMF:

- The number of vehicles is the same in both directions (AADT was divided by two).
- The TxDOT recommended traffic-lane distribution factors, shown in [Table 11](#), are applicable for calculating the percent of traffic in the outer lane.
- All vehicle types have the same polishing effect on the road surface. This assumption was employed since there is no information on the difference in polishing effects between trucks and passenger cars.

**Table 11. Lane Distribution Factor.**

Total Number of Lanes in Both Directions	Lane Distribution Factor
Less than or equal to 4	1
6	0.7
Greater than or equal to 8	0.6

## ANALYSIS OF FIELD MEASUREMENTS

This section presents the DFT and CTMeter results and a comparison between the frictional characteristics of field sections and the laboratory slabs that were tested in Phase I of this project.

The Permanent International Association of Road Congresses (PIARC) model is developed to express the International Friction Index as a function of DFT results obtained according to ASTM E 1911 (Equation 7) and skid number obtained by a skid trailer with a smooth tire according to ASTM E 274 (Equation 8). The  $S_p$  value in these two equations is a function of mean profile depth (MPD) (see Equation 9), which is obtained using the CTMeter device:

$$IFI = 0.081 + 0.732DFT_{20} e^{\frac{-40}{S_p}} \quad (7)$$

$$IFI = 0.045 + 0.925 \times 0.01 \times SN(50) e^{\frac{20}{S_p}} \quad (8)$$

$$S_p = 14.2 + 89.7MPD \quad (9)$$

The measured range of the MPD values using the CTMeter for selected pavement sections was quite wide (from 0.32 mm (0.013 inch) to 2.22 mm (0.087 inch)). Figure 20 shows the mean MPD values for the different sections. This figure shows that the PFC mixes had higher MPD values compared with Type C and Type D mixes. Type D mixes had the lowest MPD values because the gradation used in this mix is finer than in other mixes. Higher macrotexture in PFC mixes allows water to drain faster from the tire-pavement interface and increases the skid resistance at higher speeds.



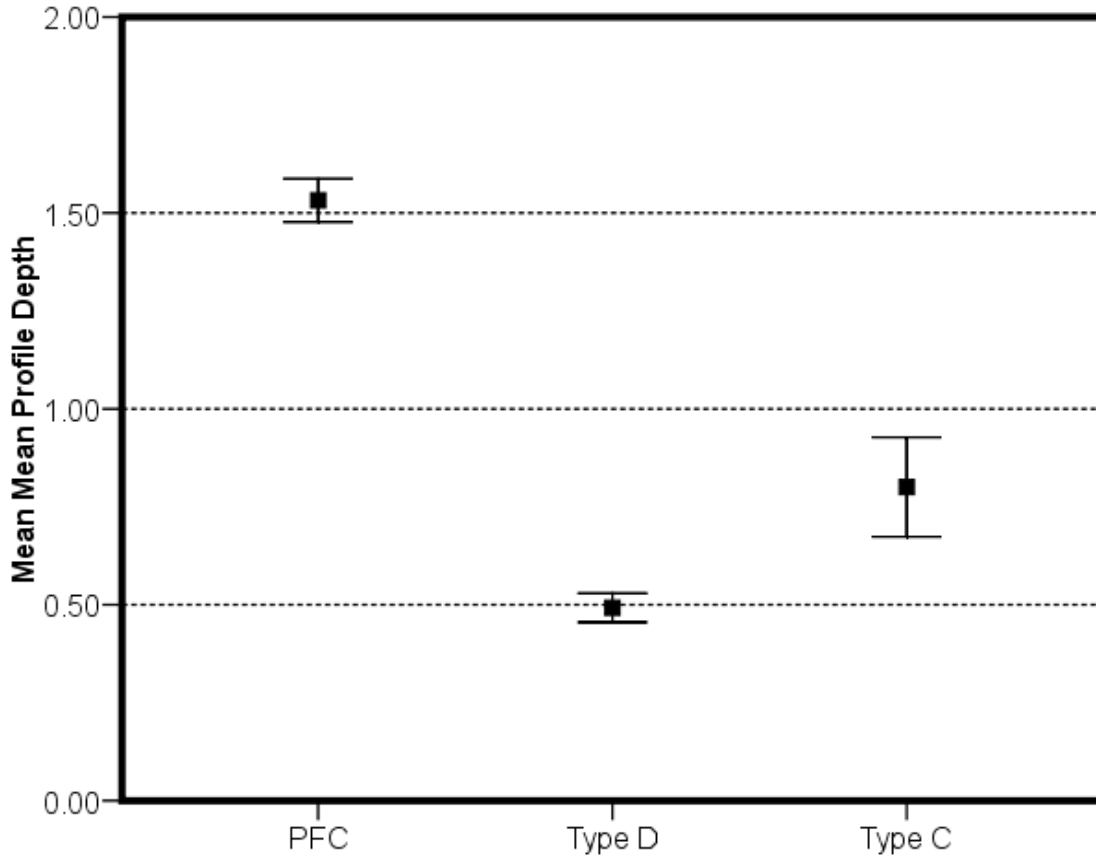


**Figure 20. Measured MPD Values for Different Mix Types.**

Table 12 shows the percent change in the measured MPD values calculated using Equation 10:

$$\text{Change in MPD} = \frac{(\text{MPD at Shoulder} - \text{MPD at Traffic Lane}) \times \text{TMF}}{1000} \quad (10)$$

This table shows that PFC mixes lost their initial macrotexture over time. However, PFC mixes composed of hard aggregates such as aggregate I lost their macrotexture less than others. Aggregate R and the combination of aggregates S and M resisted losing macrotexture reasonably well. The PFC mixture with aggregate F, which is a limestone, lost its initial macrotexture the most. It is interesting to note that macrotexture of dense-graded mixes such as Type C and Type D generally increased with time, possibly due to removal of asphalt and fine aggregate particles from the surface, thus leaving the aggregate surface exposed instead of being covered with asphalt film.

Removal of fine aggregates affects the macrotexture more in dense-graded mixtures than in open-graded mixtures since the latter has little fine aggregate in it.

**Table 12. Percent Change in MPD Values in Terms of TMF.**

Mix Type	PFC	Type D	Type C
Aggregate Type			
Aggregate M + Aggregate S	1.1%		
Aggregate M	3.6%	0.0%	
Aggregate T	3.6%		
Aggregate I	0.1%		-4.1*%
Aggregate H	2.9%		
Aggregate F	4.7%		
Aggregate R	0.6%		-0.7%
Aggregate N		1.8%	
Aggregate U		-6.1%	
Aggregate K			-2.5%

Notes: Negative values show an increase in MPD. The values were multiplied by a factor of 1000 to ease comparison for the reader.

Figure 21 shows the mean  $DFT_{20}$  for the different aggregate types used in constructing pavement sections. Dynamic friction measured at 12.4 mph measured by a DFT is a measure of microtexture (Hall et al., 2006). This figure shows that the initial microtexture level depends on aggregate type, and some aggregate such as aggregates N, H, and R provided very high microtexture initially, whereas other aggregate such as aggregate M had a low initial microtexture. Table 13 shows the microtexture change, which is similar to Equation 10 but which uses  $DFT_{20}$  instead of MPD. Among the PFC mixes, aggregate M had the highest microtexture loss among aggregates – about 7 percent for each 1000 TMF. This observation confirms findings from Phase I of this study since measurements of friction on asphalt-mix slabs with aggregate M had the lowest microtexture and highest rate of texture change. Aggregate F lost about 3 percent of its initial texture for each 1000 TMF and is the second in the list. Aggregate R and a combination of aggregates M and S maintained their initial microtexture with less than 1 percent loss for each 1000 TMF. Other aggregates such as aggregates I, T, and H preserved their initial texture with less than 2 percent texture loss for each 1000 TMF.

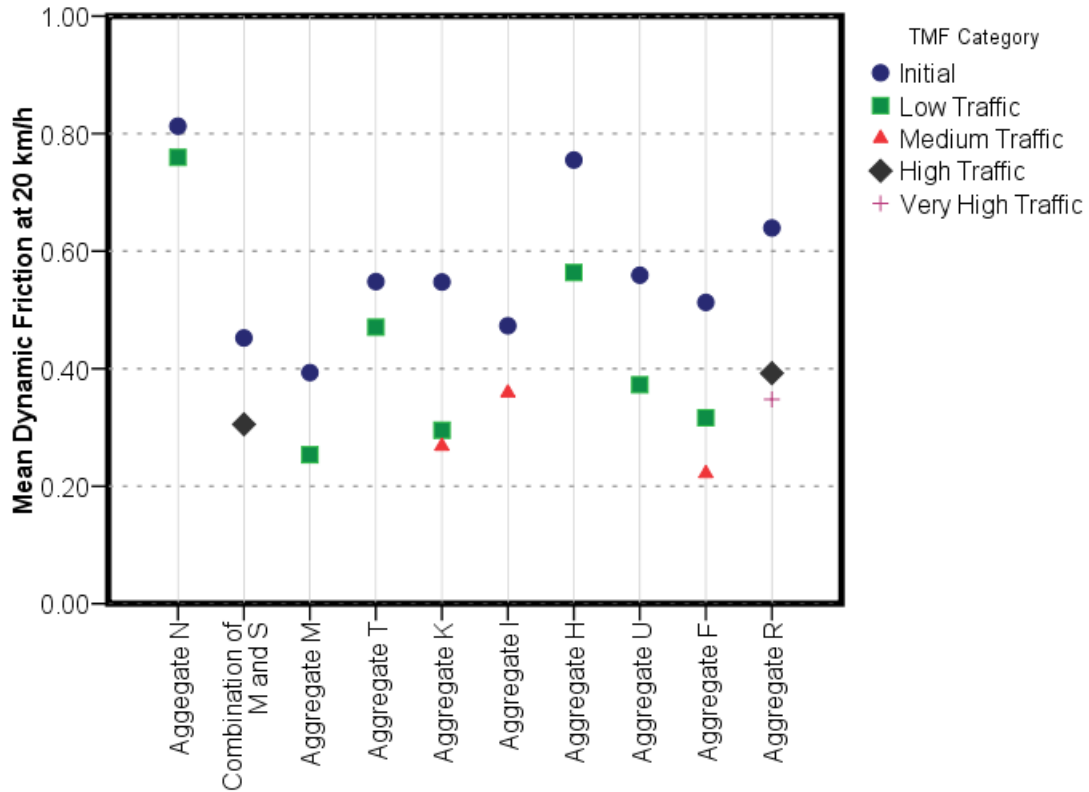


Figure 21. Mean Dynamic Friction at 12.4 mph.

Table 13. Percent Change in DFT<sub>20</sub> Values in Terms of 1000 TMF.

Aggregate Type	PFC	Type D	Type C
Aggregate M + Aggregate S	0.6%		
Aggregate M	6.8%	3.0%	
Aggregate T	1.7%		
Aggregate I	1.7%		
Aggregate H	1.8%		
Aggregate F	2.9%		11.3%
Aggregate R	0.4%		1.2%
Aggregate N		1.1%	
Aggregate U		10.8%	
Aggregate K			10.9%

Note: The values were multiplied by a factor of 1000 to ease comparison for the reader.

In the Type D mix, aggregate U lost its initial texture by 11 percent for each 1000 TMF. Aggregate M functioned better in Type D than in the PFC mix and lost about 3 percent of its initial texture for each 1000 TMF. Aggregate N was the most resistant aggregate in this group with only 1.1 percent texture loss.

In Type C mixes, aggregates F and K were the most sensitive aggregates to traffic loading and lost about 11 percent of their initial texture for each 1000 TMF. In the laboratory and field-data analysis, aggregate K had poor frictional characteristics. Aggregate R preserved its initial microtexture with only 1.2 percent loss. It is worthwhile to mention that aggregate F lost 11 percent in Type C mixes, whereas the percent loss for this aggregate was about 3 percent in the PFC mix. This observation is in agreement with skid-trailer data analysis in which it was shown that this aggregate had satisfactory frictional performance in the PFC mix with a skid number of about 30 for a high traffic level, whereas it did not have good frictional characteristics with a skid number of around 20 in the Type C mix.

Figure 22 shows very high scatter in the relationship between measured skid number and MPD. This relationship can be significantly improved by dividing the data into mixture categories as shown in Figure 23. In this figure the measured skid number does not correlate to MPD values in PFC mixes. Type C and Type D mixes correlate well to a change in MPD. Thus, a change in macrotexture will directly affect the measured SN values in these two mixes. It should be noted that these are dense-graded mixes and have low MPD values (about 0.5 mm (0.02 inch)).

Figure 24 shows that there is high scatter in the relationship between dynamic friction at 12.4 mph and measured skid value. Separate plots for all mixtures are depicted in Figure 25. These plots show the SN value to have some correlation to the dynamic friction measured at 12.4 mph. These results indicate that mixes with larger aggregate sizes (PFC and Type C) were more dependent on the DFT, which is an indication of microtexture. From comparing these results with the results depicted in Figure 23, researchers realized that the measured skid number was more affected by macrotexture in mixes with smaller aggregate size (Type C and Type D), whereas skid number was slightly more affected by microtexture for mixes with large aggregates. The correlation of measured dynamic friction at 50 mph and measured skid number was studied. Figure 26

shows that there is a strong correlation between the measured dynamic friction at 50 mph and measured skid numbers for Type C and Type D mixes, whereas there was almost no correlation between dynamic friction at 50 mph and measured skid numbers for PFC mixes.

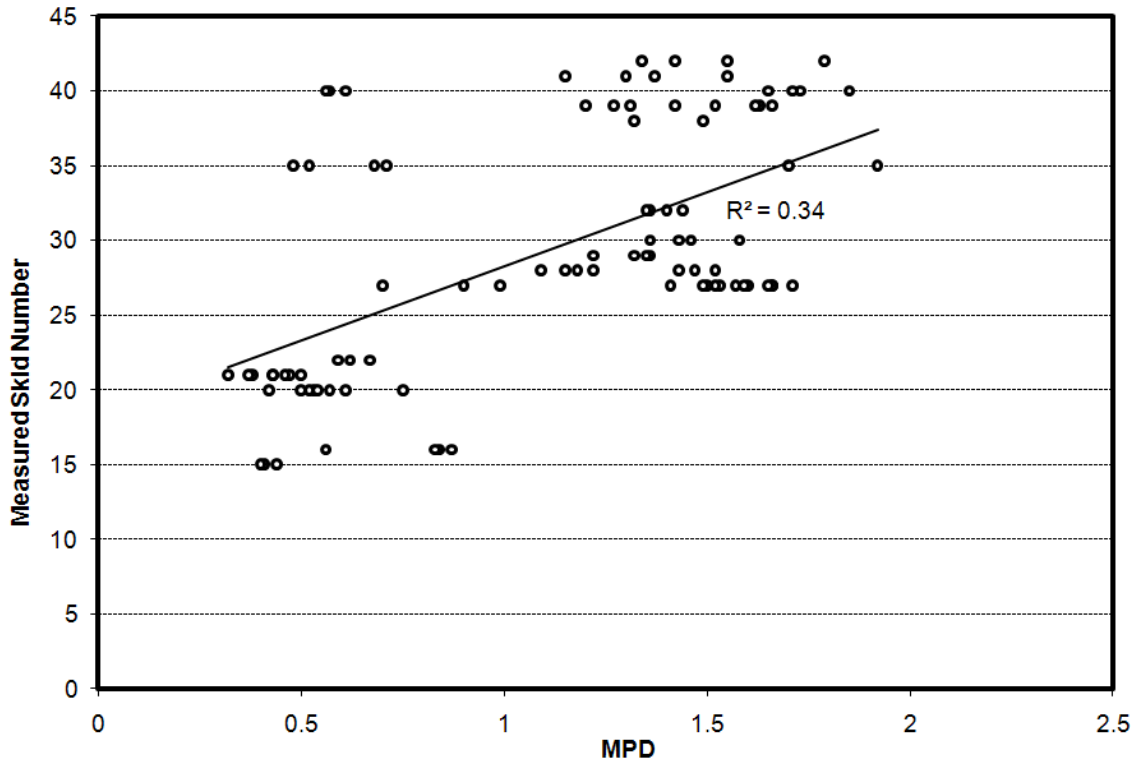
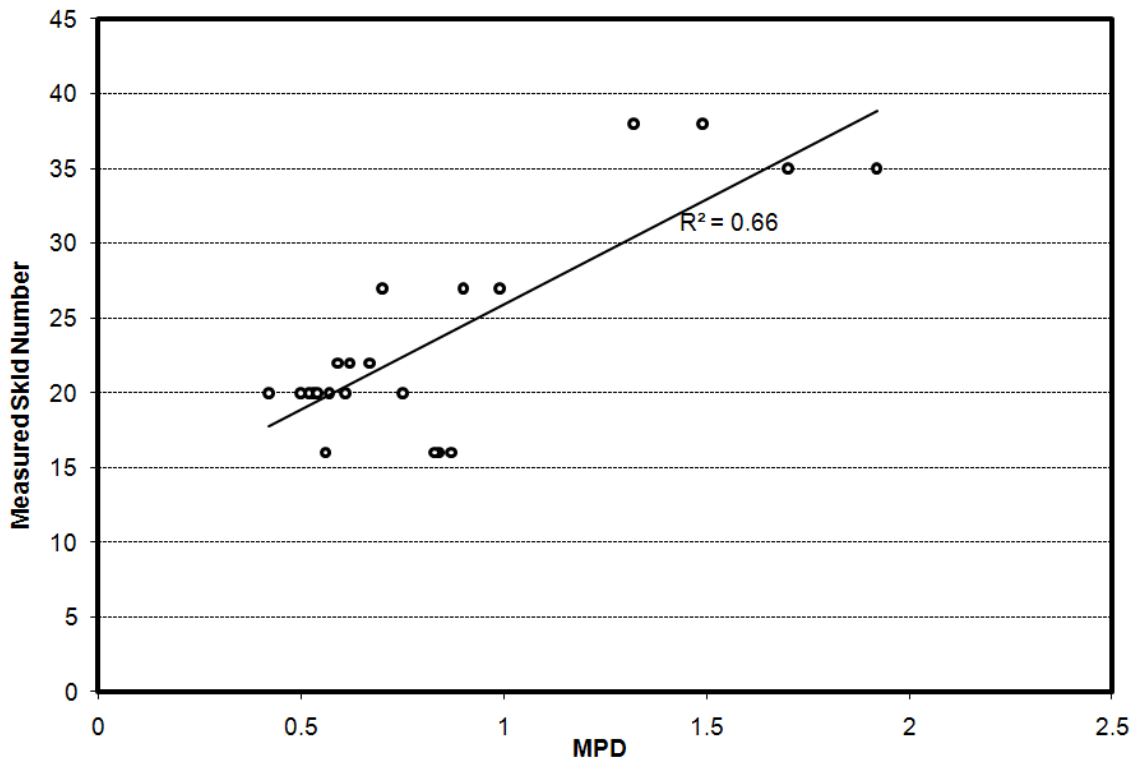
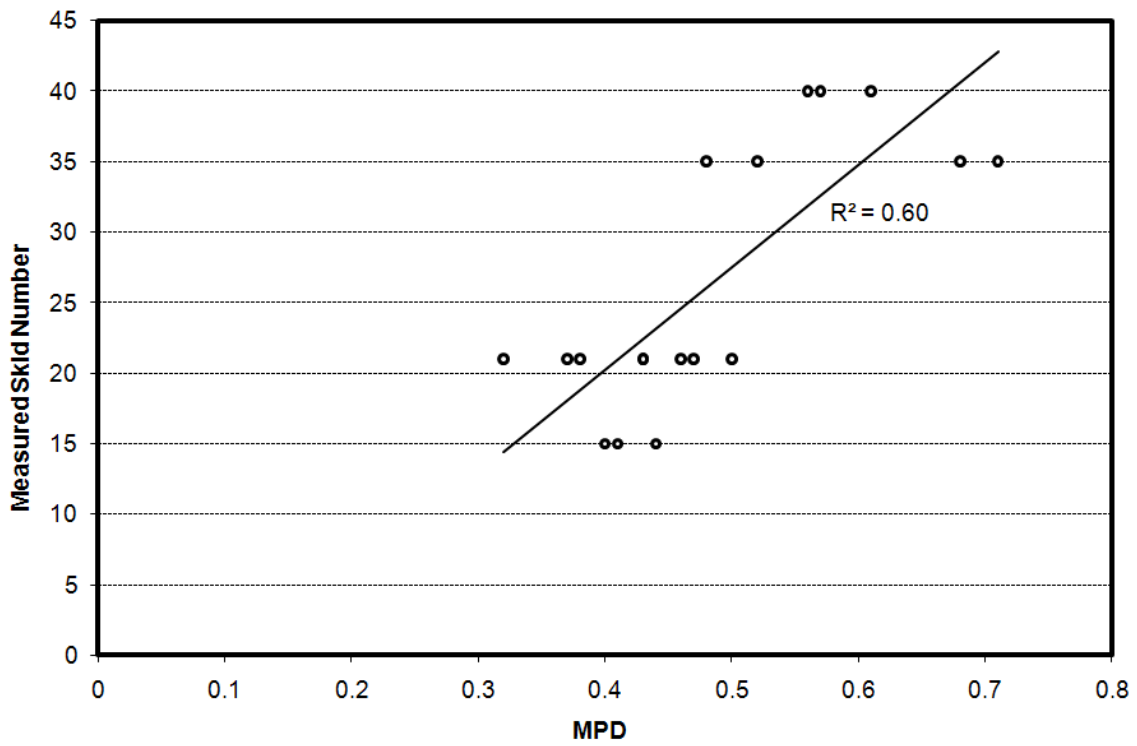


Figure 22. Mean Profile Depth versus Measured Skid Number.



(a) Type C



(b) Type D

**Figure 23. Mean Profile Depth versus Measured Skid Number**

for Different Mix Types.

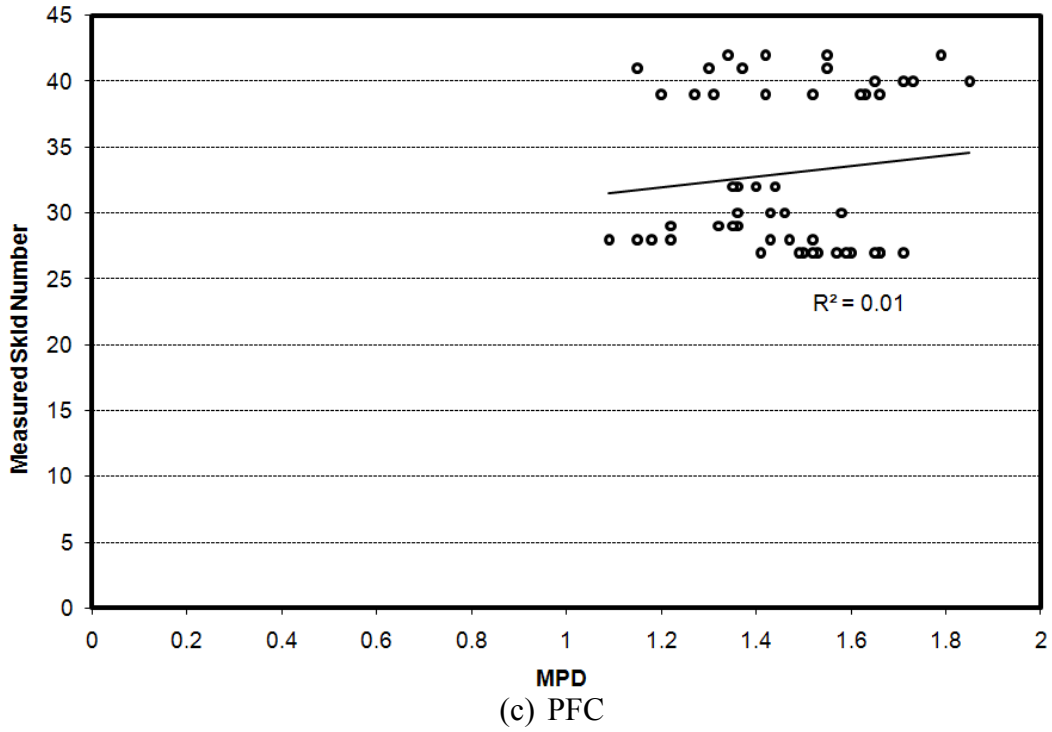


Figure 23. Mean Profile Depth versus Measured Skid Number for Different Mix Types (Continued).

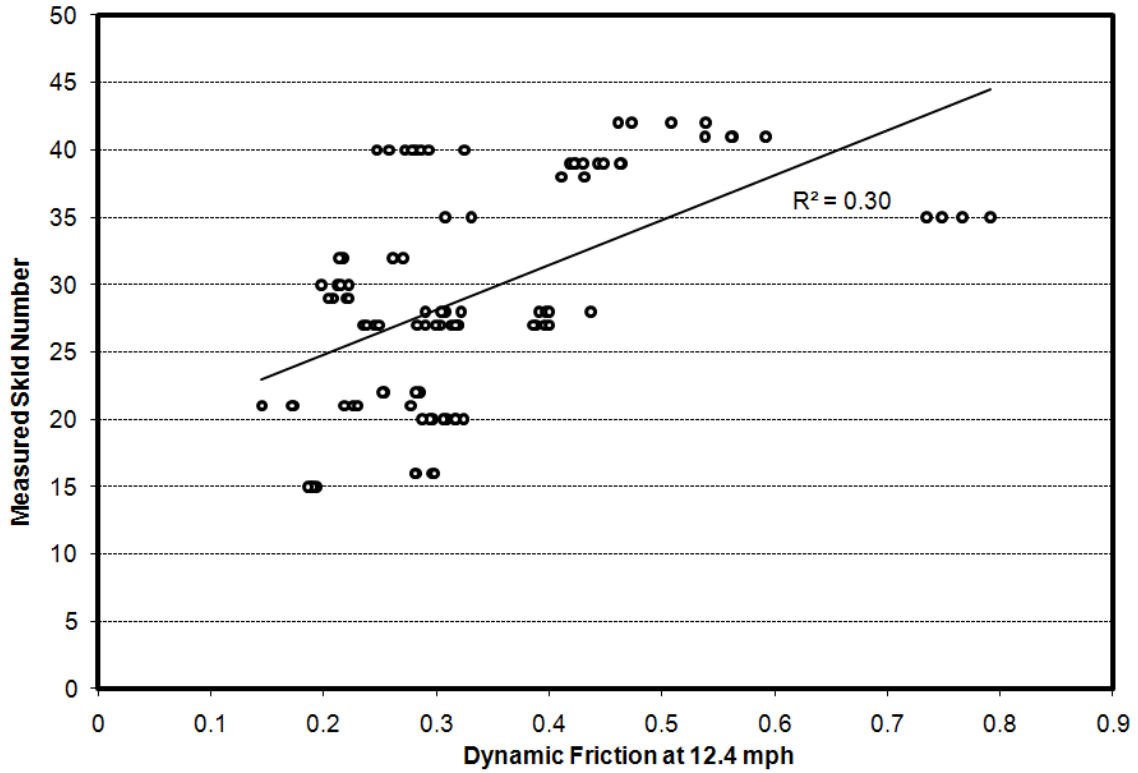
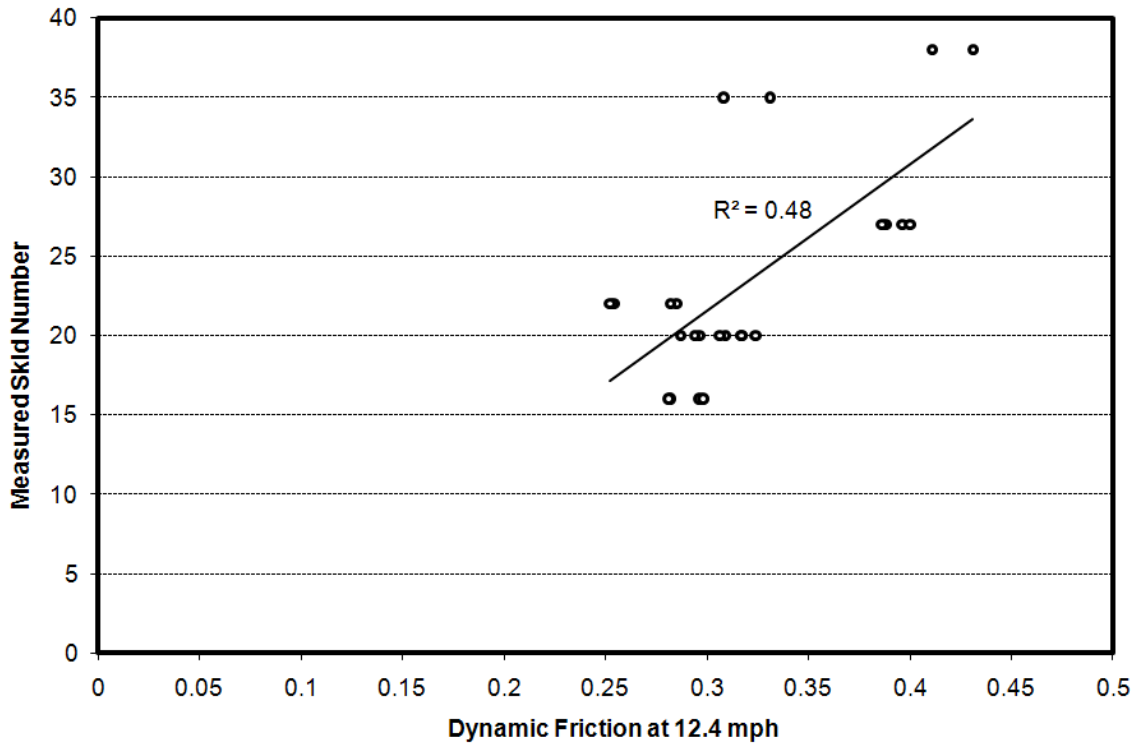
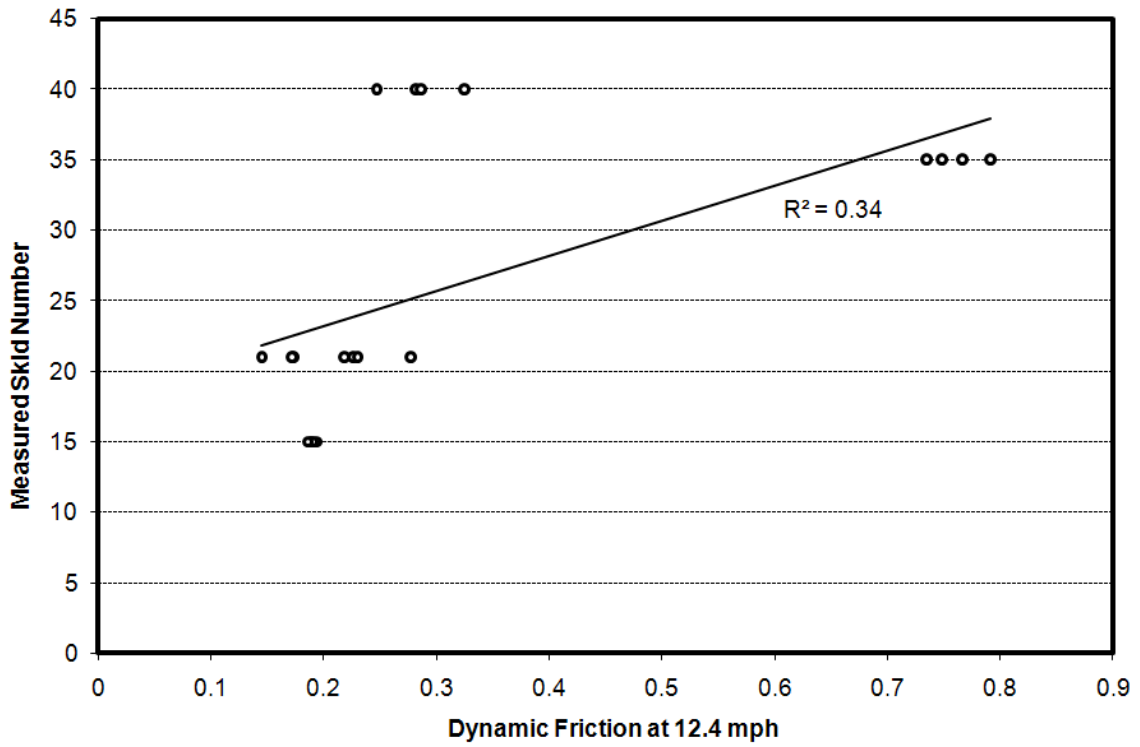


Figure 24. Dynamic Friction at 12.4 mph versus Measured Skid Number.



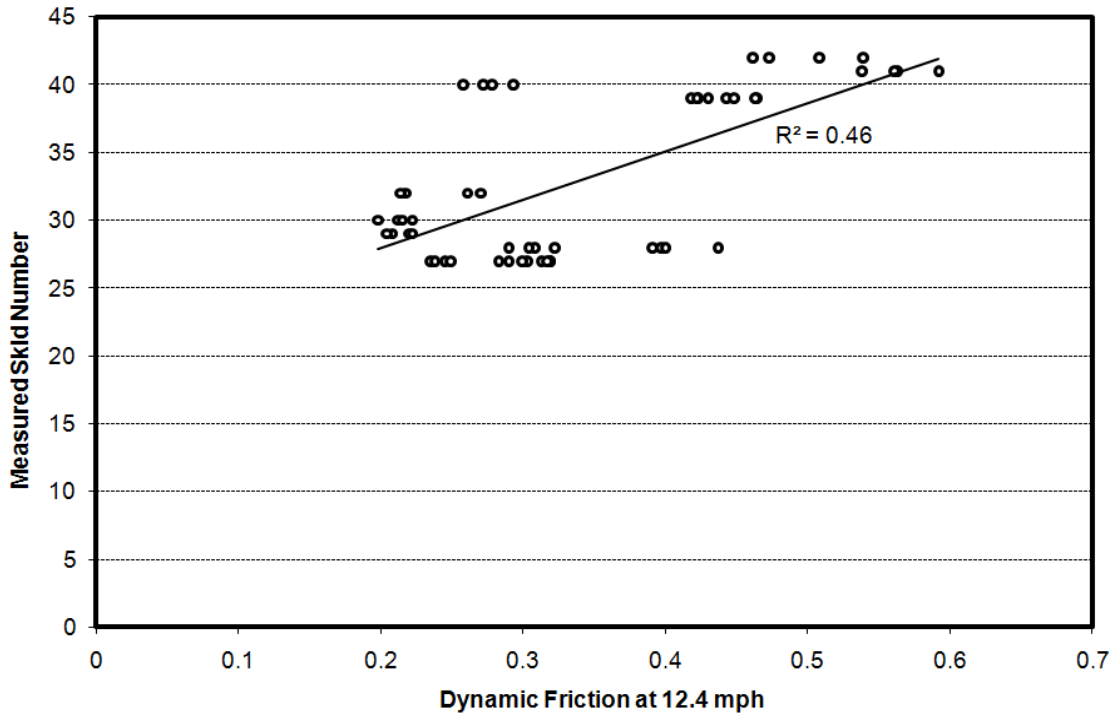
(a) Type C



(b) Type D

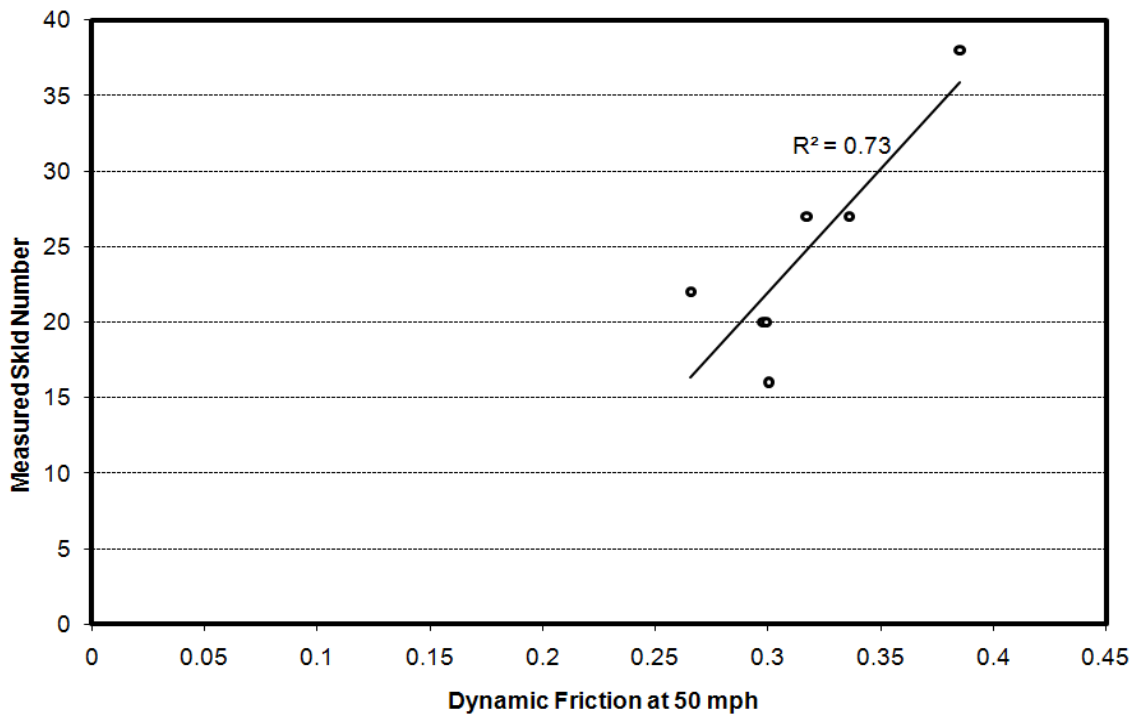
**Figure 25. Dynamic Friction at 12.4 mph versus Measured Skid Number for Different Mix Types.**





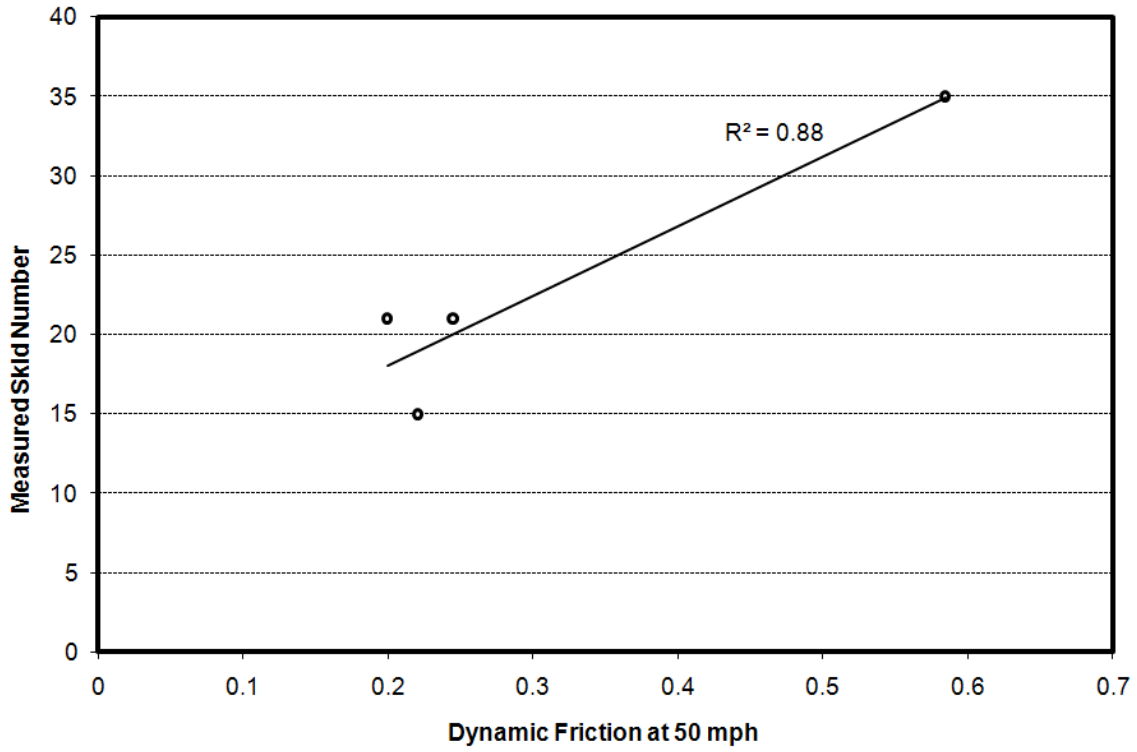
(c) PFC

**Figure 25. Dynamic Friction at 12.4 mph versus Measured Skid Number for Different Mix Types (Continued).**

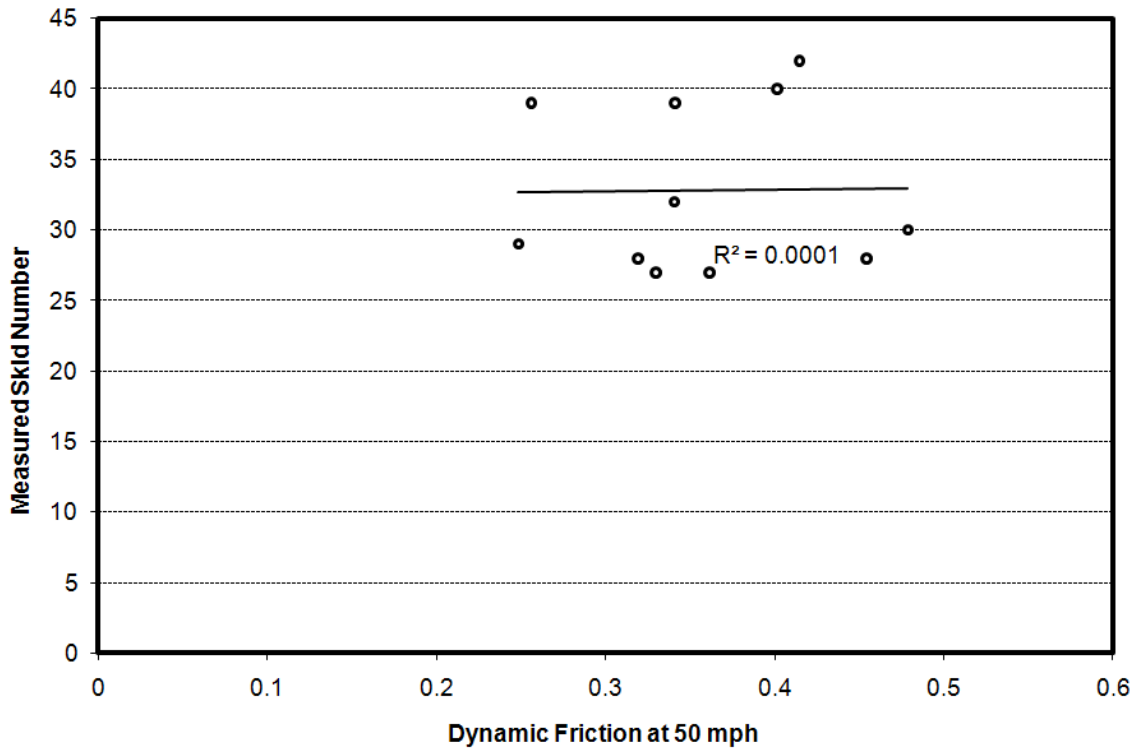


(a) Type C

**Figure 26. Dynamic Friction at 50 mph versus Measured Skid Number for Different Mix Types.**



(b) Type D



(c) PFC

**Figure 26. Dynamic Friction at 12.4 mph versus Measured Skid Number for Different Mix Types (Continued).**

## **RELATIONSHIP OF FIELD MEASUREMENTS TO AGGREGATE PROPERTIES**

In order to study the effect of each aggregate characteristic on the skid resistance, a simple regression analysis was performed. R-square and significance of the regression coefficients at 5 percent significance level were tabulated in [Table 14](#) and [15](#). The significance of each aggregate parameter was analyzed under two broad categories: mixture types ([Table 14](#)) and traffic level ([Table 15](#)). These analyses were done based on the values measured by a CTMeter and DFT in the field.

The results of analysis showed all material properties are significant factors in explaining the variation of the Type C mix except texture measurements by AIMS before and after Micro-Deval, and percent change in angularity before and after Micro-Deval. The angularity after Micro-Deval, percent weight loss in Micro-Deval, Los Angeles abrasion percent weight loss, and angularity before Micro-Deval have the highest coefficient of determination, respectively. These results suggest that the frictional performance of the Type C mix is more affected by aggregate shape characteristics than aggregate surface characteristics. Aggregate angularity is more effective in providing the friction of Type C mixes than their texture.

[Table 14](#) also shows that all aggregate characteristics are significant in explaining the variation of frictional properties of PFC mixes over time. Among all aggregate characteristics, texture after Micro-Deval, texture before Micro-Deval, angularity before Micro-Deval, and polish-stone value (PSV) are the most important ones. These results suggest both aggregate shape and surface characteristics are significant in explaining the variation of frictional properties of PFC. The comparison between coefficients of determination shows that the aggregate texture is more important than the angularity and therefore controls the frictional characteristics of PFC mixes, generally.

Unfortunately, there are not enough data points, at this moment, to determine the significant aggregate characteristics in explaining the frictional characteristics of the Type D mix.

[Table 15](#) shows the effect of aggregate properties in different traffic levels. It can be realized that the initial pavement friction could only be explained by aggregate texture before and after Micro-Deval. Moreover, other aggregate properties do not contribute in

providing the initial skid resistance. All aggregate properties are significant in explaining the variation of skid number in low traffic except LA percent weight loss, percent angularity change before and after Micro-Deval, and angularity after Micro-Deval. Unlike low traffic level, all aggregate properties become significant in medium traffic level except percent angularity change before and after Micro-Deval. Comparably, aggregate texture indices become more significant in medium traffic level due to the higher coefficient of determination.

Table 16 shows the R-square and significance of different aggregate properties in explaining the rate of change in skid number (measured by TxDOT skid trailers). This table indicates that only the percent change in texture before and after Micro-Deval measured by AIMS and polished-stone values are significant factors. It is worthwhile to know that the change in texture and polished-stone value was shown to be significant in the laboratory phase of this study.

**Table 14. R-Square and Significance of Different Aggregate Properties for Different Mixes.**

Property	LA % Wt. Loss		PSV		Mg. % Wt. Loss		MD % Wt. Loss		Angularity BMD		Percent Angularity Change BMD and AMD		Texture BMD		% Texture Change BMD and AMD		Texture AMD			
	R <sup>2</sup>	Sig.	R <sup>2</sup>	Sig.	R <sup>2</sup>	Sig.	R <sup>2</sup>	Sig.	R <sup>2</sup>	Sig.	R <sup>2</sup>	Sig.	R <sup>2</sup>	Sig.	R <sup>2</sup>	Sig.	R <sup>2</sup>	Sig.		
Mix Type	0.35	Yes	0.03	No	0.23	Yes	0.37	Yes	0.32	Yes	0.001	No	0.38	Yes	0.07	No	0.13	Yes	0.08	No
Type C	NA*	NA	NA	NA	0.14	Yes	NA	NA	NA	NA	NA	NA	NA	NA	NA	NA	NA	NA	NA	NA
Type D	0.08	Yes	0.22	Yes	0.03	No	0.06	Yes	0.24	Yes	0.09	Yes	0.01	No	0.26	Yes	0.19	Yes	0.27	Yes
PFC	0.001	No	0.11	Yes	0.16	Yes	0.28	Yes	0.44	Yes	0.04	No	0.1	Yes	0.19	Yes	0.28	Yes	0.16	Yes

\* NA = not enough data points.

Note: Before Micro-Deval (BMD), after Micro-Deval (AMD).

**Table 15. R-Square and Significance of Different Aggregate Properties for Different Traffic Level.**

Property	LA % Wt. Loss		PSV		Mg. % Wt. Loss		MD % Wt. Loss		Angularity BMD		% Angularity Change BMD and AMD		Texture BMD		% Texture Change BMD and AMD		Texture AMD			
	R <sup>2</sup>	Sig.	R <sup>2</sup>	Sig.	R <sup>2</sup>	Sig.	R <sup>2</sup>	Sig.	R <sup>2</sup>	Sig.	R <sup>2</sup>	Sig.	R <sup>2</sup>	Sig.	R <sup>2</sup>	Sig.	R <sup>2</sup>	Sig.		
Traffic Level	0.001	No	0.05	No	0.03	No	0.04	No	0.05	No	0.001	No	0.02	No	0.28	Yes	0.08	No	0.27	Yes
Initial	0.06	No	0.31	Yes	0.13	Yes	0.16	Yes	0.34	Yes	0.04	No	0.03	No	0.24	Yes	0.4	Yes	0.31	Yes
Low	0.48	Yes	0.58	Yes	0.9	Yes	0.85	Yes	0.92	Yes	0.001	No	0.77	Yes	0.76	Yes	0.83	Yes	0.89	Yes
Medium	0.11	No	NA	NA	NA	NA	NA	NA	NA	NA	NA	NA	NA	NA	NA	NA	NA	NA	NA	NA
High																				

**Table 16. R-Square and Significance of Different Aggregate Properties to Explain SN Change.**

Property	LA % Wt. Loss		PSV		Mg. % Wt. Loss		MD % Wt. Loss		Angularity BMD		% Angularity Change BMD and AMD		Texture BMD		% Texture Change BMD and AMD		Texture AMD			
	R <sup>2</sup>	Sig.	R <sup>2</sup>	Sig.	R <sup>2</sup>	Sig.	R <sup>2</sup>	Sig.	R <sup>2</sup>	Sig.	R <sup>2</sup>	Sig.	R <sup>2</sup>	Sig.	R <sup>2</sup>	Sig.	R <sup>2</sup>	Sig.		
% SN Change	0.01	No	0.24	Yes	0.03	No	0.03	No	0.002	No	0.15	No	0.14	No	0.01	No	0.32	Yes	0.001	No

## RELATIONSHIP BETWEEN FIELD MEASUREMENTS AND LABORATORY MEASUREMENTS

In the interest of finding the relationship between measured skid resistance by skid trailer and DFT/CTMeter combination, the PIARC procedure for finding the IFI value was used, and the IFI values were calculated using the DFT, CTMeter, and skid number using [Equations 7 to 9](#).

In principle, [Equations 7 and 8](#) should give the same value for the IFI. Therefore, the IFI calculated from [Equation 7](#) can be substituted in [Equation 8](#) to find the SN(50). As illustrated in [Figure 27](#), the measured value of SN by skid trailer is greater than the calculated value using the PIARC equation. The R-squared value for the relation is 0.72 and is comparable to the R-squared value of 0.61 reported by [Kowalski \(2007\)](#) for such a relationship. There are two main factors that could explain this difference between SN(50) obtained from [Equation 8](#) and measured values. The first is the propagation of errors. Error is present in the PIARC regression equation and is propagated during the mathematical manipulation required to backcalculate the SN. The second factor is experimental error. Each friction-measuring device will generate some experimental error due to the equipment design and human factors. The presence of these errors could account for the differences between the measured and calculated SN.

Based on the relationship between measured and calculated SN values, [Equation 8](#) was modified to account for the difference between calculated and measured skid numbers. [Equation 11](#) shows the modified form of [Equation 8](#) to predict the field skid number:

$$SN(50) = 5.135 + 128.486(IFI - 0.045) e^{\frac{-20}{S_p}} \quad (11)$$

Where,

$$S_p = 14.2 + 89.7MPD \quad (9)$$

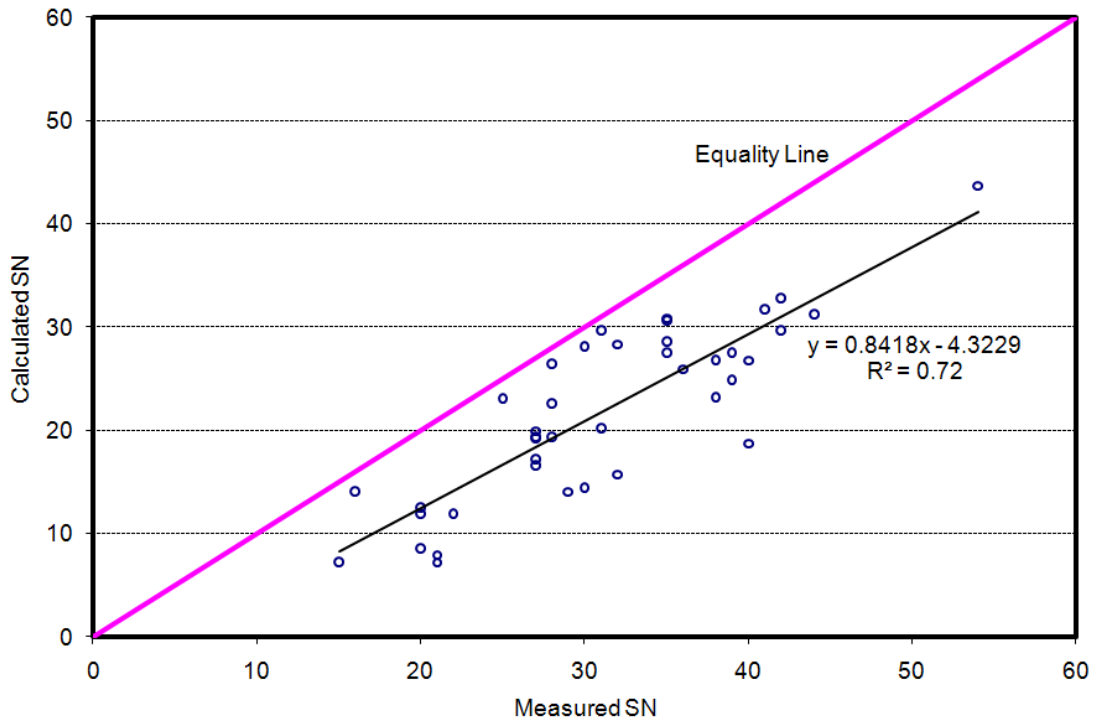


**Figure 27. Measured Skid Number versus Calculated Skid Number Using PIARC Equation.**

Figure 28 shows the measured and calculated skid number values using the modified PIARC equation (Equation 11). It is evident that the calculated and measured values are relatively close, and the modified equation can be used to predict the measured skid number.

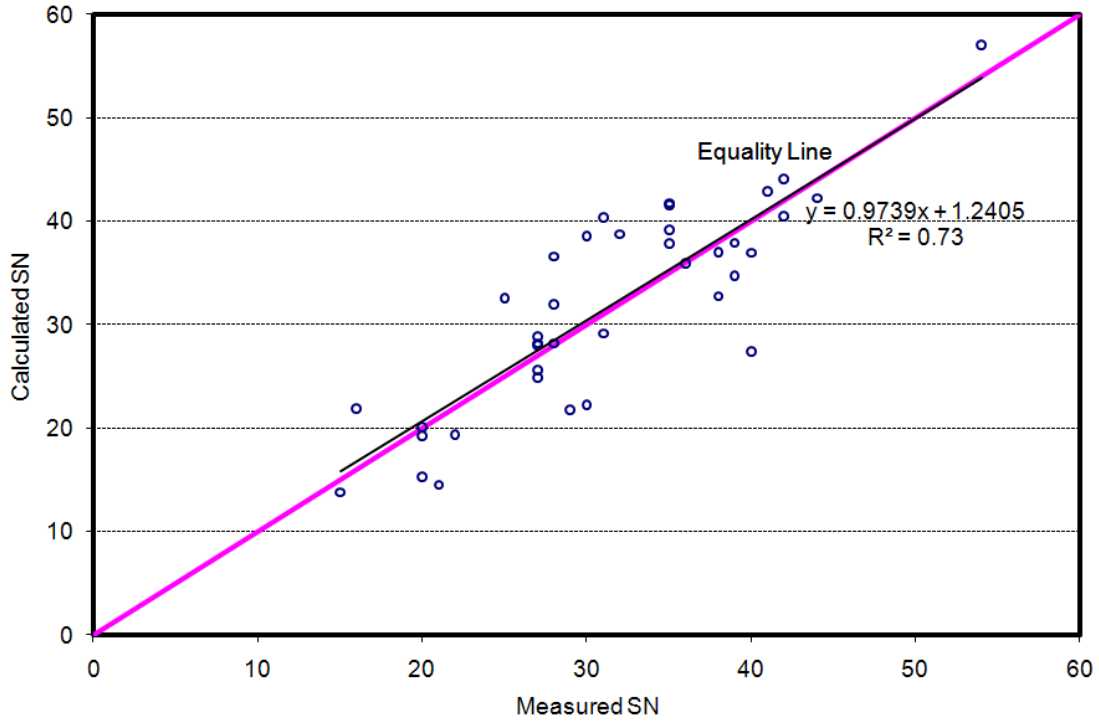


**Figure 28. Measured Skid Number versus Calculated Skid Number Using Modified PIARC Equation.**

$$SN(50) = 5.135 + 128.486(IFI - 0.045) e^{\frac{-20}{S_p}} \quad (11)$$

**SUMMARY OF THE RESULTS OF THE FIELD MEASUREMENT**

During Phase II of TxDOT Project 0-5627, 25 road sections were selected for testing using DFT and CTMeter devices. The selection covered a wide range of material-type and traffic conditions, and more importantly it included some of the mixtures that were tested in the laboratory in Phase I of this study. CTMeter and DFT devices were used to take measurements from the farthest outside lane on the inner wheel path and from the shoulder.

The results of the macrotexture measurements by the CTMeter showed that the PFC mixes had higher MPD values compared to that of Type C and Type D mixes. Type D had the lowest MPD values due to its finer gradation. The results also indicated that the macrotexture of PFC mixes decreased over time, and the rate of decrease in



macrotexture depended on aggregate type. The rate of decrease for some aggregates such as aggregates I and R was low – less than 1 percent for each 1000 TMF. However, the rate of decrease in skid number for other aggregate types such as aggregate F was high (about 5 percent). The macrotexture of Type C and Type D mixes was found to increase to some extent over time possibly due to removal of asphalt and fine aggregates from the surface. The removal of asphalt, however, occurs during the very early stage of pavement service life. The rate of increase in macrotexture was also found to be dependent on aggregate type. This trend had been observed in the laboratory for Type D mixes.

The  $DFT_{20}$  values, which are an indication of microtexture, showed that the initial pavement microtexture depended on aggregate type. For instance, the level of microtexture provided by aggregate H mixtures was different from that provided by aggregate M mixtures. Moreover, mixes containing aggregates H and R had higher initial microtexture compared to that containing other aggregate types such as aggregate M. Results of the analysis showed PFC mixes containing aggregate M had the highest rate of polishing. This finding conforms to the results of the laboratory study in which it was shown that aggregate M had the highest polishing rate and lowest friction level in PFC mixes. Aggregate sources such as aggregate R had a low polishing rate compared with other aggregates. In Type C mixes, aggregates F and K had a considerably high polishing rate (about 10 to 12 percent for each 1000 TMF). Aggregate R had an acceptable polishing rate of about 1.2 percent per each 1000 TMF. In Type D mixes, aggregate U had the highest rate of polishing with about 11 percent texture loss per 1000 TMF, whereas aggregate N had the lowest polishing rate of 1.1 percent.

The results showed there was a correlation between the MPD values and measured skid number in Type C and Type D mixes. However, no correlation was found between MPD values and measured skid number in PFC mixes. The results also indicate that there was a fair correlation between  $DFT_{20}$  and measured skid number for all mixes. Furthermore, a fairly strong correlation was found between the results of the measured dynamic friction at 50 mph (80 km/h) and measured skid number for Type C and Type D mixes. Similar to MPD, no correlation was found between the measured dynamic friction at 50 mph (80 km/h) and skid number for PFC mixes. The results of this analysis suggest

the measured skid number is affected by macrotexture in dense-graded mixes, whereas microtexture governs the frictional performance of PFC mixes.

The results of the analysis of the measured skid number and aggregate characteristics indicate that the frictional performance including terminal condition and rate of change in skid number for both Type C and PFC mixes in low and high traffic levels is affected by aggregate shape properties such as texture change before and after Micro-Deval, angularity after Micro-Deval, and angularity before Micro-Deval.

The skid number backcalculated from field measurements using the PIARC equation was less than the measured skid number. A relatively strong relationship, however, was found between the calculated and measured skid number. The PIARC equation was modified to improve the prediction of the SN value from the measurements obtained using a DFT and CTMeter.

## **CHAPTER V – A SYSTEM FOR PREDICTING SKID NUMBER OF ASPHALT PAVEMENTS**

### **INTRODUCTION**

The results of Phases I and II of this project have shown that the influence of a certain aggregate type on mixture skid resistance depends on the mixture design. Therefore, a method is presented in this chapter to predict the skid number of asphalt pavements as a function of traffic based on aggregate characteristics and mixture design. This system will be very valuable to select the optimum combination of aggregate type and mixture design in order to achieve the desired level of skid resistance. Some of the equations presented earlier in this report will also be included in this chapter in order to present a complete procedure for predicting the field skid number without having the reader referred to equations presented in various parts of this report.

### **DEVELOPMENT OF SYSTEM FOR PREDICTING SKID NUMBER**

As discussed in Chapter II of this report, a method was developed in Phase I for predicting the IFI as a function of the number of loading cycles (N) using the National Center for Asphalt Technology (NCAT) polishing device. As shown in [Equations 12 to 16](#), the parameters of the relationship of IFI versus N are dependent on aggregate texture measurements using AIMS before and after polishing in the Micro-Deval and on aggregate gradation.

$$\text{IFI (N)} = a_{\text{mix}} + b_{\text{mix}} \cdot \exp(-c_{\text{mix}} \cdot N) \quad (12)$$

$$F(x; \kappa, \lambda) = 1 - \exp[-(x/\lambda)^\kappa] \quad (13)$$

$$a_{\text{mix}} = \frac{18.422 + \lambda}{118.936 - 0.0013 \times (\text{AMD})^2} \quad (14)$$

$$a_{\text{mix}} + b_{\text{mix}} = 0.4984 \ln(5.656 \times 10^{-4} (a_{\text{agg}} + b_{\text{agg}})) + 5.846 \times 10^{-2} \lambda - 4.985 \times 10^{-2} \kappa + 0.8619 \quad (15)$$

$$c_{mix} = 0.765 \cdot e^{\left( \frac{-7.297 \cdot 10^{-2}}{c_{agg}} \right)} \quad (16)$$

where:

$a_{mix}$ : terminal IFI value for the mix,

$a_{mix} + b_{mix}$ : initial IFI value for the mix,

$c_{mix}$ : rate of change in IFI for the mix,

AMD: aggregate texture after Micro-Deval,

$a_{agg} + b_{agg}$ : aggregate initial texture using texture model,

$c_{agg}$ : aggregate texture rate of change using texture model,

k-value: shape factor of Weibull distribution used to describe aggregate gradation,  
and

$\lambda$ -value: scale factor of Weibull distribution used to describe aggregate gradation.

The  $a_{agg} + b_{agg}$  and  $c_{agg}$  are obtained from measuring aggregate texture after several time intervals of polishing in the Micro-Deval. It would be desirable to be able to predict these values from only two texture measurements of aggregates using AIMS before Micro-Deval and after Micro-Deval polishing for 105 minutes, which is the standard time currently used by TxDOT. For this purpose, nonlinear regression analysis was used to examine the possibility of predicting  $a_{agg}$ ,  $b_{agg}$ , and  $c_{agg}$  from AMD and BMD texture. A total of nine aggregate samples were used in this regression analysis. Moreover, these samples were part of a database of AIMS measurements of aggregates in Phase I plus three other aggregate sources. It was found that the following equations can be used to determine the texture model coefficients:

$$a_{agg} + b_{agg} = 0.9848BMD + 3.1735 \quad R^2 = 0.99 \quad (17)$$

$$c_{agg} = 0.0217 \left( \frac{ARI}{TL} \right)^{-0.131} \quad R^2 = 0.66 \quad (18)$$

$$ARI = \frac{\left( \frac{AMD}{BMD} \right)^2}{\left( 1 - \left( \frac{AMD}{BMD} \right)^2 \right)} \quad (18a)$$

$$TL = \left( \frac{BMD - AMD}{BMD} \right) \quad (18b)$$

where:

ARI: Aggregate Roughness Index and

TL: texture loss.

Equations 17 and 18 were used along with Equations 14 and 16 to calculate the polishing rate ( $c_{mix}$ ) and the terminal friction value ( $a_{mix}$ ) of an asphalt mixture. Next, a statistical correlation analysis was performed using SPSS 15, a statistical software, to check whether these two parameters were correlated. If the parameters were correlated, then cross correlation would occur in any comparison and lower the validity of the results. Two statistical indices were used to determine the degree of correlation between the two parameters: coefficient of determination ( $R^2$ -value) and significance of correlation (p-value). The  $R^2$ -value described the degree of linear relationship among variables, and the p-value described the statistical significance of the regression equation. A low p-value (below  $\alpha = 0.05$ ) indicates high confidence in the regression equation (parameters are correlated). An  $R^2$ -value between 0.5 and 0.8 implies fair correlation between the two parameters, while an  $R^2$ -value below 0.5 implies a low correlation. The correlation analysis resulted in an  $R^2$ -value of 0.002 and a p-value of 0.1, implying that the polishing rate ( $c_{mix}$ ) and the terminal friction value ( $a_{mix}$ ) are not correlated and are statistically independent parameters. This finding justifies the selection of these two parameters for comparing the frictional characteristics of different mixes.

The next step is to determine the gradation parameters ( $\lambda$  and  $\kappa$ ) for different gradations used in the state of Texas. Researchers included eight mix designs in this analysis as shown in Table 17. The gradation boundaries for these mix designs were extracted from a TxDOT specification manual, and the cumulative Weibull distribution was used to describe the percent passing as a function of aggregate size using nonlinear regression analysis and Solver in Microsoft® Excel®. It is worthwhile to know that for most cases the coefficient of determination of the regression was more than 0.95.

**Table 17. Calculated Scale and Shape Factors for Different Mixes.**

Mix Design	Scale Parameter $\lambda$	Shape Parameter $\kappa$
Type C	5.605	0.830
Type D	4.052	0.864
PFC	10.054	3.954
SMA-D	9.201	1.494
Crack Attenuating Mixture (CAM)	3.168	1.000
SMA-C	9.431	1.276
CMHB-C	8.578	1.077
CMHB-F	5.574	1.415

Finally the results of the lab measurements and field measurements were used to develop a relationship between lab polishing and field polishing in terms of number of polishing cycle in the lab (N) and TMF. The proposed equation has a high R-square value and can be used to estimate the variation of the IFI in the field in terms of TMF.

Equation 12 was developed for predicting the IFI values in a mixture as a function of N (number of cycles in terms of 1000 cycles in the NCAT polishing device). In this study, analysis was conducted to correlate N to TMF. Based on the measured  $DFT_{20}$  values and macrotexture measurements by the CTMeter, the IFI values were determined using Equations 19 and 20 for each road section:

$$IFI = 0.081 + 0.732DFT_{20} e^{\frac{-40}{S_p}} \quad (19)$$

$$S_p = 14.2 + 89.7MPD \quad (20)$$

The IFI values were determined for sections with different TMFs. Then, Equation 12 was used to determine the N value that would give the same IFI that is calculated using Equation 19. It should be mentioned that the coefficients  $a_{mix}$ ,  $b_{mix}$ , and  $c_{mix}$  that were substituted in Equation 12 were for the same mixtures that were tested in the field. A statistical analysis was performed to determine the outliers that were removed from the analysis. Researchers performed a nonlinear regression analysis to find the relationship between TMF and number of polishing cycles (N) as in Equation 21 and Figure 29.

$$TMF = \frac{A}{1 + B e^{-CN}} \quad (21)$$

where A, B, and C are regression coefficients and have the values of 35600, 15.96, and  $4.78 \times 10^{-2}$ , respectively. N in [equation 21](#) is the number of polishing cycles.

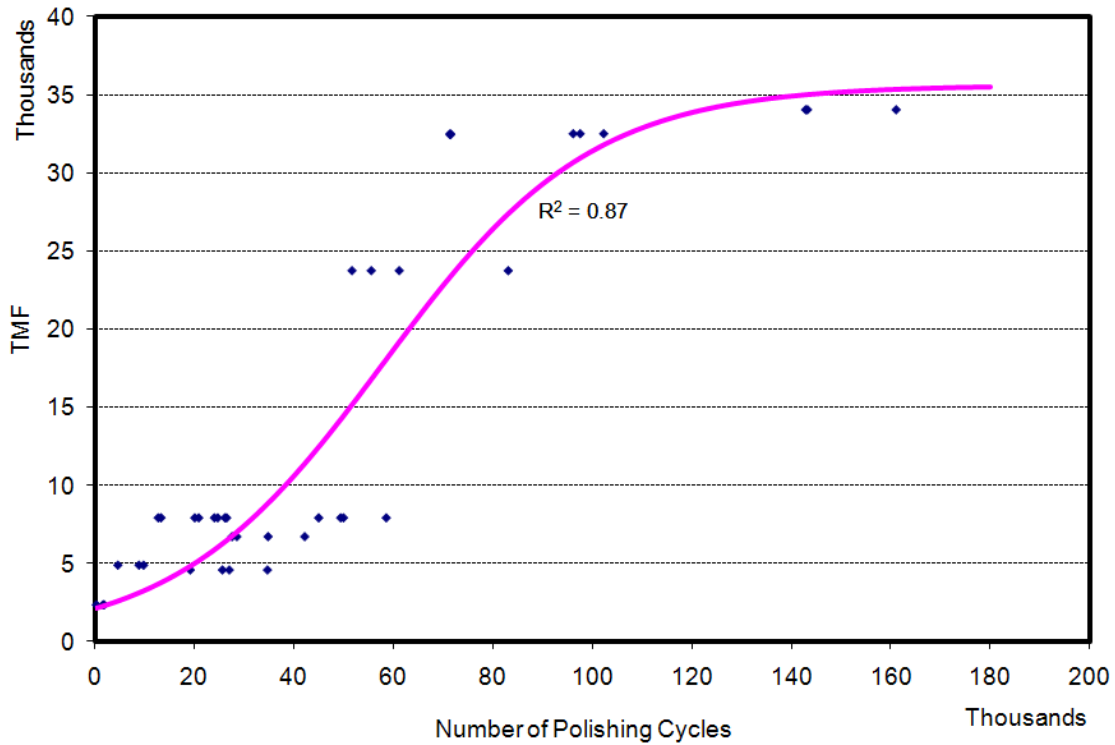


**Figure 29. TMF versus Number of Polishing Cycles.**

The last step in the analysis is to predict the SN value given the IFI. For this purpose, [Equation 22](#) is used:

$$SN(50) = 5.135 + 128.486(IFI - 0.045)e^{\frac{-20}{S_p}} \quad (22)$$

However, [Equation 22](#) includes the  $S_p$  value, which is a function of MPD as follows:

$$S_p = 14.2 + 89.7MPD \quad (23)$$

It is known that macrotexture, which is represented by MPD, is a function primarily of mixture gradation. Therefore, nonlinear regression analysis was conducted to determine MPD as a function of the gradation parameters  $\lambda$  and  $\kappa$ . The best correlation found between measured MPD and these gradation parameters is shown in Equation 24 and in Figure 30. Figure 30 shows the relationship between measured and calculated MPD values.

$$MPD = 1.8 - \frac{3.041}{\lambda} - \frac{0.382}{\kappa^2} \quad (24)$$

$$R^2 = 0.90$$

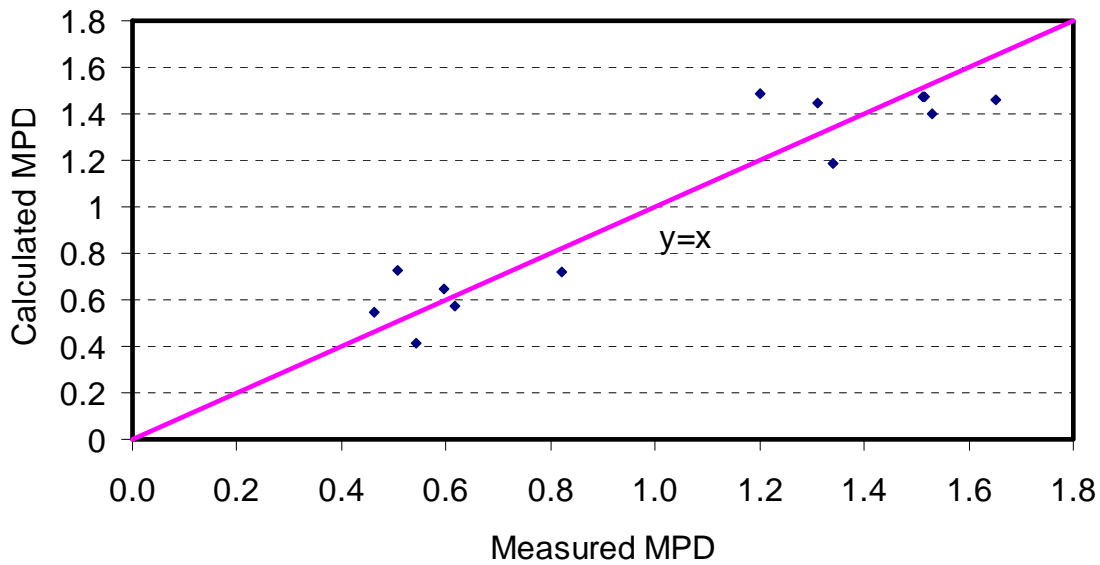


**Figure 30. Relationship between Measured and Calculated MPD Values.**

### **SENSITIVITY ANALYSIS OF PREDICTION SYSTEM**

The sensitivity analysis was conducted using several aggregate types and mixture designs. Aggregates were selected to represent a wide spectrum of texture values representing the minimum, maximum, first quartile, second quartile, and third quartile of terminal texture ( $a_{agg}$ ) and polishing rate ( $c_{agg}$ ) as shown in Tables 18 and 19, respectively.



**Table 18. Selected Aggregates Based on Terminal Texture.**

Sample	Quartile	Terminal Texture $a_{mix}$	Polish Rate	Material Type	Material Group
1	Minimum	26.67	0.0233	Crushed Limestone (LS)	3. LS-Dolomites
2	1st	56.34	0.0094	Crushed Limestone	3. LS-Dolomites
3	Median	72.46	0.0145	Crushed Limestone	3. LS-Dolomites
4	3rd	92.43	0.0049	Crushed Sandstone	2. Sandstone
5	Maximum	216.34	0.0298	Crushed Limestone Rock Asphalt	6. Miscellaneous

**Table 19. Selected Aggregates Based on Polishing Rate.**

Sample	Quartile	Polish Rate $c_{mix}$	Terminal Texture $a_{mix}$	Aggregate Type	TxDOT Aggregate Group
6	Minimum	0.0001	84.55	Crushed Siliceous & LS Gravel	4. Gravels
7	1st	0.0182	216.34	Crushed LS Rock Asphalt	6. Miscellaneous
8	Median	0.0227	109.58	Crushed Limestone	3. LS-Dolomites
9	3rd	0.0253	69.17	Crushed Limestone	3. LS-Dolomites
10	Maximum	0.0364	279.45	Crushed LS Rock Asphalt	6. Miscellaneous

Using [Equations 14, 16, 17, and 18](#), the terminal friction value and polish rate were calculated. [Figure 31](#) shows the terminal friction values for different aggregates and mix designs.

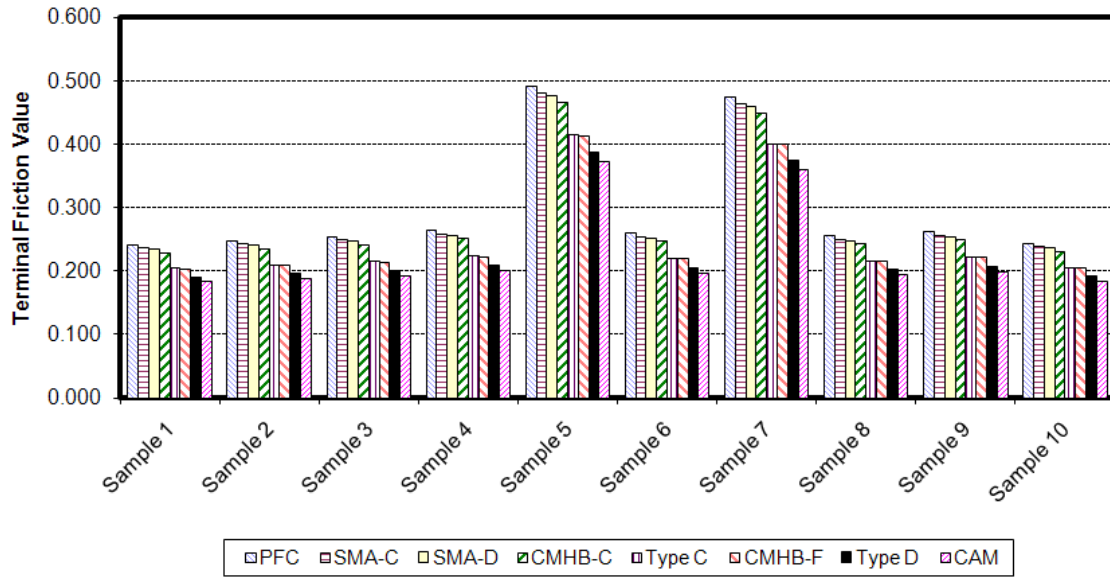


**Figure 31. Terminal Friction Values for Different Aggregates and Mix Designs.**

It is evident the PFC mixes have the highest terminal friction values. SMA-C, SMA-D, and CMHB-C are the next mixes in the list. The terminal polish values of the Type C and CHMB-F mixes are almost the same. The Type D mix and CAM mix have the lowest terminal friction among all mixes. Among the aggregates, samples 7 and 5 have the highest terminal friction values. These values can be attributed to the high texture index after Micro-Deval. The difference among other aggregates is not significant. [Figure 32](#) shows the polishing rate for different aggregates.

Given polishing rate and initial and terminal friction values, the IFI can be calculated using [Equations 12](#) and [21](#) as a function of TMF and plotted. For instance, [Figures 33](#) and [34](#) illustrate the IFI values for samples 1 and 8. The SN values were calculated using [Equation 22](#) and [23](#) as a function of TMF and plotted in [Figures 35](#) and [36](#). These figures indicate the model is able to predict the variation of skid number as a function of traffic. Moreover, in both aggregates the PFC mix has the highest terminal skid number, and Type C and CHMB-F mixes have the lowest terminal friction. SMA mixes containing these aggregate types provide the highest level of friction.

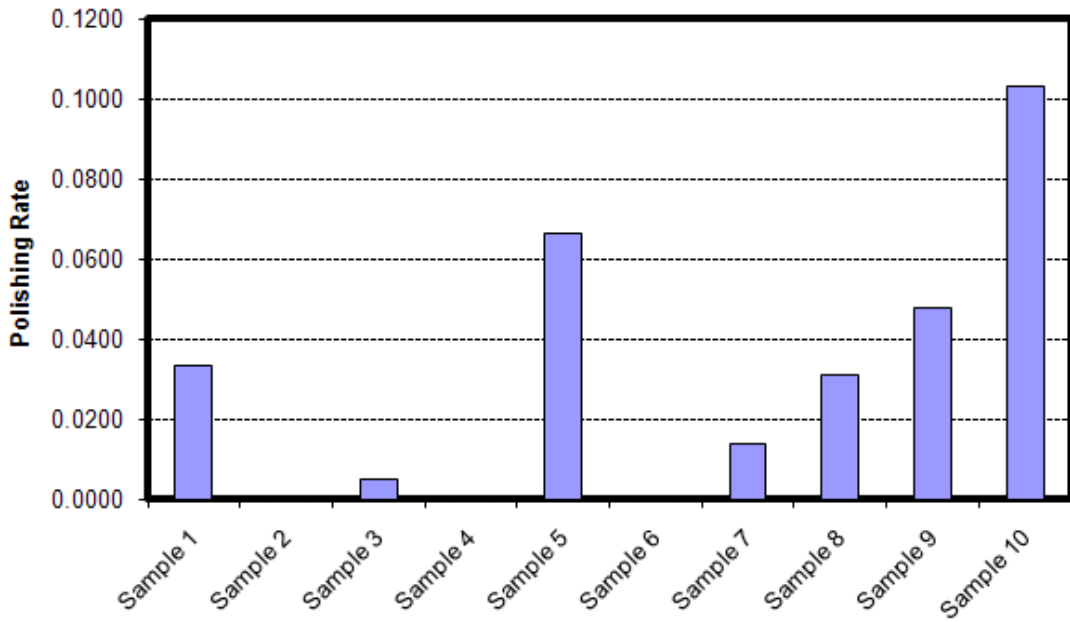


Figure 32. Polishing Rate for Different Aggregates.

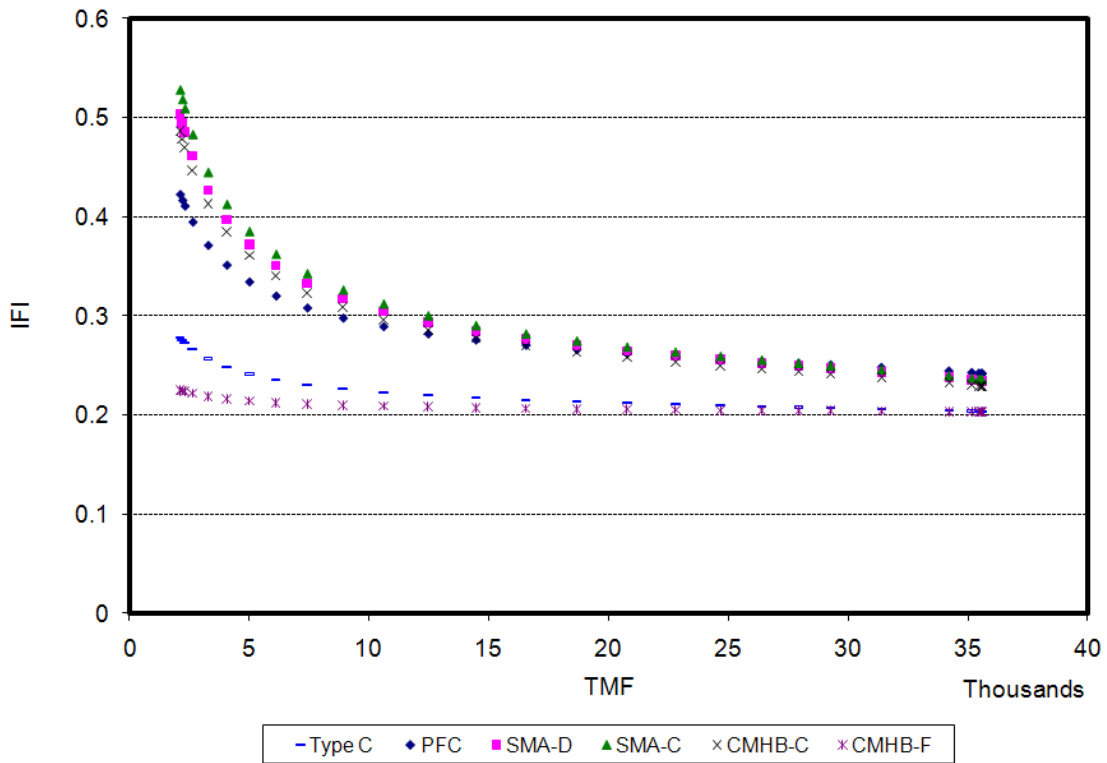


Figure 33. IFI Values as a Function of TMF for Sample 1.

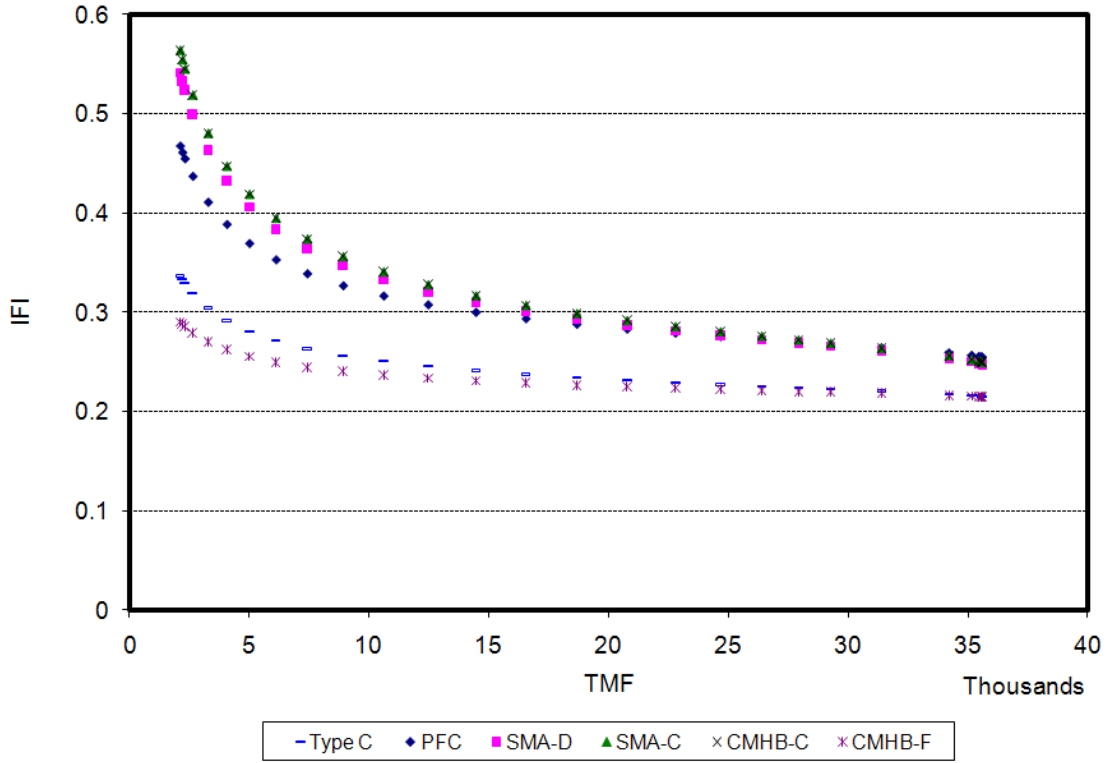


Figure 34. IFI Values as a Function of TMF for Sample 8.

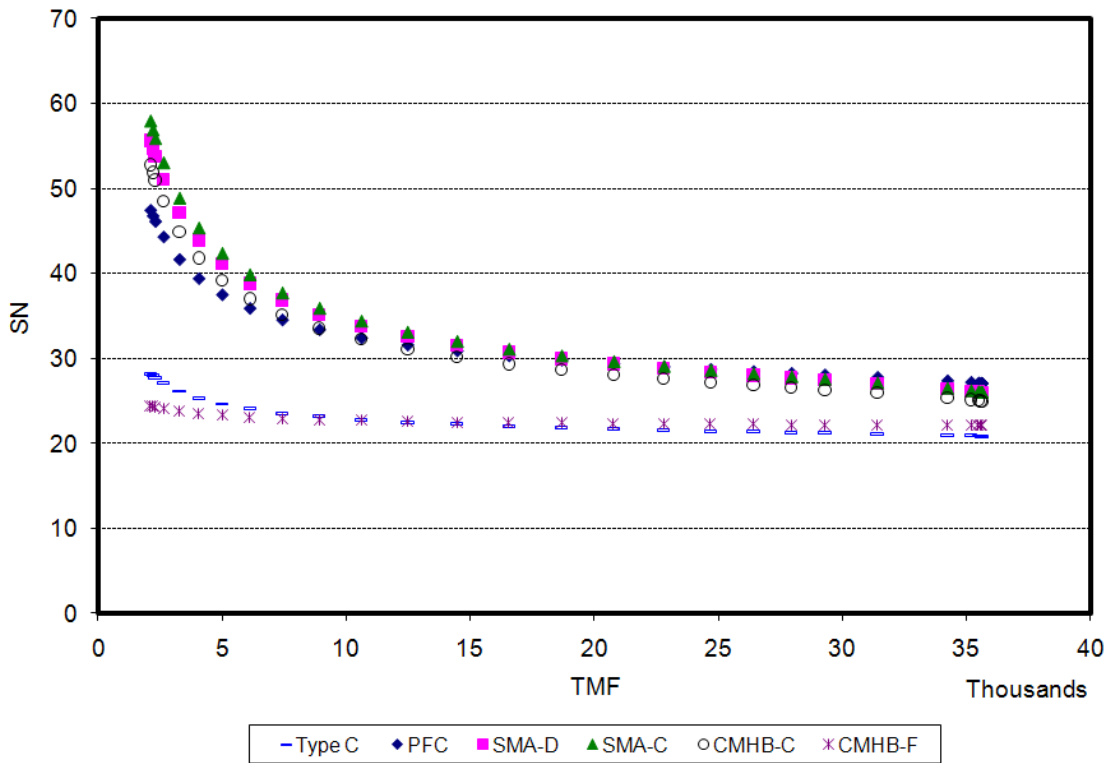
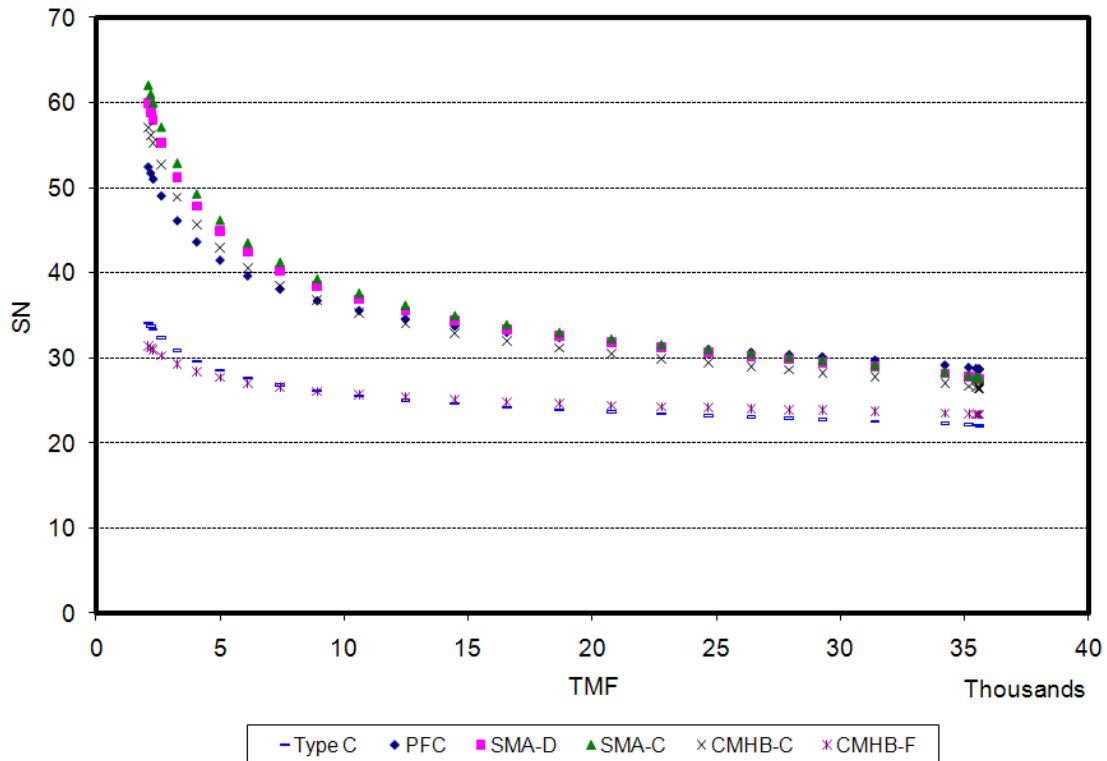


Figure 35. SN Values as a Function of TMF for Sample 1.



**Figure 36. SN Values as a Function of TMF for Sample 8.**

## RECOMMENDED SYSTEM FOR PREDICTING SKID NUMBER

This chapter presented a system for predicting the skid number of asphalt mixtures. This system consists of the following steps:

- Measure aggregate texture using AIMS before Micro-Deval.
- Measure aggregate texture using AIMS after Micro-Deval.
- Calculate  $a_{agg} + b_{agg}$  using Equation 17.
- Calculate the Aggregate Roughness Index (ARI) using Equation 18a.
- Calculate texture loss (TL) using Equation 18b.
- Calculate  $c_{agg}$  using Equation 18.
- Determine the gradation parameters ( $\lambda$  and  $\kappa$ ) from Table 17 or by fitting the cumulative Weibull function (Equation 2) to the gradation curve.
- Calculate  $a_{mix}$  using Equation 14.
- Calculate  $a_{mix} + b_{mix}$  using Equation 15.
- Calculate  $c_{mix}$  using Equation 16.

- Calculate MPD using [Equation 24](#).
- Calculate  $S_p$  using [Equation 23](#).
- Calculate IFI as a function of N using [Equation 12](#).
- Calculate TMF in terms of N using [Equation 21](#).
- Calculate SN using [Equation 22](#).

## **CHAPTER VI – CONCLUSIONS AND RECOMMENDATIONS**

### **SUMMARY OF THE RESULTS OF THE FIELD-DATA ANALYSIS**

In Phase I of this study, researchers conducted laboratory experiments to determine the influence of aggregate properties and mixture design on the skid resistance of asphalt-mixture slabs. The work in Phase I has led to the development of a method to predict International Friction Index values as a function of aggregate texture measured using AIMS and aggregate gradation.

In Phase II of the project, skid data from different road sections with different material and mix types were collected. Traffic, mix type, and aggregate type were the main factors that were considered in the analysis of the measured skid numbers. To facilitate comparing different road categories in their current service life, a single factor, denoted the traffic multiplication factor, was defined. This factor is the product of AADT in the design lane times years in service divided by 1000. This factor considers both traffic level and years of operation.

The results of the data analysis showed the measured skid number decreases as TMF increases. The measured skid numbers had less variation at higher TMF levels. This phenomenon could be attributed to mixtures reaching close to terminal skid condition, which is associated with aggregates approaching their equilibrium (or terminal) state of texture after a high number of polishing or loading cycles.

Skid numbers measured by TxDOT skid trailers were considered for four types of surfaces (surface treatment grade 3, surface treatment grade 4, PFC, and Type C). The analyses of these skid numbers showed that surface treatments generally had higher skid numbers than Type C, which is a conventional dense-graded mix. Additionally, PFC mixes exhibited better skid resistance than Type C mixes and surface-treatment mixes. The results showed the PFC mixes had the lowest variation in skid number, while surface-treatment mixes had the highest variability.

The effect of aggregate type was studied, and the results showed that there was high interaction between aggregate performance, the mix type in which the aggregate is used, and traffic level. In general, it is hard to classify aggregates without specifying

mixture type and traffic levels. Some aggregates performed poorly in certain mixture types, while their performance was acceptable in other mixture types.

For the most part, the results of the field-data analysis were in agreement with the laboratory findings in Phase I. It was interesting to find that the same equation form (i.e., [Equation 1](#)) that was used to describe aggregate rate of polishing can be used to describe skid number versus TMF values in the field and to describe skid number versus polishing cycles in the laboratory.

In Phase II, 25 road sections were selected for testing using DFT and CTMeter devices. The selection covered a wide range of material types and traffic conditions, and more importantly included some of the mixtures that were tested in the laboratory in Phase I of this study. CTMeter and DFT devices were used to take measurements on the left wheel path of the farthest outside lane and on the shoulder.

The results of the macrotexture measurements by the CTMeter showed that the PFC mixes had higher MPD values compared with Type C and Type D mixes. Type D had the lowest MPD values due to its finer gradation. The results also indicated that the macrotexture of PFC mixes decreased over time, and the rate of decrease in macrotexture depended on aggregate type. The macrotexture of Type C and Type D mixes was found to increase to some extent over time possibly due to removal of fine aggregates from the surface (raveling). The friction measured using the DFT, which is an indication of microtexture, showed the initial pavement microtexture depended on aggregate type.

The results showed there was a correlation between the MPD values and measured skid number in Type C and Type D mixes. However, no correlation was found between MPD values and measured skid number in PFC mixes. The results also indicate that there was a fair correlation between dynamic friction at 12.4 mph and measured skid number for all mixes. Furthermore, a fairly strong correlation was found between the results of the measured dynamic friction at 50 mph and measured skid number for Type C and Type D mixes. Similar to MPD, no correlation was found between the measured dynamic friction at 50 mph (80 km/h) and skid number for PFC mixes. The results of this analysis suggest the measured skid number is affected by macrotexture in dense-graded mixes, whereas microtexture governs the frictional performance of PFC mixes.



The results of the analysis of the measured skid number and aggregate characteristics indicated the frictional performance including terminal condition and rate of change in skid number for both Type C and PFC mixes in low and high traffic levels is affected by aggregate shape properties such as texture change before and after Micro-Deval, angularity before Micro-Deval, and angularity after Micro-Deval. A relationship was developed to predict the SN in the field based on DFT and CTMeter measurements.

The data collected in Phases I and II were analyzed, and a system was developed to predict the skid number of asphalt mixtures as a function of traffic level. This system requires input parameters that can be easily obtained. These input parameters are aggregate texture measured using AIMS with aggregates before and after Micro-Deval, and aggregate gradation.

## **RECOMMENDATIONS**

The system that was developed in this study is very promising and has been verified using the data collected in this study. However, researchers recommend gathering more data that represent a wider range of mixtures and aggregates to further validate this system and make it applicable to all mixture types and aggregates in Texas.



## REFERENCES

- ASTM. 2008. *Annual Book of ASTM Standards*, Vol. 04.03. American Society for Testing and Materials, West Conshohocken, PA.
- Chelliah, T., Stephanos, P., Shah, M.G., and Smith, T. 2003. Developing a Design Policy to Improve Pavement Surface Characteristics. Presented at 82nd Transportation Research Board Annual Meeting, Washington, D.C.
- Davis, R.M., Flintsch, G.W., Al-Qadi, I.L.K., and McGhee, K. 2002. Effect of Wearing Surface Characteristics on Measured Pavement Skid Resistance and Texture. Presented at 81st Transportation Research Board Annual Meeting, Washington, D.C.
- FHWA. 1990. *Nationwide Personal Transportation Survey*. NPTS Databook, FHWA Report FHWA-PL-94-010, Federal Highway Administration, U.S. Department of Transportation, Washington, D.C.
- Fulop, I.A., Bogardi, I., Gulyas, A., and Csicsely-Tarpay, M. 2000. Use of Friction and Texture in Pavement Performance Modeling. *ASCE Journal of Transportation Engineering*, Vol. 126, No. 3.
- Gandhi, P.M., Colucci, B., and Gandhi, S.P. 1991. Polishing of Aggregates and Wet Weather Accident Rate for Flexible Pavements. *Transportation Research Record* 1300, Transportation Research Board, National Research Council, Washington, D.C.
- Giles, C.G., Sabey, B.E., and Cardew, K.H.F. 1964. Development and Performance of the Portable Skid Resistance Tester. Road Research Technical Paper 66, Road Research Laboratory, Department of Scientific and Industrial Research, HMSO, London, United Kingdom.
- Goodman, S.N., Hassan, Y., and Abd El Halim, A.O. 2006. Preliminary Estimation of Asphalt Pavement Frictional Properties from Superpave Gyrotory Specimen and Mix Parameters. *Transportation Research Record* 1949, Transportation Research Board, National Research Council, Washington, D.C.

- Hall, J.W., Glover, L.T., Smith, K.L., Evans, L.D., Wambold, J.C., Yager, T.J., and Rado, Z. 2006. *Guide for Pavement Friction*. Project No. 1-43, Final Guide, National Cooperative Highway Research Program, Transportation Research Board, National Research Council, Washington, D.C.
- Hanson, D.I., and Prowell, B.D. 2004. *Evaluation of Circular Texture Meter for Measuring Surface Texture of Pavements*. NCAT Report 04-05, National Center for Asphalt Technology, Auburn, AL.
- Henry, J.J. 1996. *Overview of the International PIARC Experiment to Compare and Harmonize Texture and Skid Resistance Measurements: The International Friction Index*. Proceedings of the 3rd International Symposium on Pavement Surface Characteristics, Christchurch, New Zealand, September.
- Kamel, N., and Gartshore, T. 1982. *Ontario's Wet Pavement Accident Reduction Program*. ASTM Special Technical Publication 763, American Society of Testing and Materials, Philadelphia, PA.
- Kowalski, K.J. 2007. *Influence of Mixture Composition on the Noise and Frictional Characteristics of Flexible Pavements*. Ph.D. Dissertation, Purdue University, West Lafayette, IN.
- Kuempel, D.A., Sontag, R.C., Crovetto, J., Becker, A.Y., Jaeckel, J.R., and Satanovsky, A. 2000. *Noise and Texture on PCC Pavements*. Final report in multi-state study, Report Number WI/SPR-08-99, Wisconsin Department of Transportation, Madison, WI.
- Mahmoud, E.M. 2005. *Development of Experimental Method for the Evaluation of Aggregate Resistance to Polish, Abrasion, and Breakage*. M.S.C.E Thesis, Texas A&M University, College Station, TX.
- McCullough, B.V., and Hankins, K.D. 1966. Skid Resistance Guidelines for Surface Improvements on Texas Highways. *Transportation Research Record* 131, Transportation Research Board, National Research Council, Washington, D.C.
- Miller, M.M., and Johnson, H.D. 1973. *Effects of Resistance to Skidding on Accidents: Surface Dressing on an Elevated Section of the M4 Motorway*. Report No. LR 542, Transport and Road Research Laboratory, Berkshire, United Kingdom.

- Noyce D.A., Bahia, H.U., Yambó, J.M., and Kim, G. 2005. *Incorporating Road Safety into Pavement Management: Maximizing Asphalt Pavement Surface Friction for Road Safety Improvements*. Midwest Regional University Transportation Center Traffic Operations and Safety (TOPS) Laboratory.
- Rizenbergs, R.L., Burchett, J.L., and Napier, C.T. 1972. *Skid Resistance of Pavements*. Report No. KYHPR-64-24, Part II, Kentucky Department of Highways, Lexington, KY.
- Smith, H. 1976. Pavement Contributions to Wet-Weather Skidding Accident Reduction. *Transportation Research Record 622*, Transportation Research Board, National Research Council, Washington, D.C.
- SPSS Manual. 2009. *The SPSS Two Step Cluster Component*. Technical Report. [http://www.spss.ch/upload/1122644952\\_The%20SPSS%20TwoStep%20Cluster%20Component.pdf](http://www.spss.ch/upload/1122644952_The%20SPSS%20TwoStep%20Cluster%20Component.pdf). Accessed: Feb. 3, 2009.
- TxDOT. 2004. Standard Specifications for Construction and Maintenance of Highways, Streets, and Bridges. <ftp://ftp.dot.state.tx.us/pub/txdot-info/des/specs/specbook.pdf>. Accessed: Jan. 25, 2009.
- Wallman, C.G., and Astron, H. 2001. *Friction Measurement Methods and the Correlation between Road Friction and Traffic Safety*. Swedish National Road and Transport Research Institute, VTI Meddelande 911A, Linköping, Sweden.
- Wambold, J.C., Antle, C.E., Henry J.J., and Rado, Z. 1995. *PIARC (Permanent International Association of Road Congress) Report*. International PIARC Experiment to Compare and Harmonize Texture and Skid Resistance Measurement, C-1 PIARC Technical Committee on Surface Characteristics, France.
- West, T.R., Choi, J.C., Bruner, D.W., Park, H.J., and Cho, K.H. 2001. Evaluation of Dolomite and Related Aggregates Used in Bituminous Overlays for Indiana Pavements. *Transportation Research Record 1757*, Transportation Research Board, National Research Council, Washington, D.C.



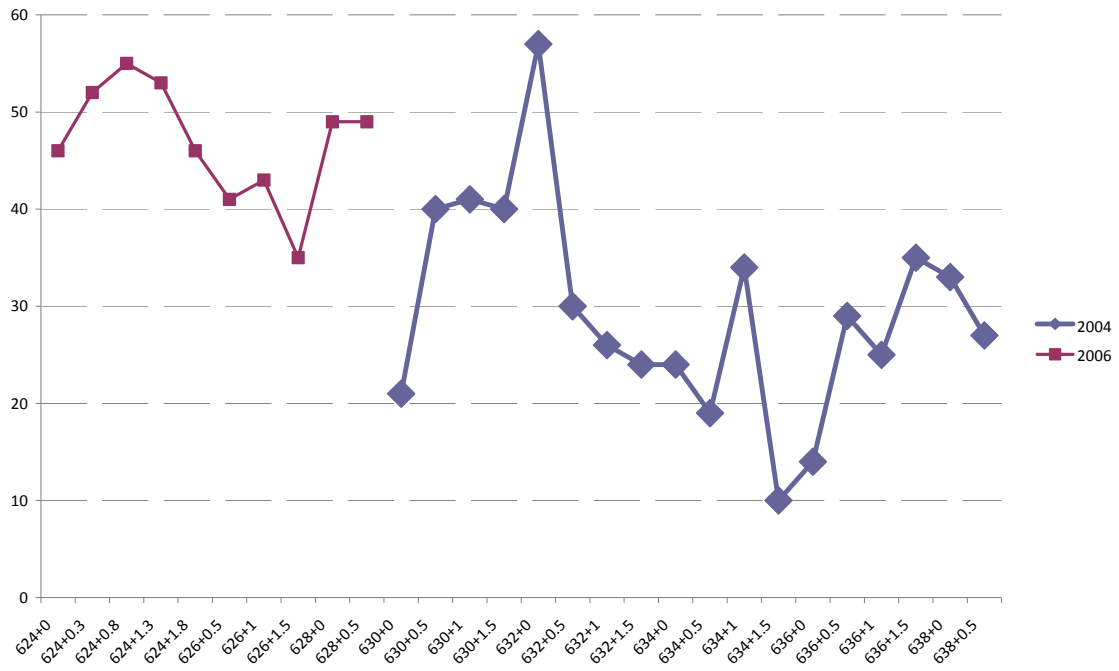
## **APPENDIX**

### **Skid Data Variability for different Road Sections**

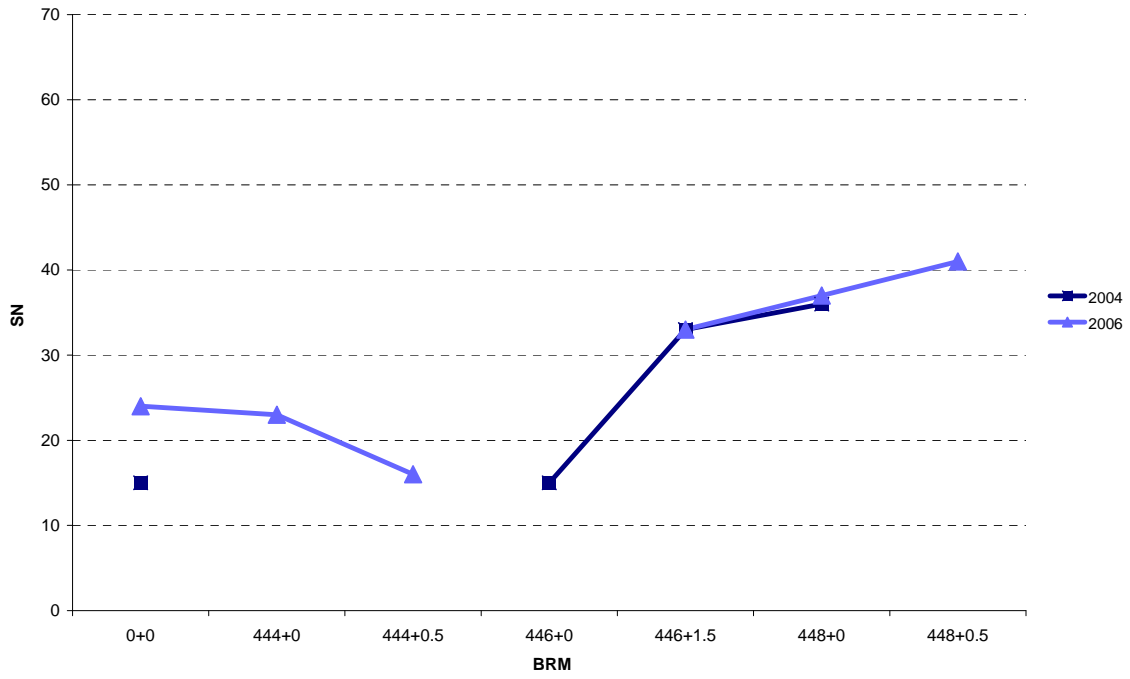




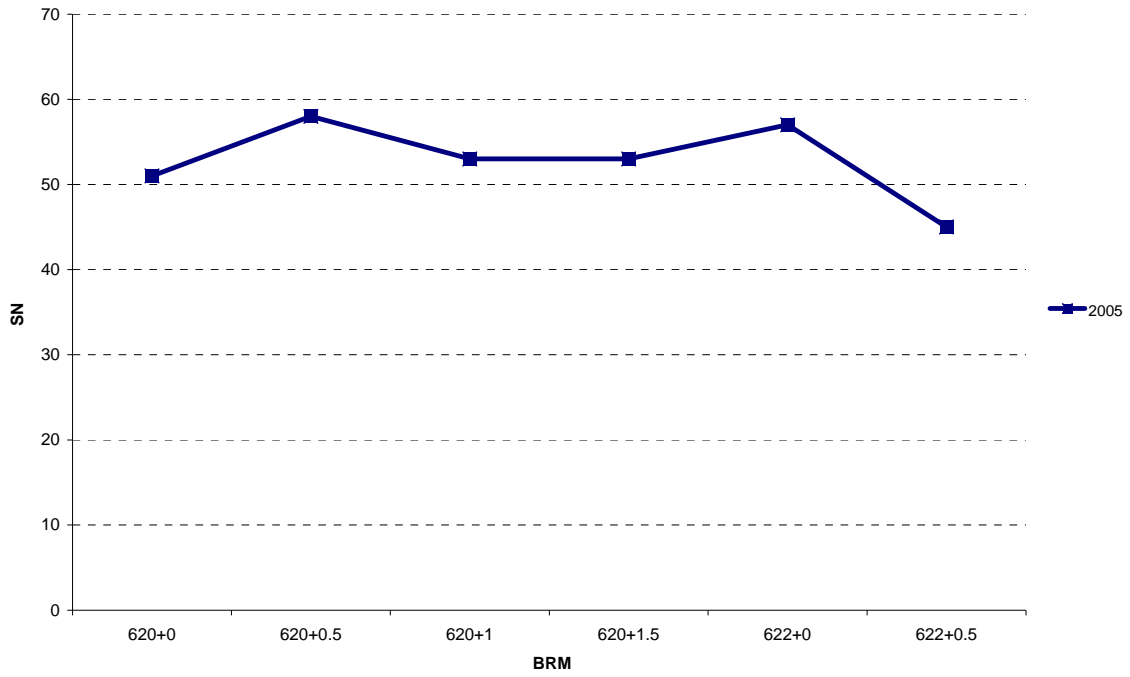
### BU0077VK



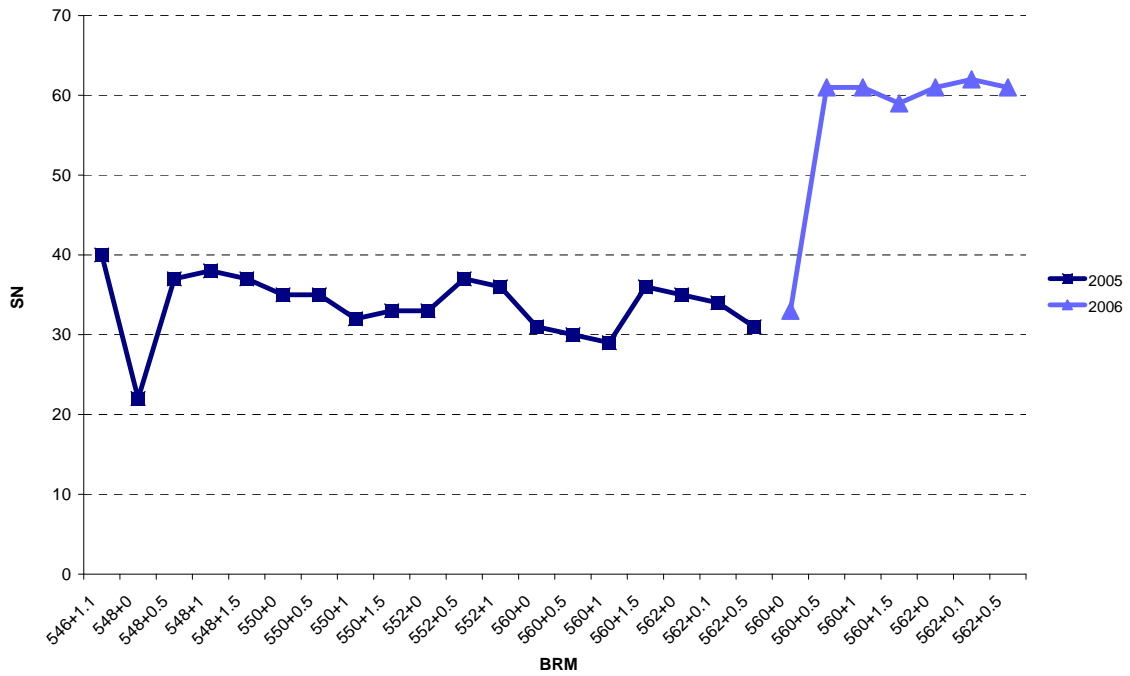
### BU0290FK



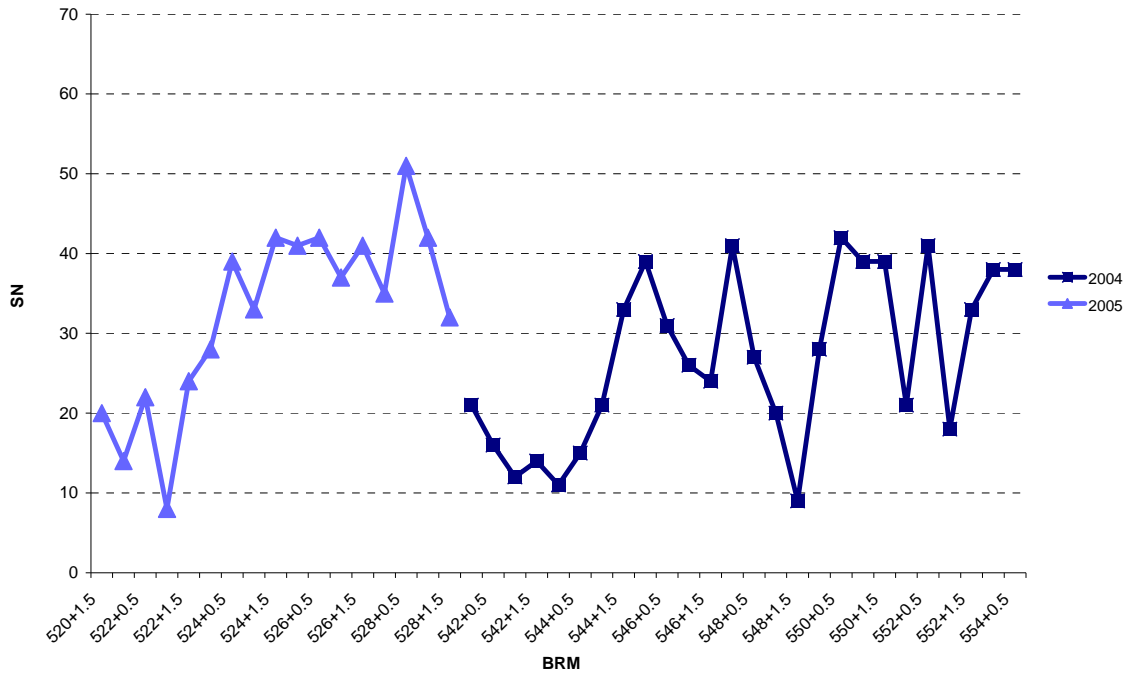
FM0024 K



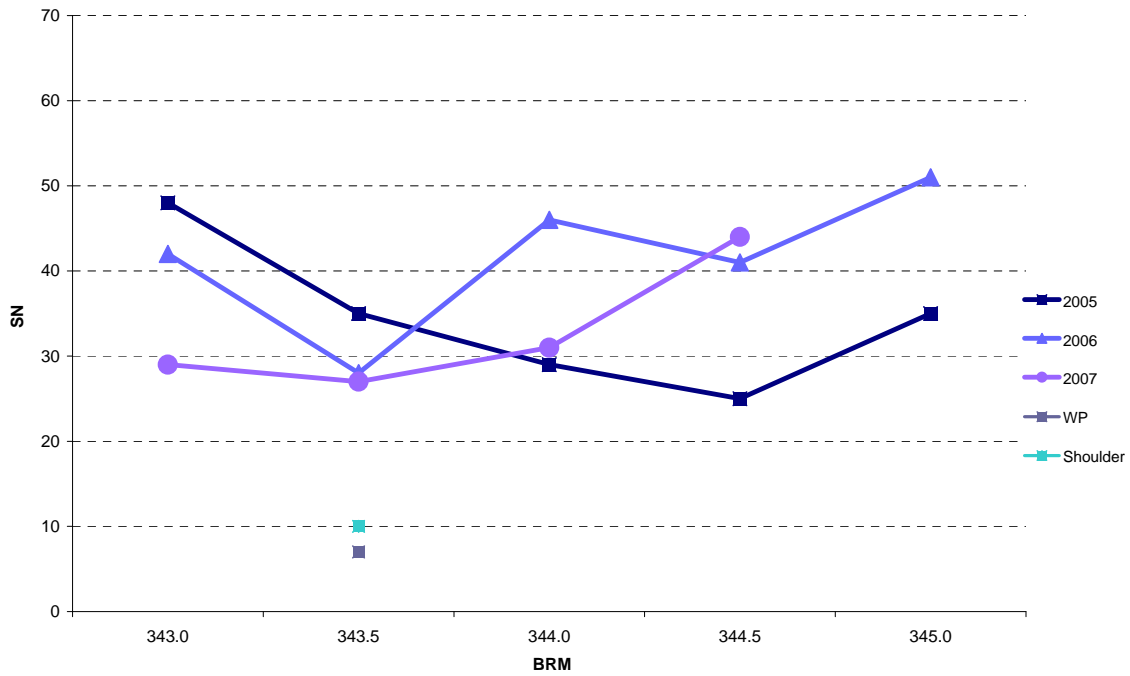
FM0624 K



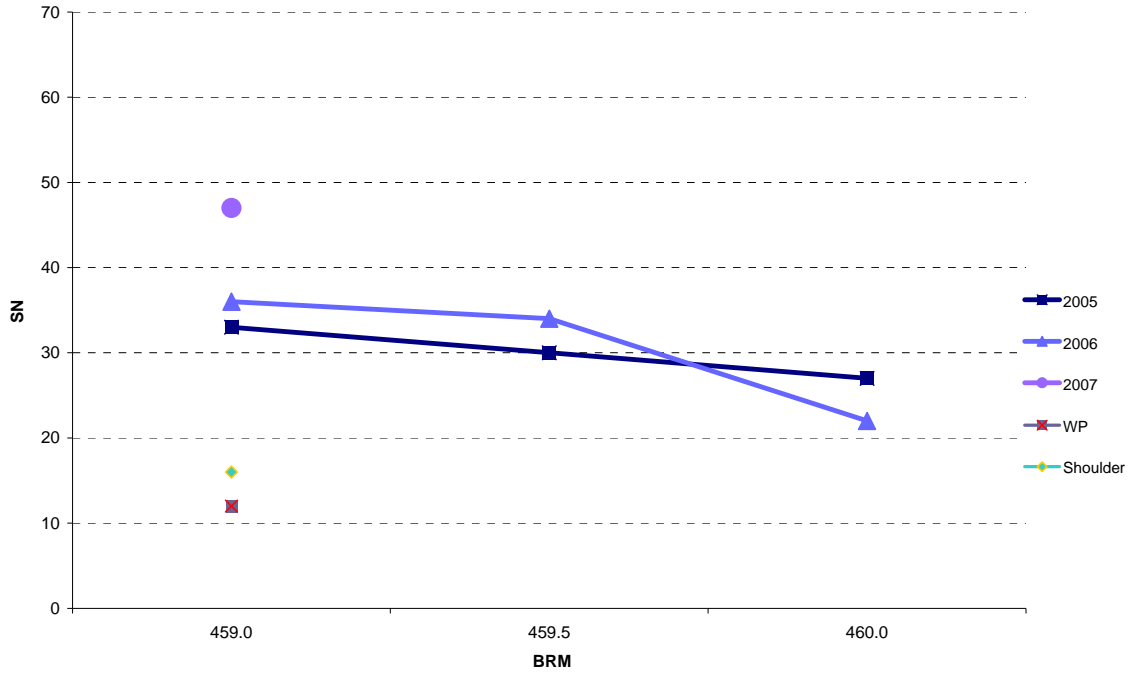
FM0665 K



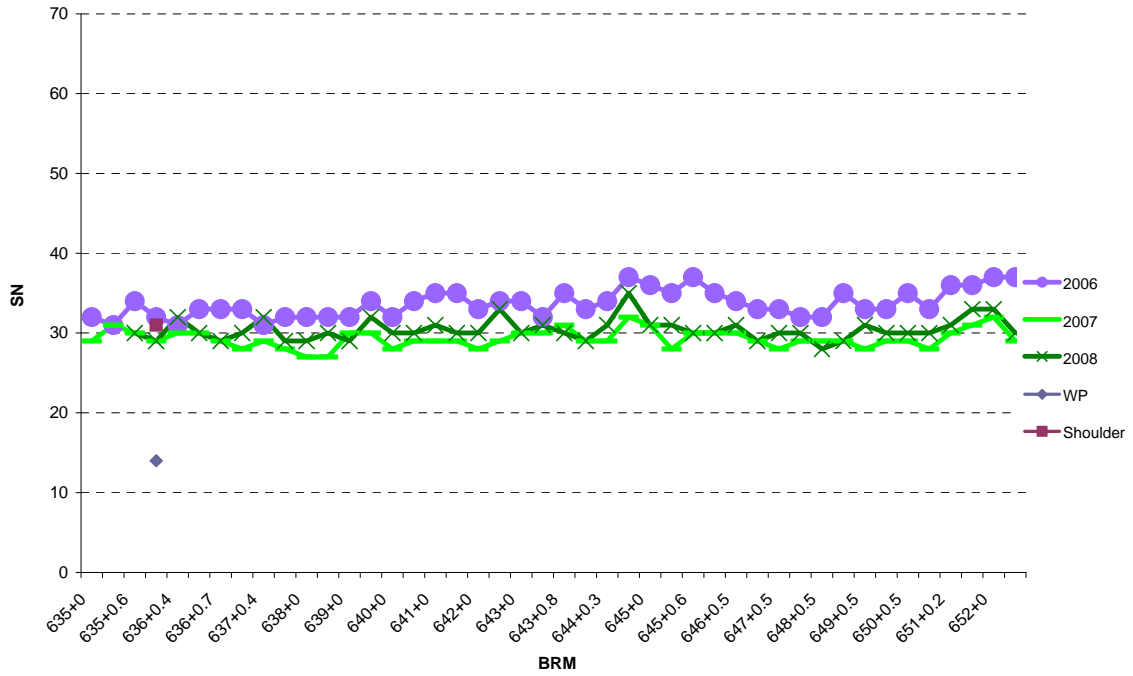
FM2524 K



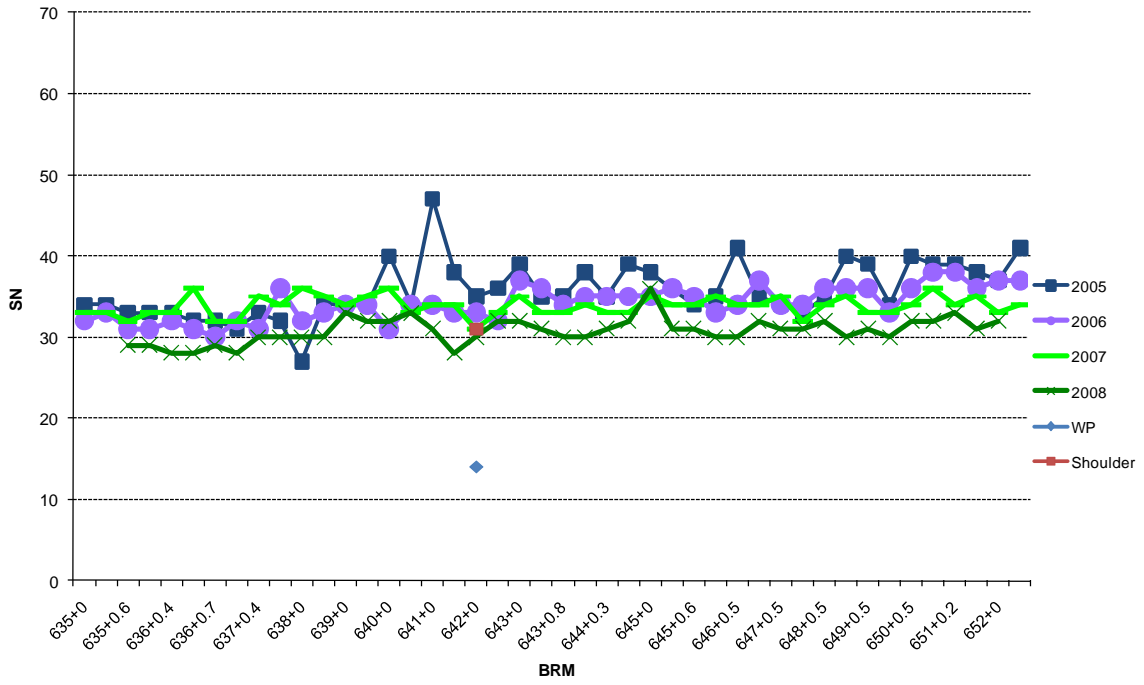
FM3064 K



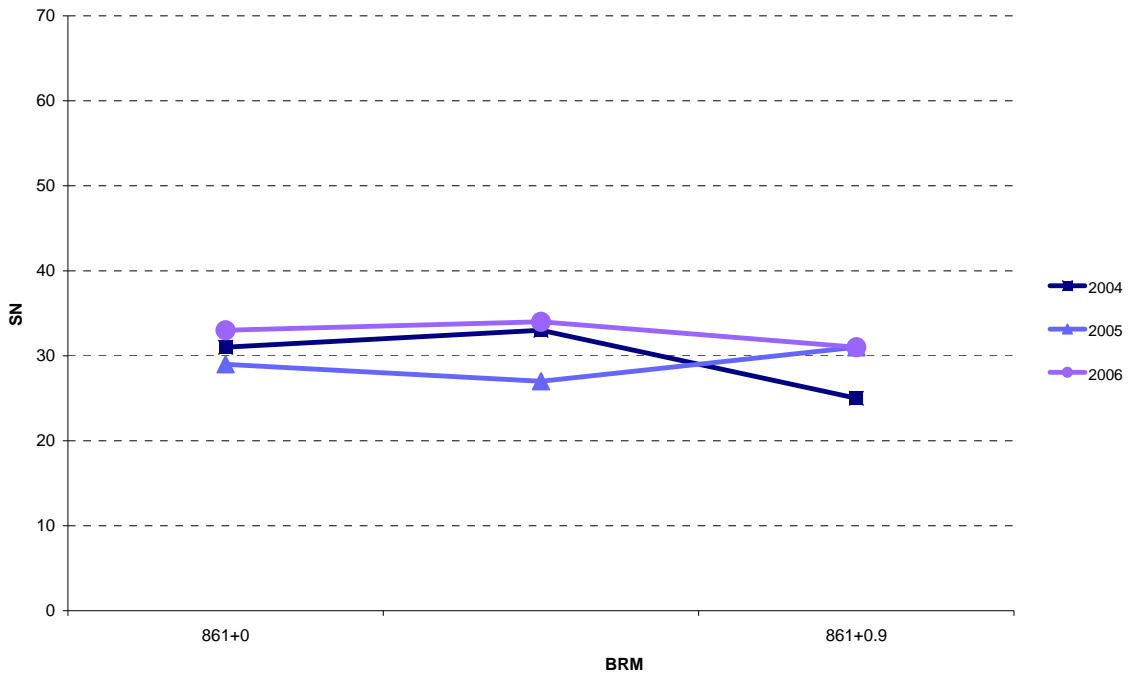
IH0010 L



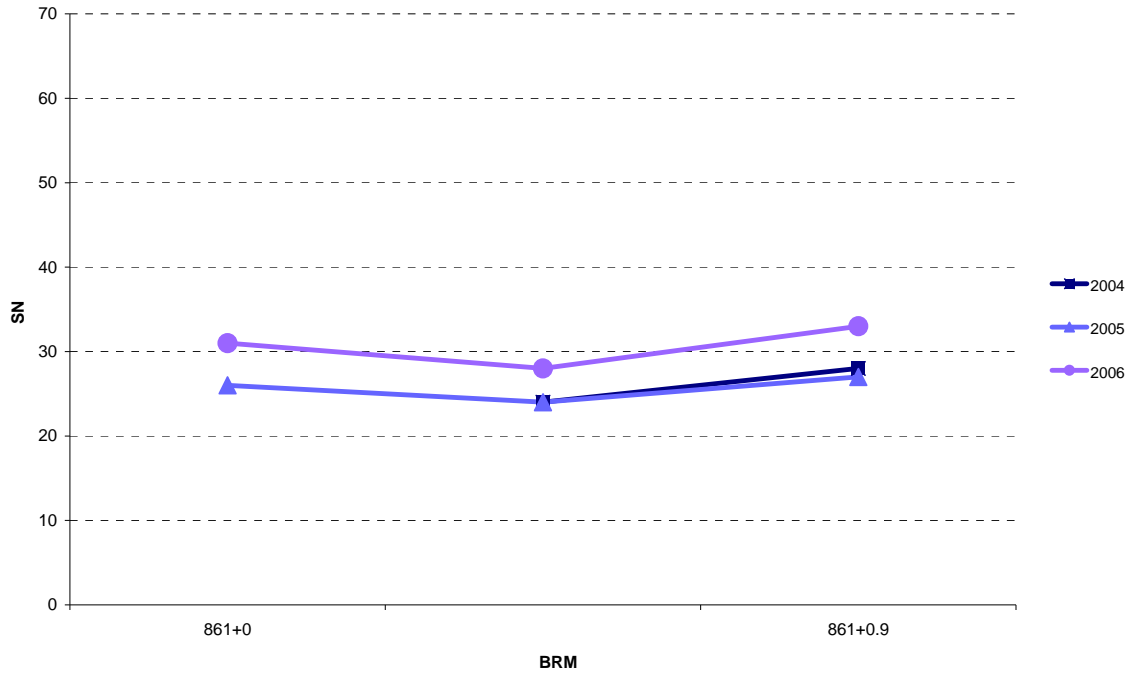
IH0010 R



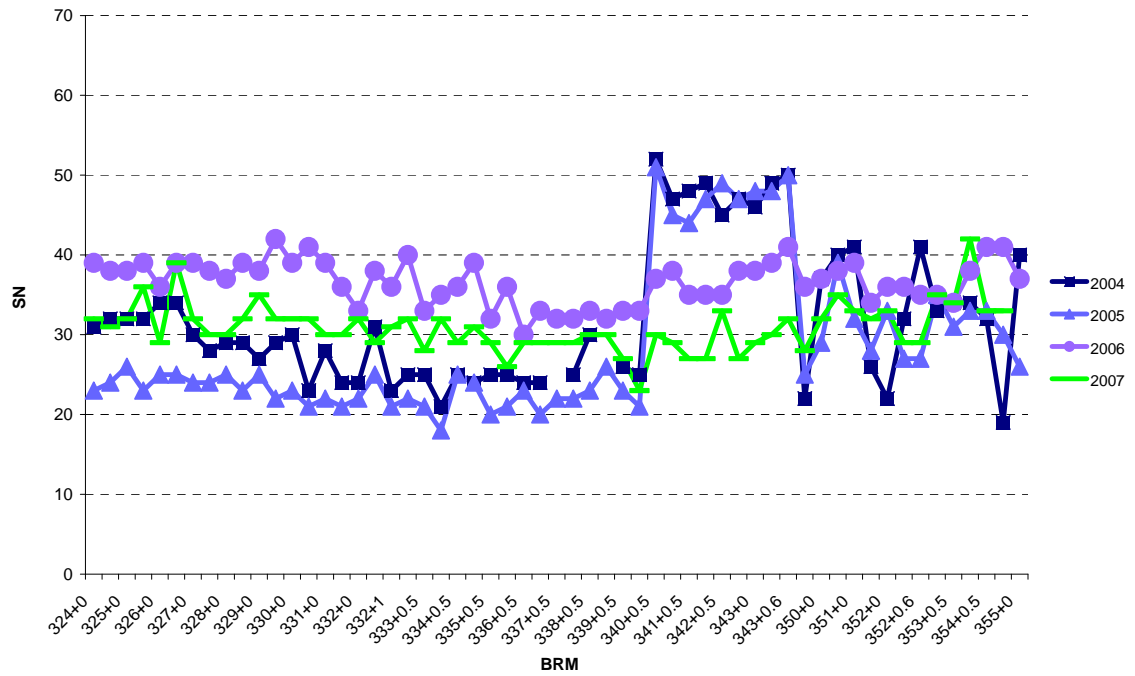
IH0010 L



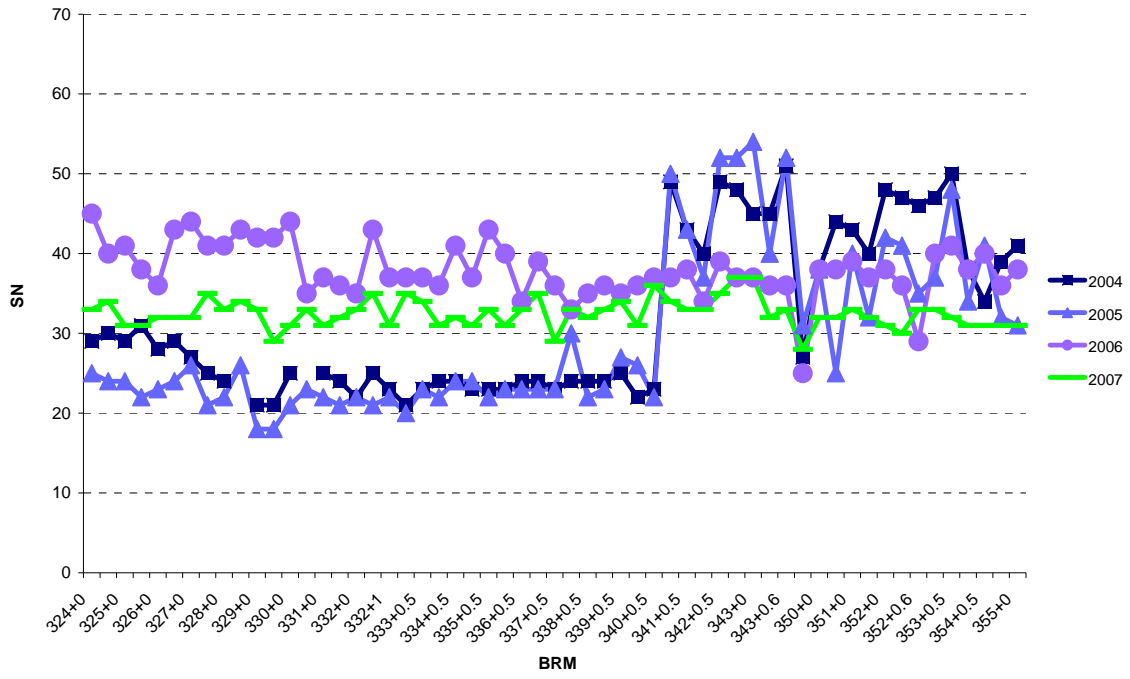
### IH0010 R



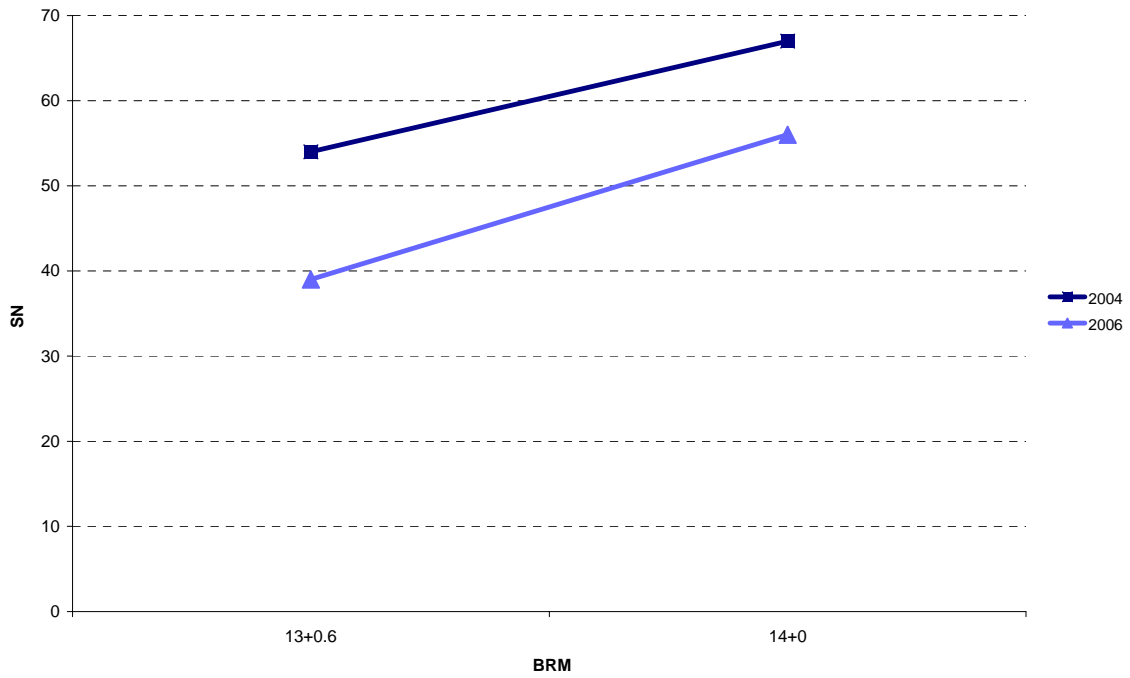
### IH0020 L



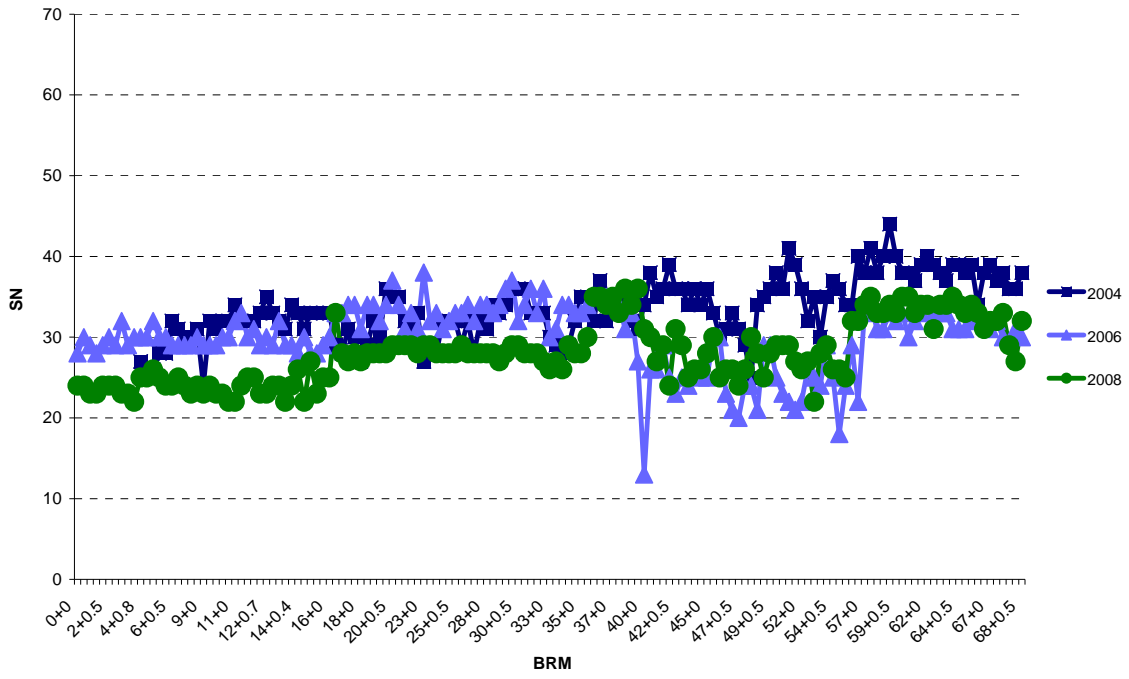
IH0020 R



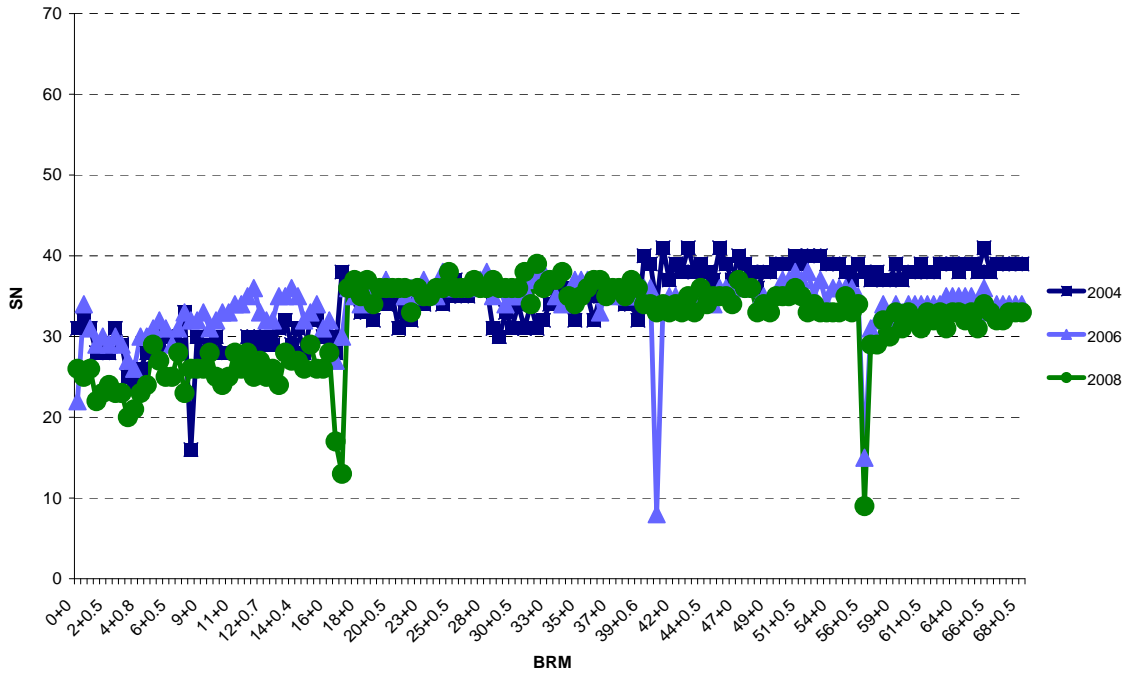
IH0037 A



IH0037 L

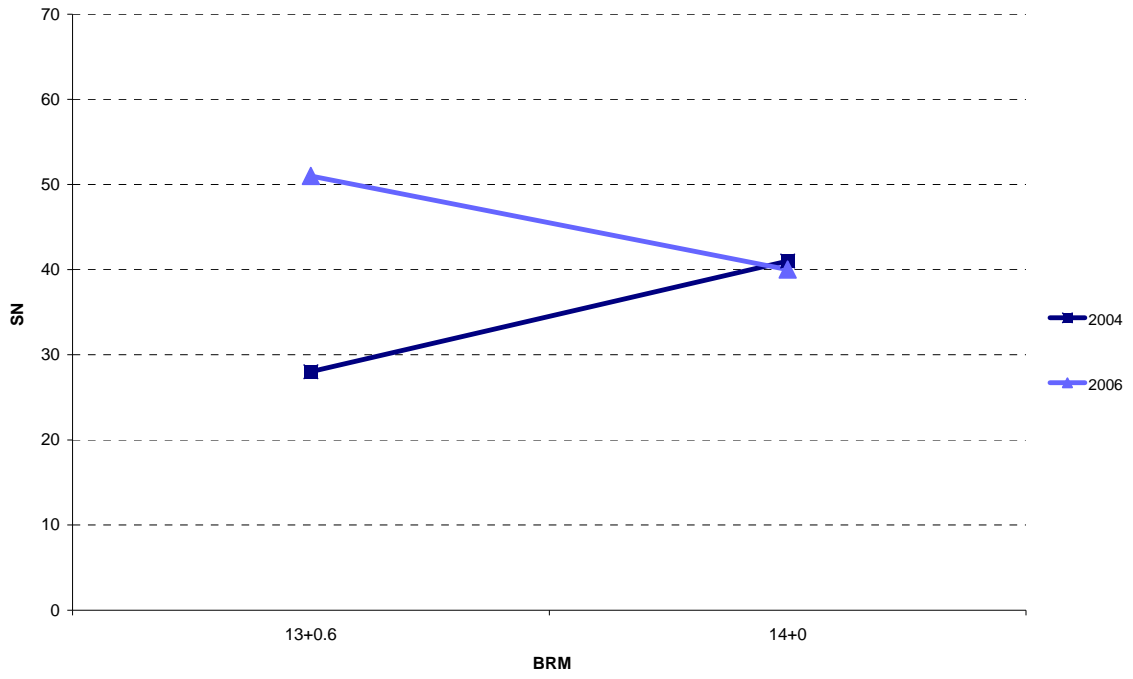


IH0037 R

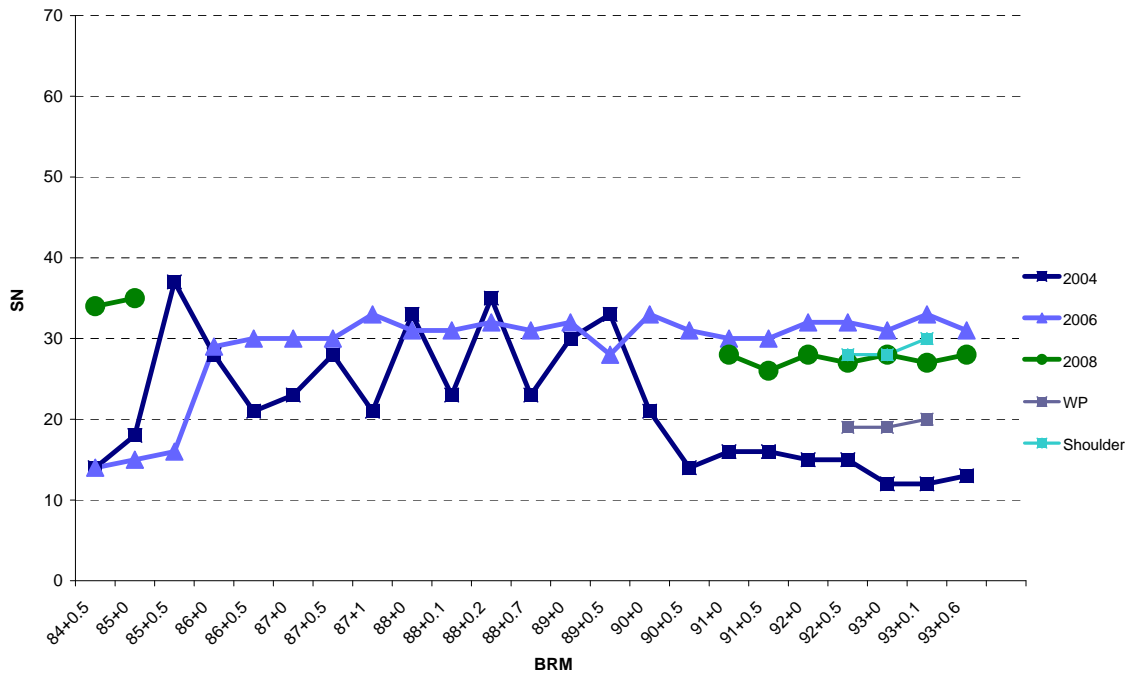




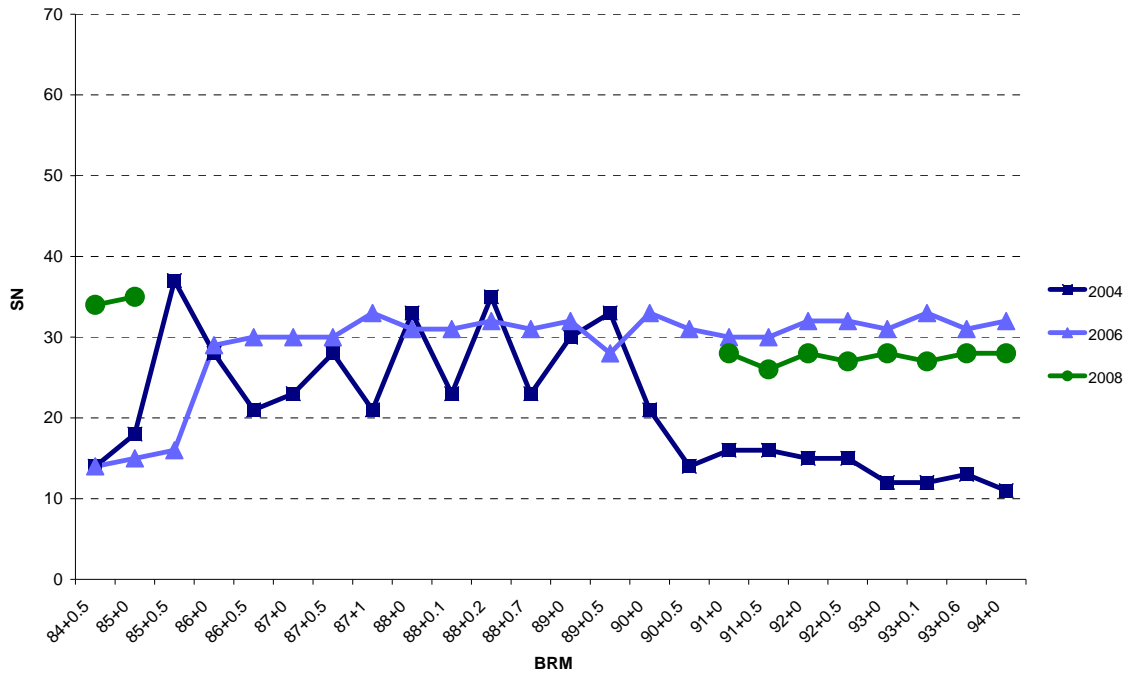
IH0037 X



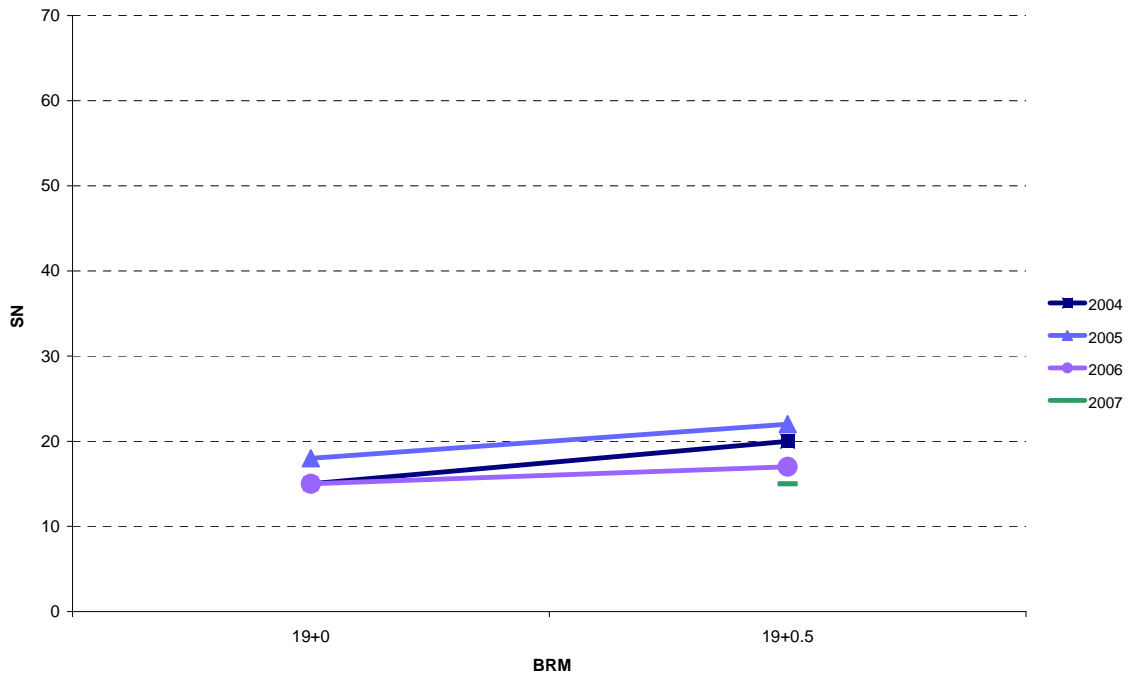
IH0045 L



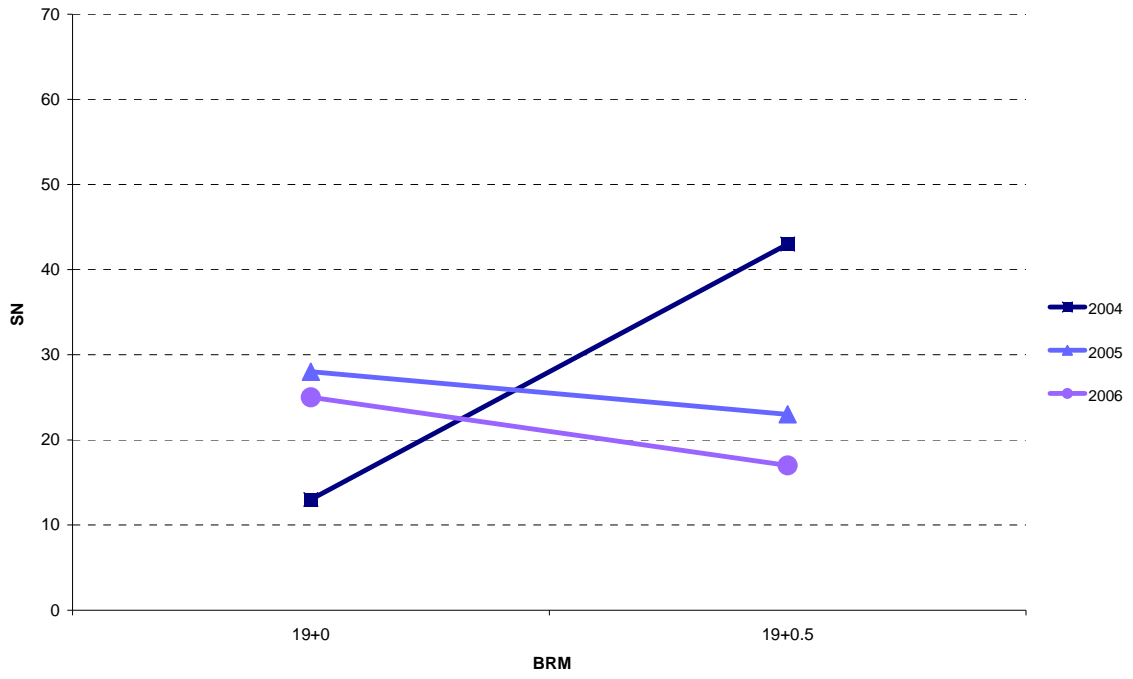
IH0045 R



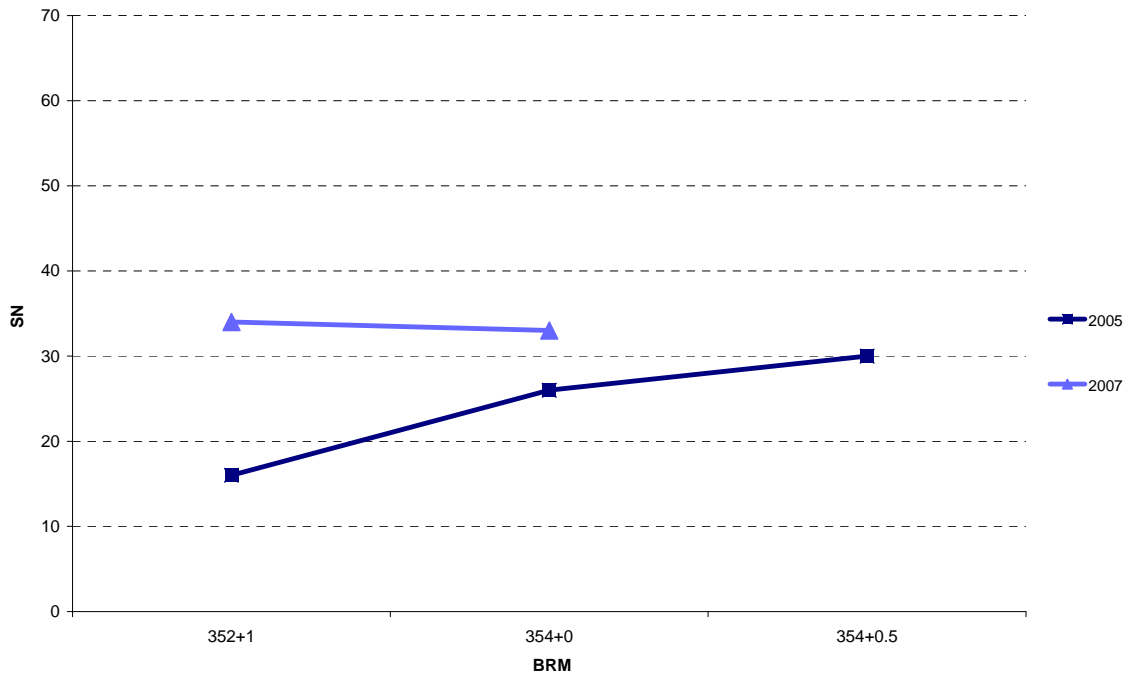
IH0410 L



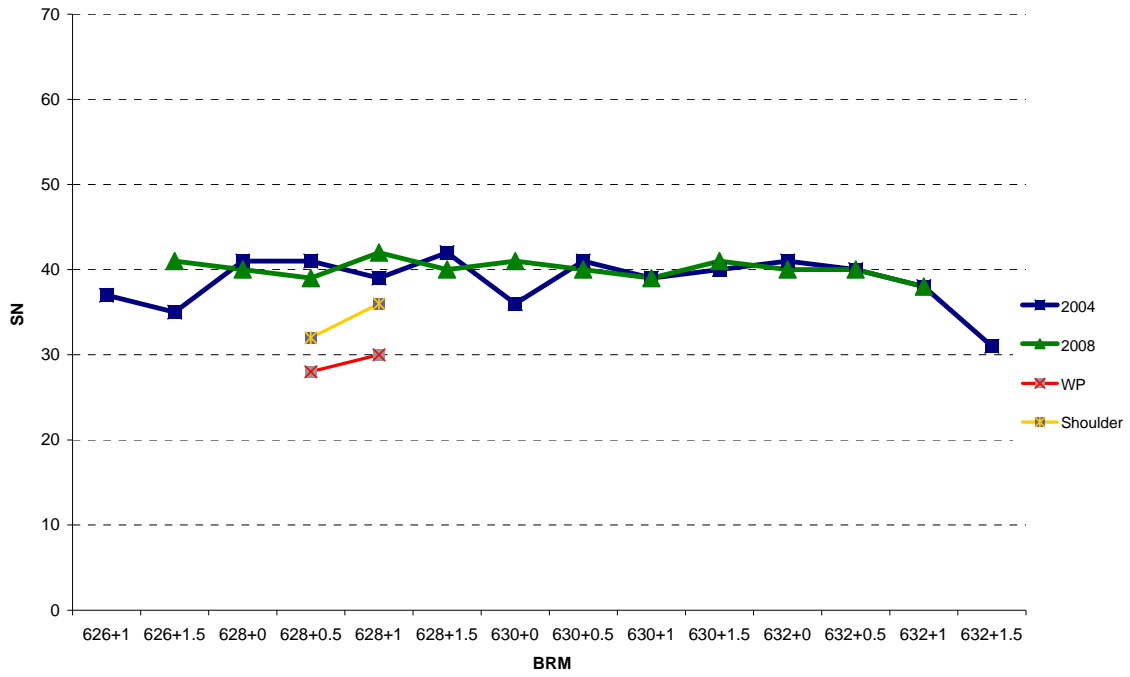
### IH0410 R



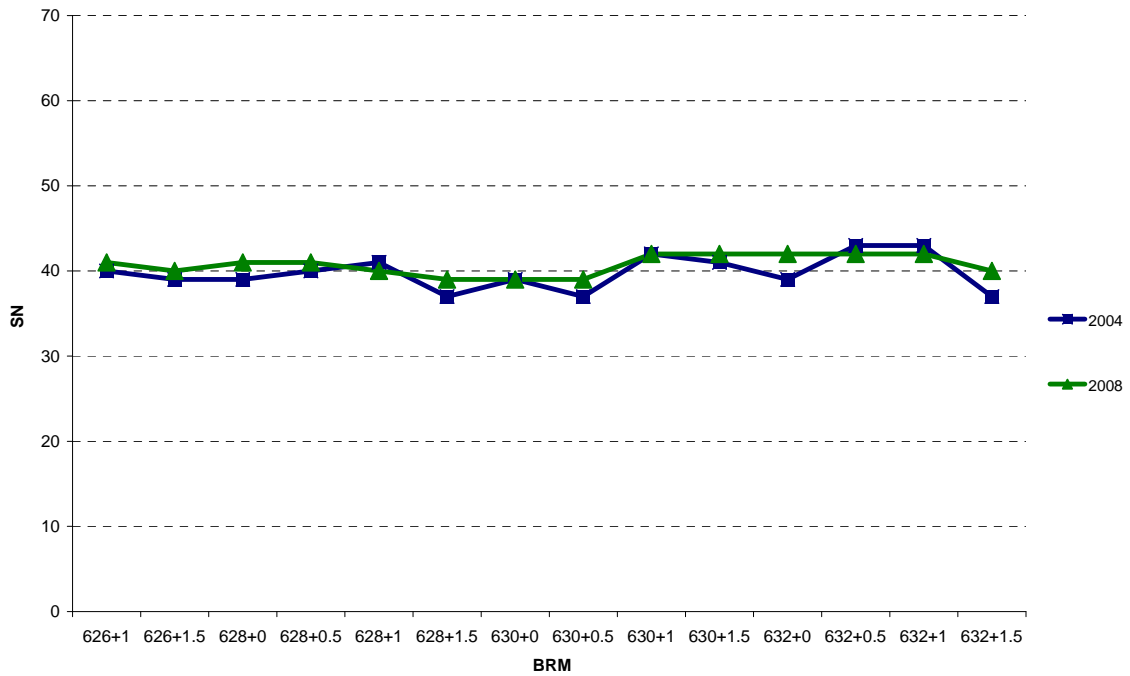
### SH0006 K



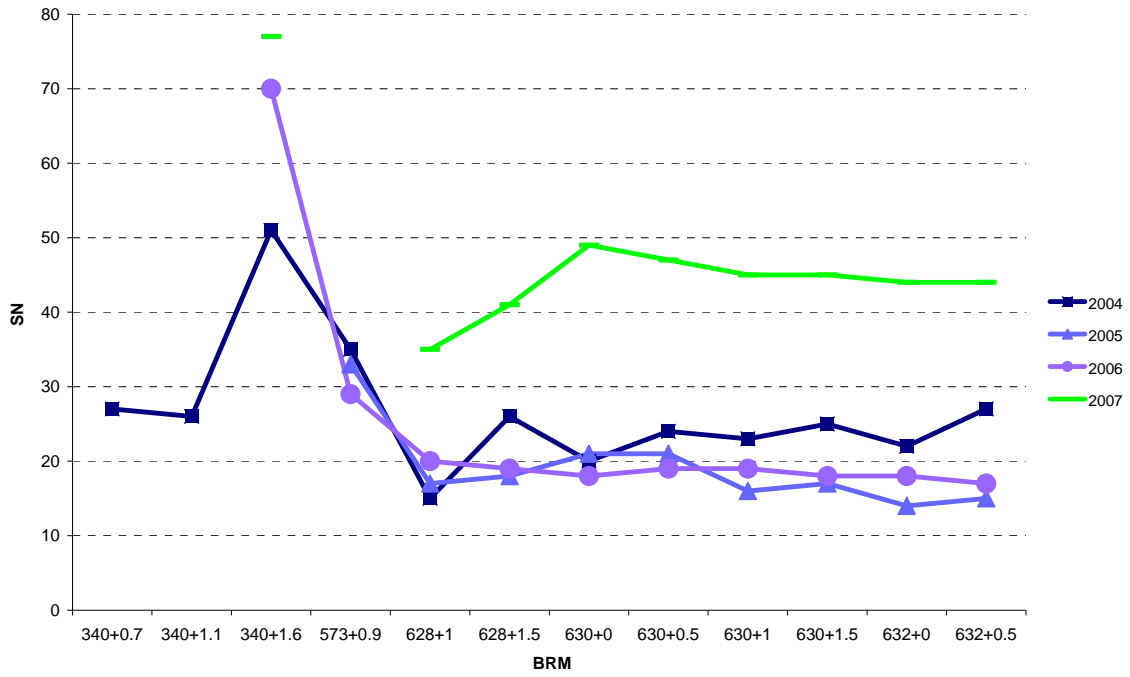
SH0006 L



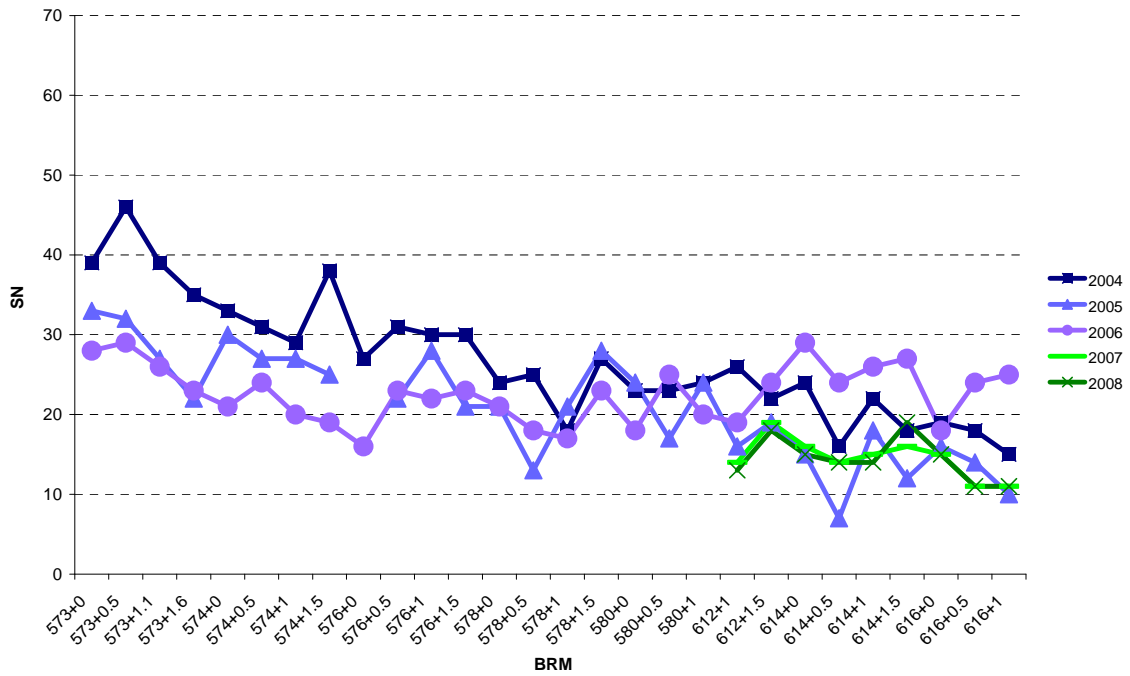
SH0006 R



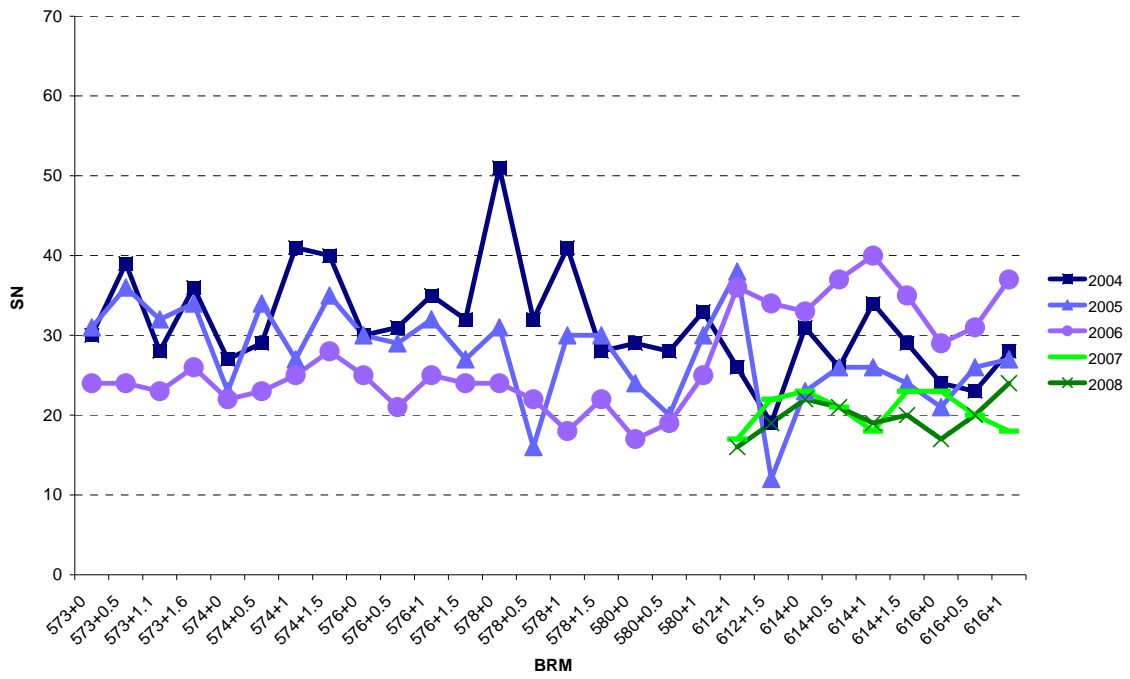
SH0016 K



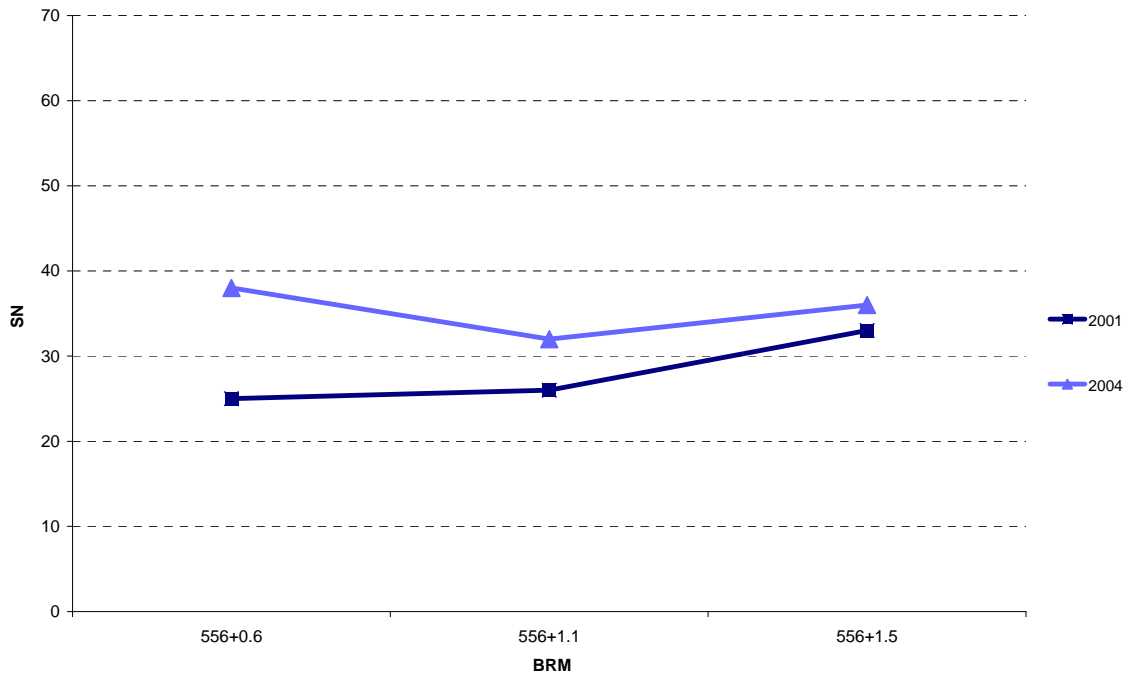
SH0016 L



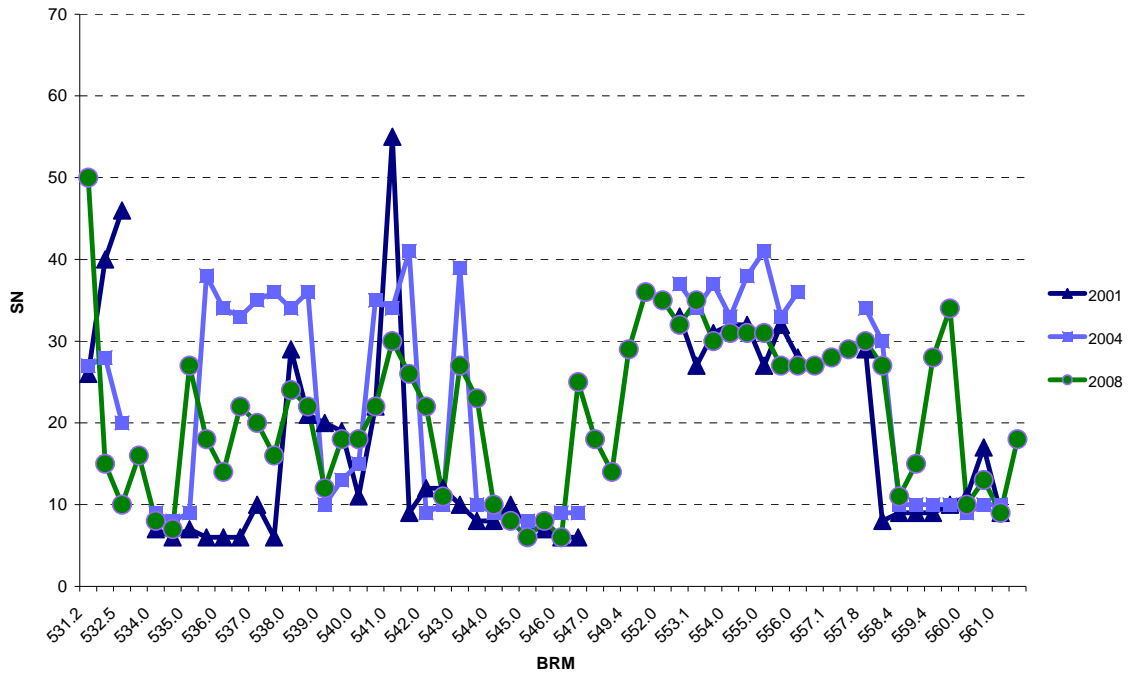
SH0016 R



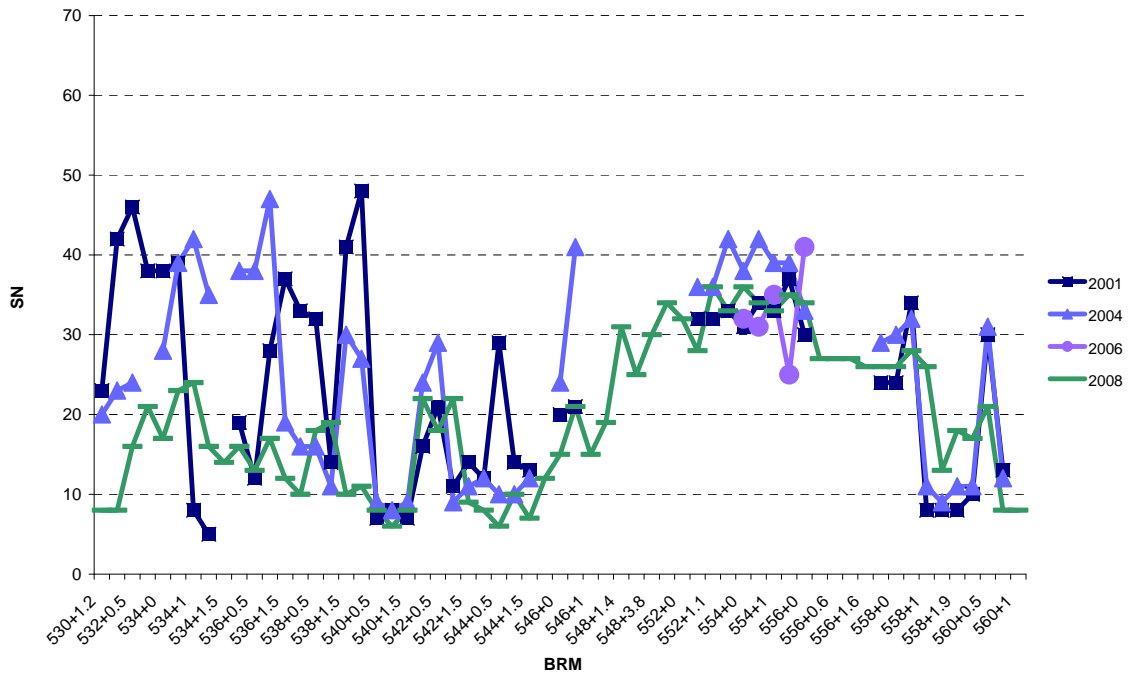
SH0044 K



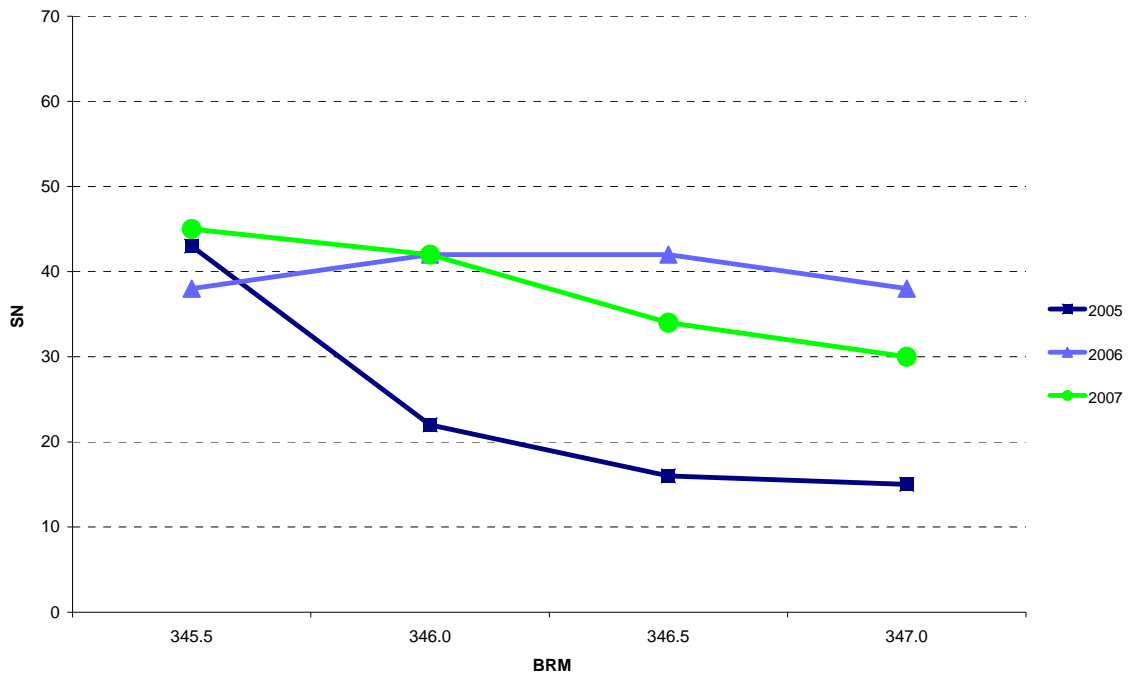
SH0044 L



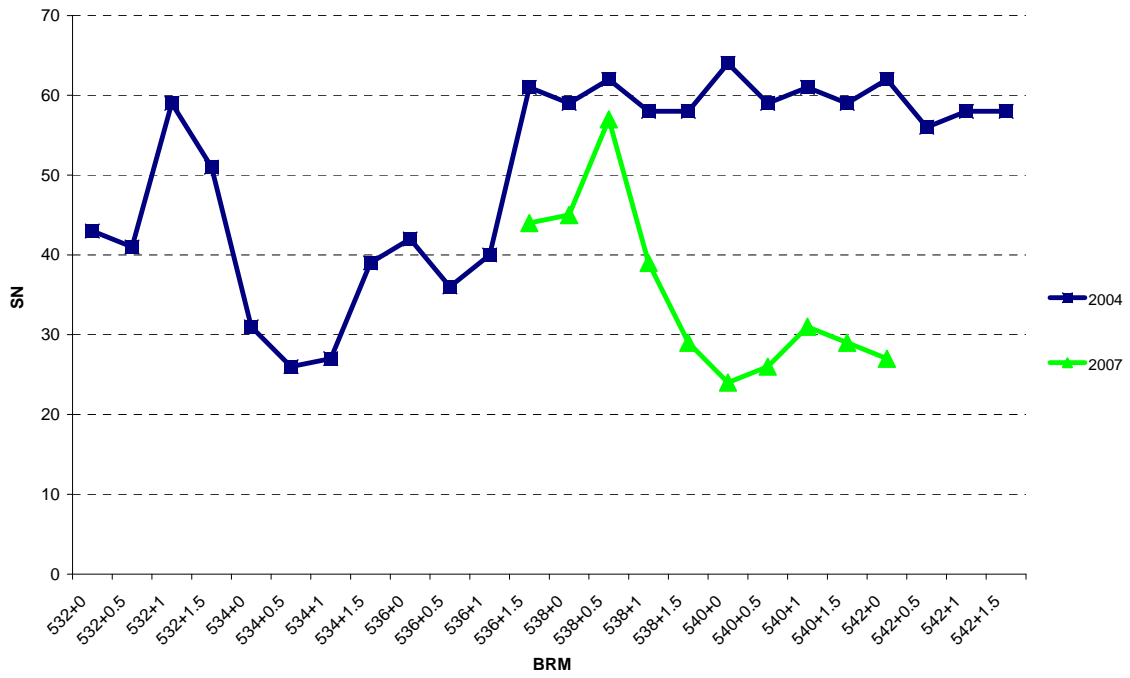
SH0044 R



SH0279 K

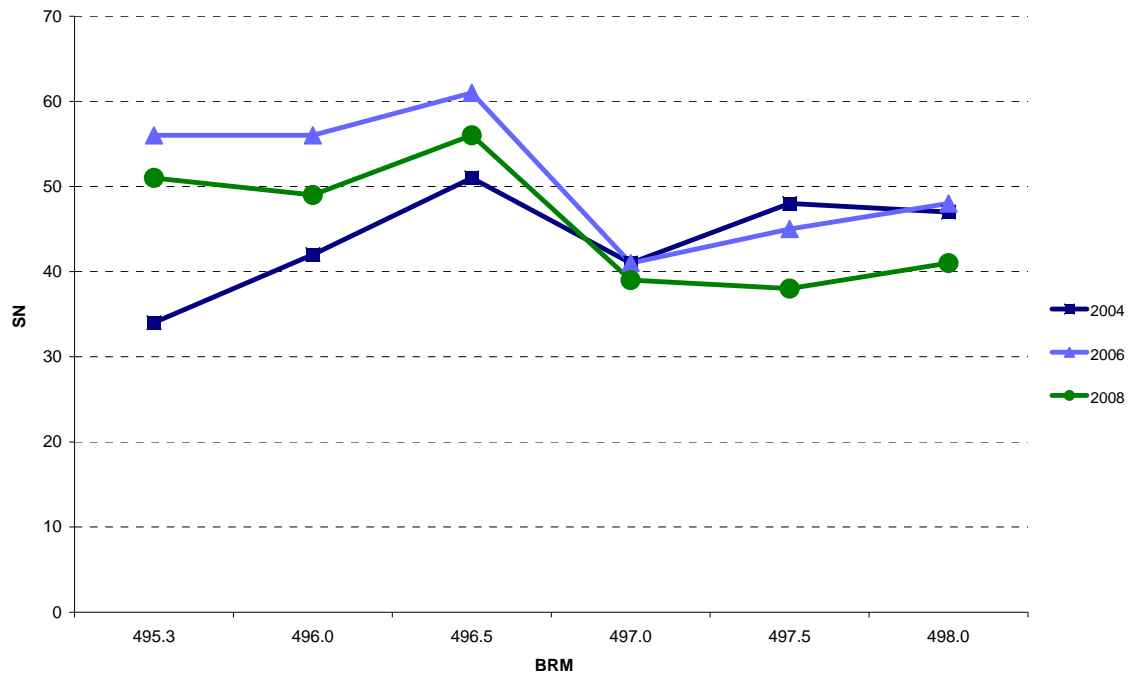


SH0285 K

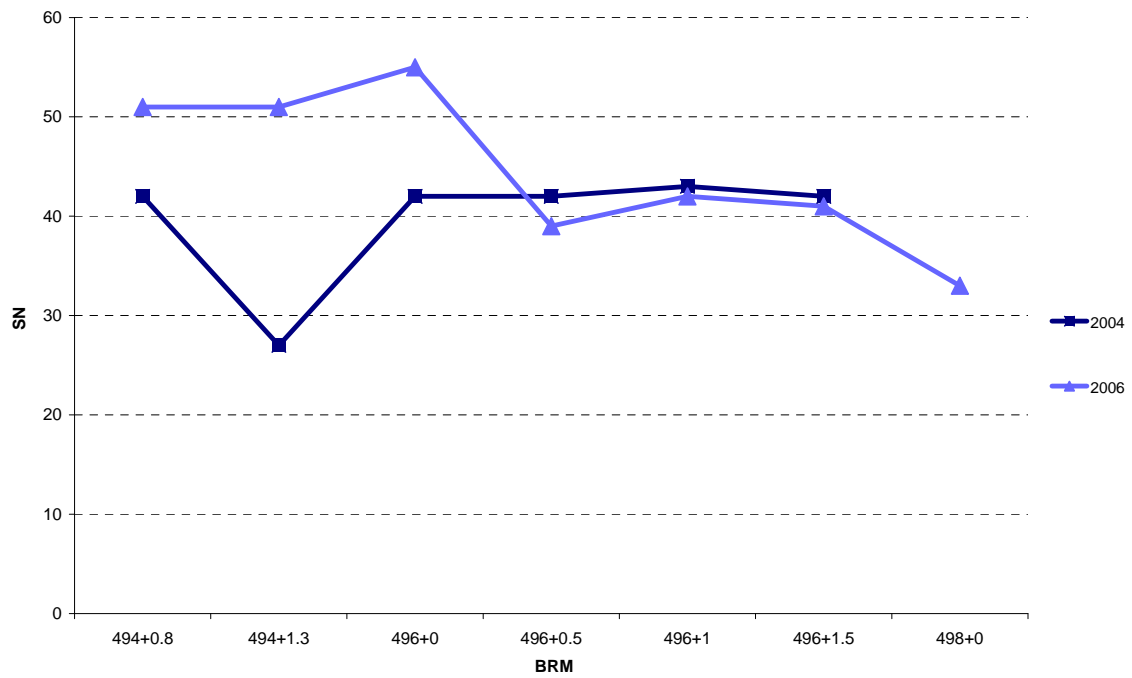


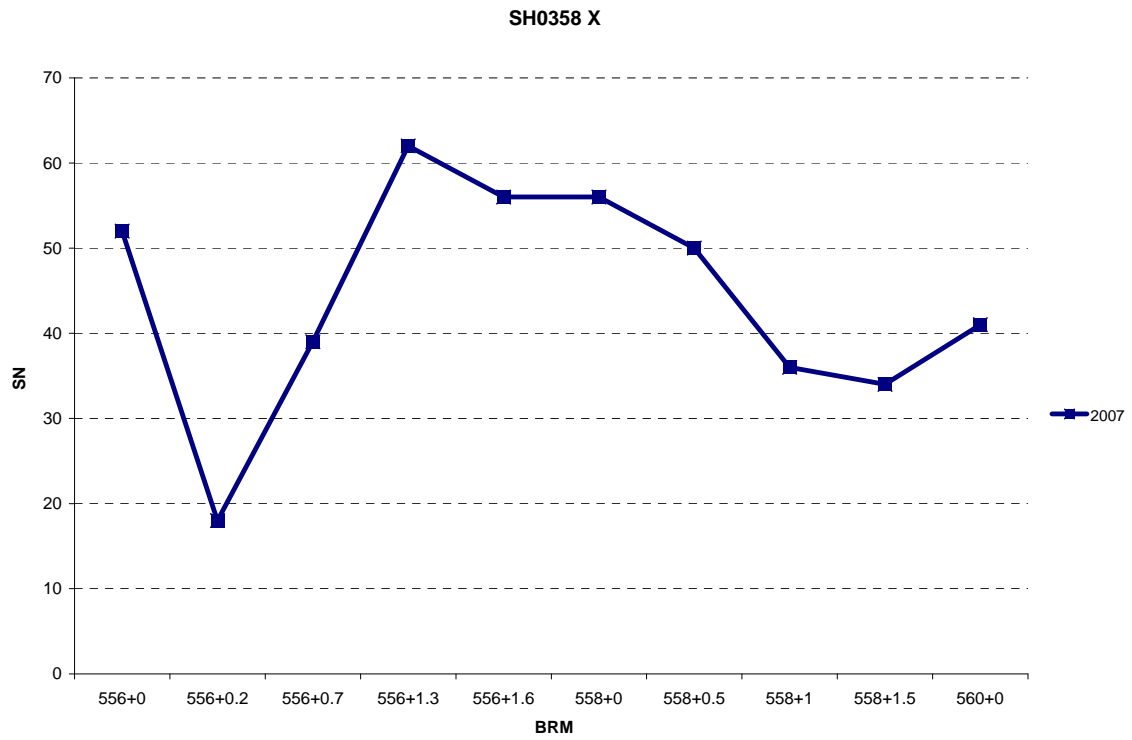
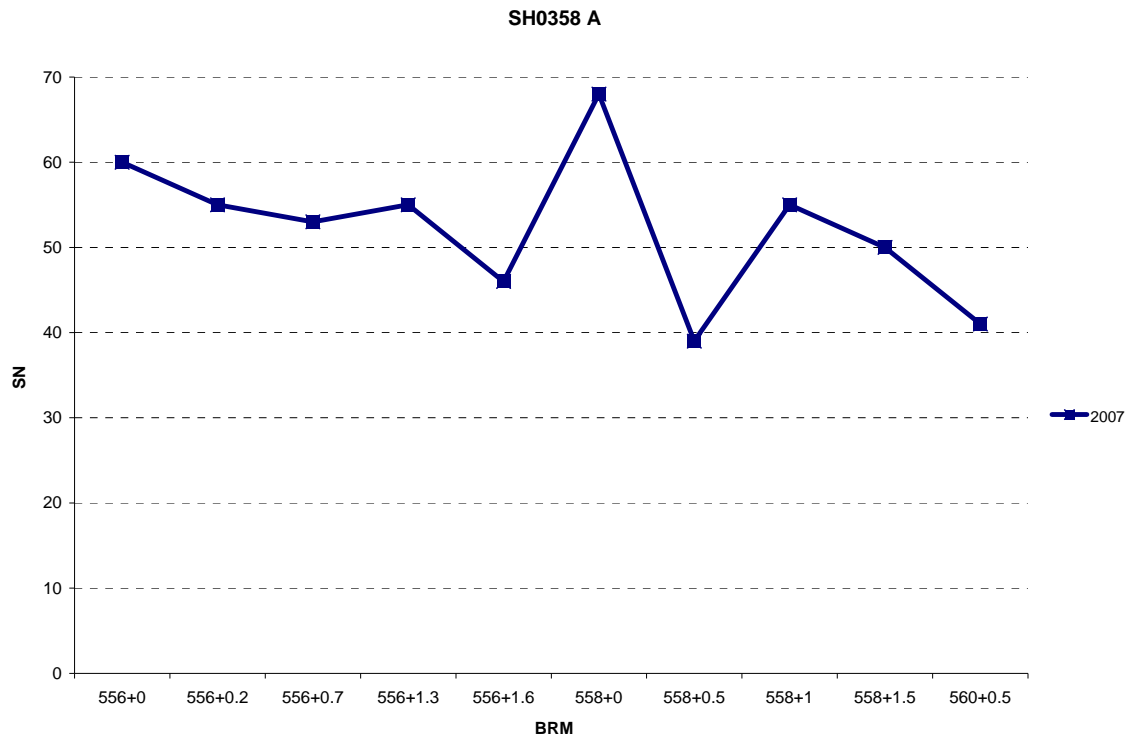


SH0288 A

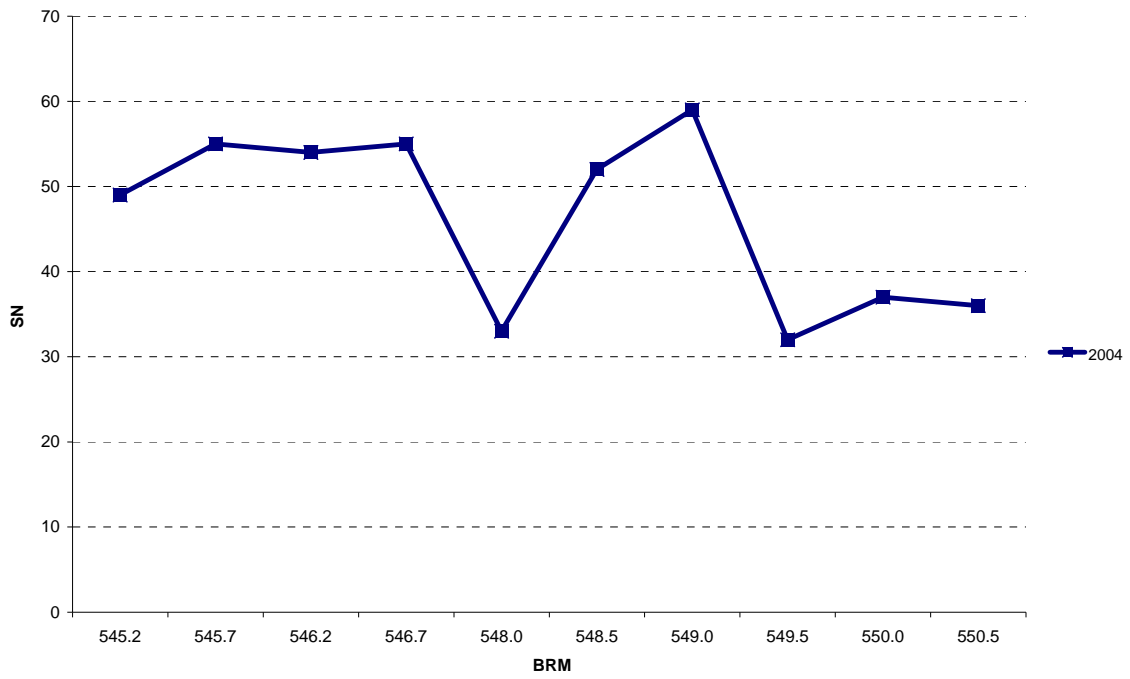


SH0288 X

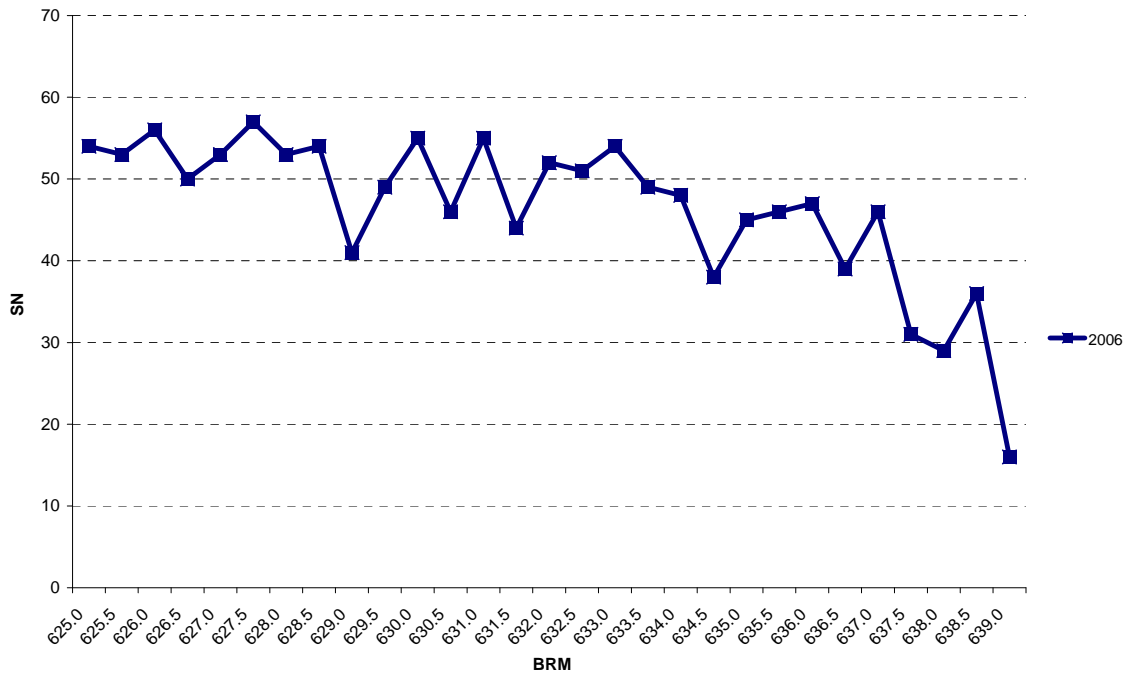




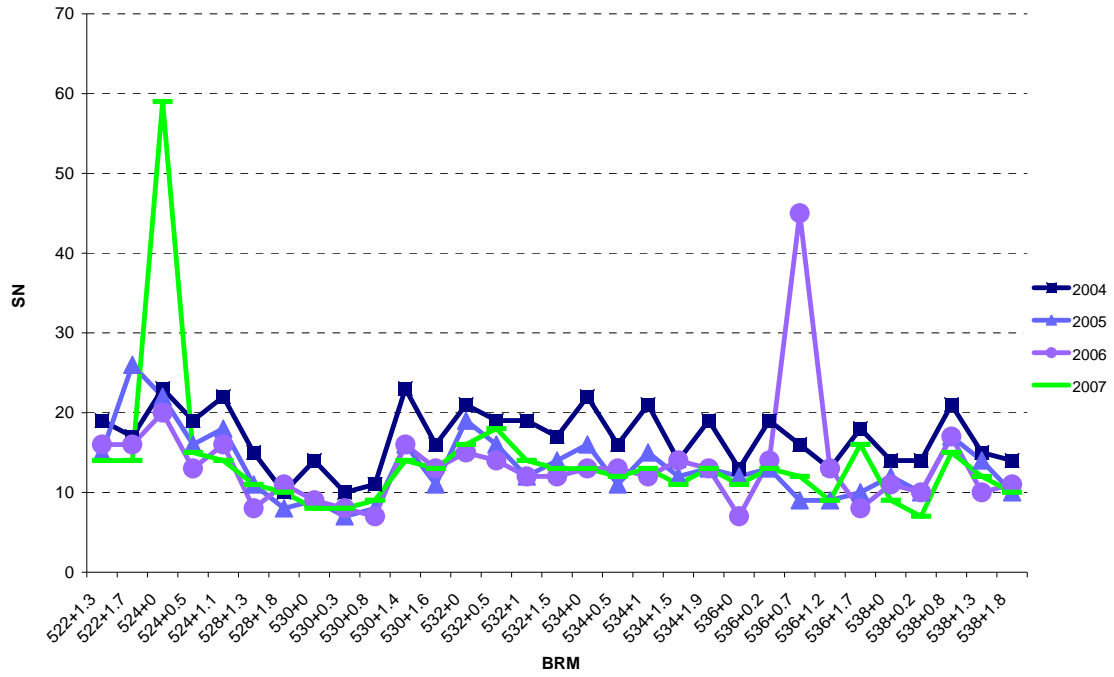
SH0359 K



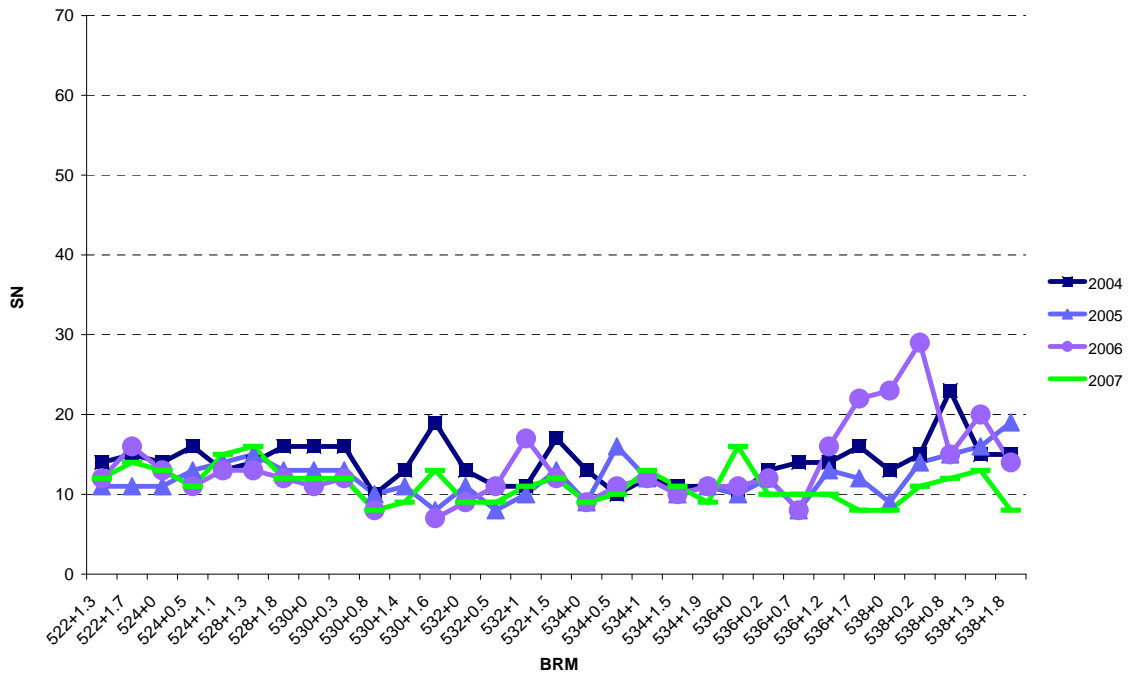
SH0361 K



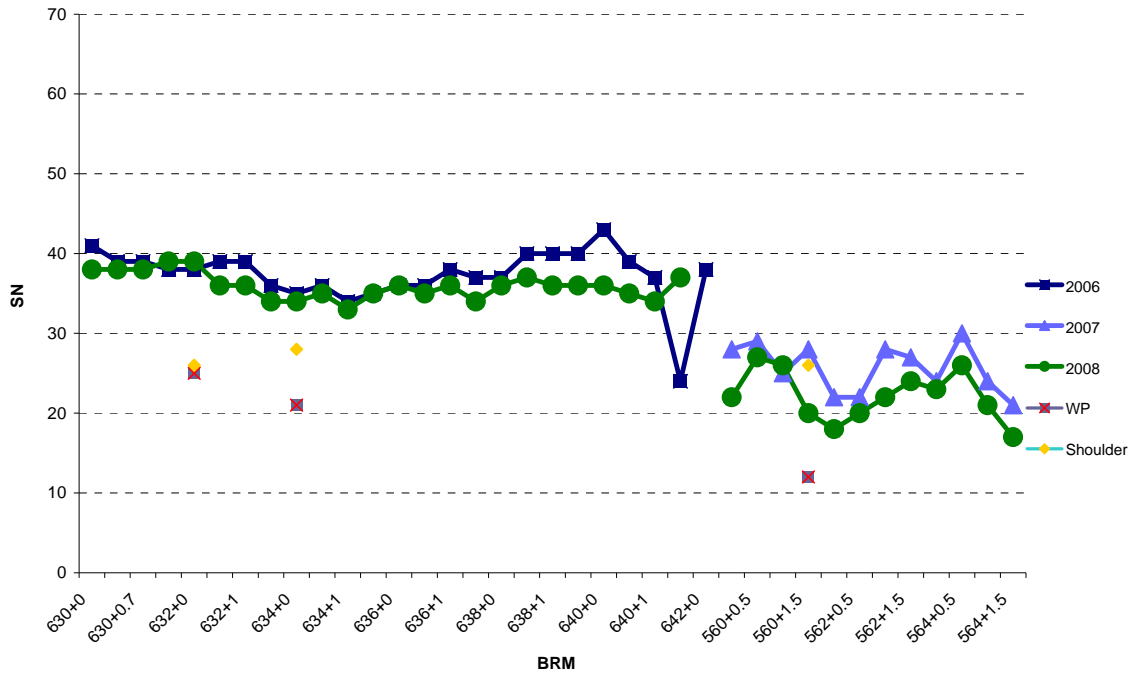
SL1604 L



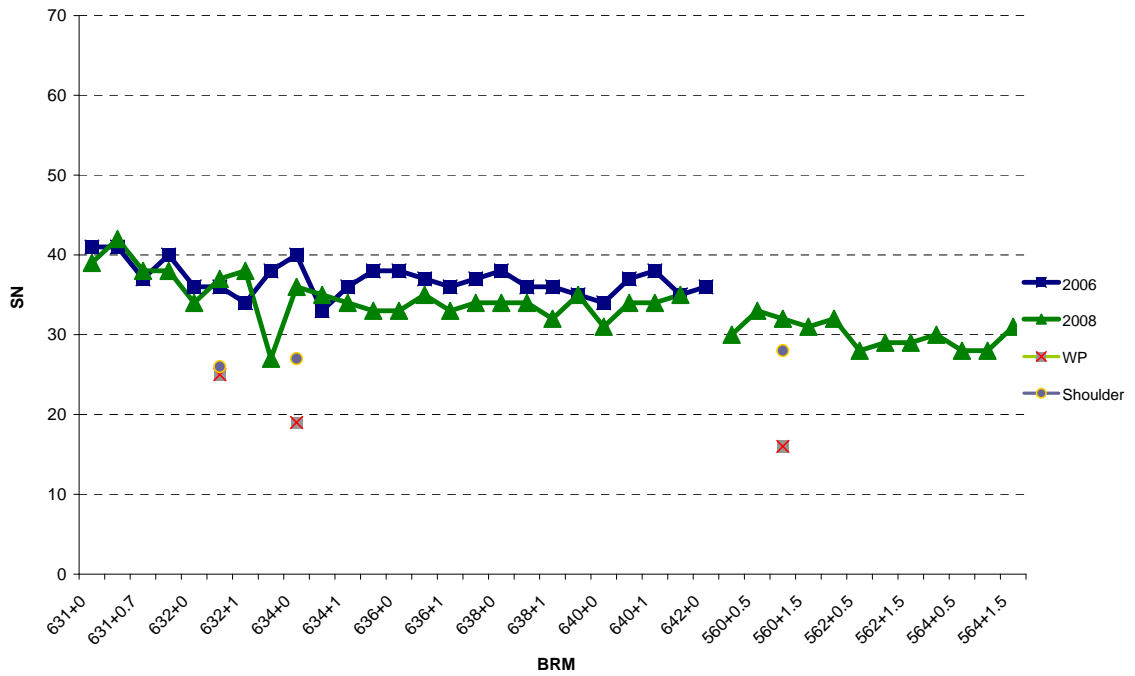
SL1604 R



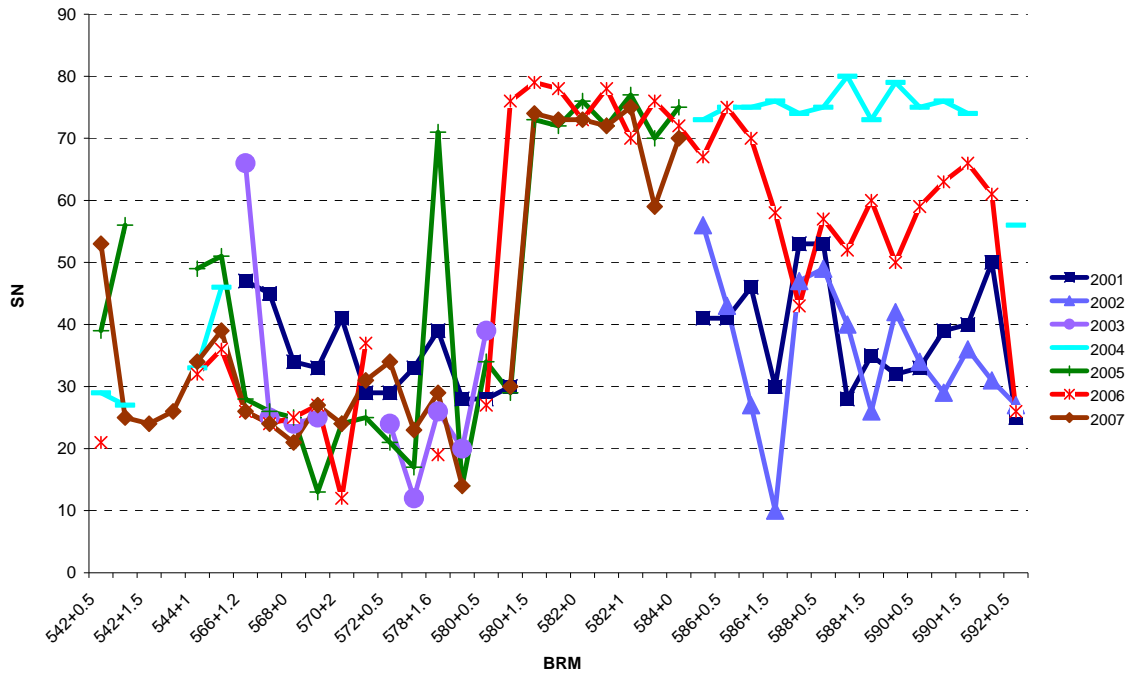
US0059 L



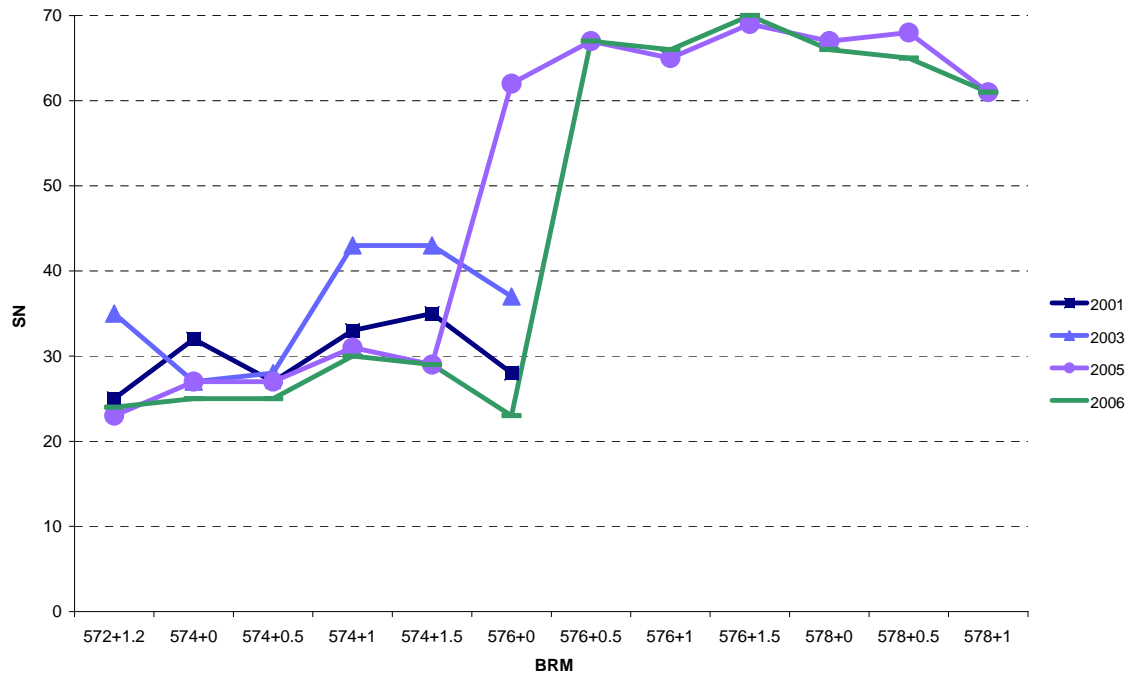
US0059 R



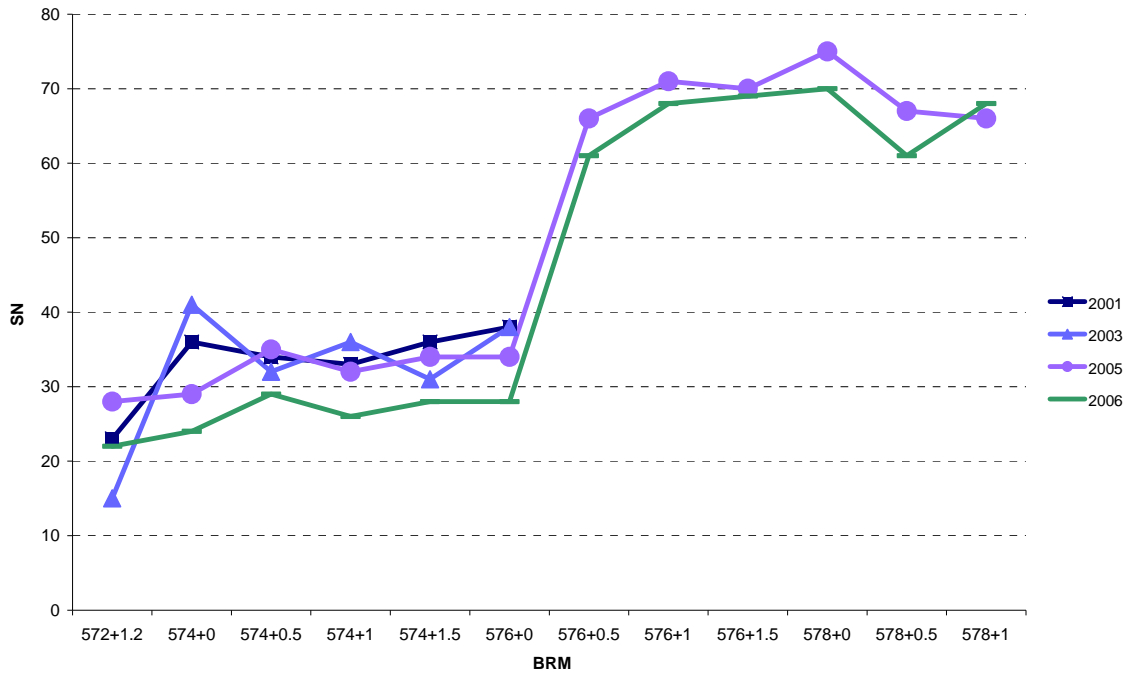
US0067 K



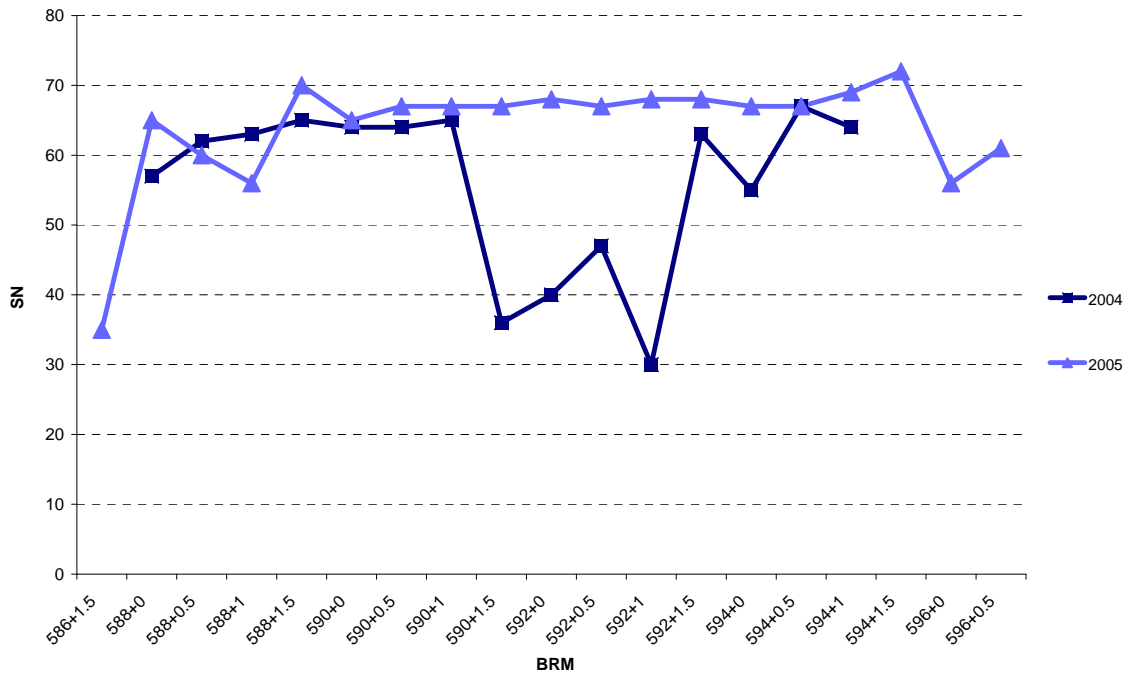
US0067 L



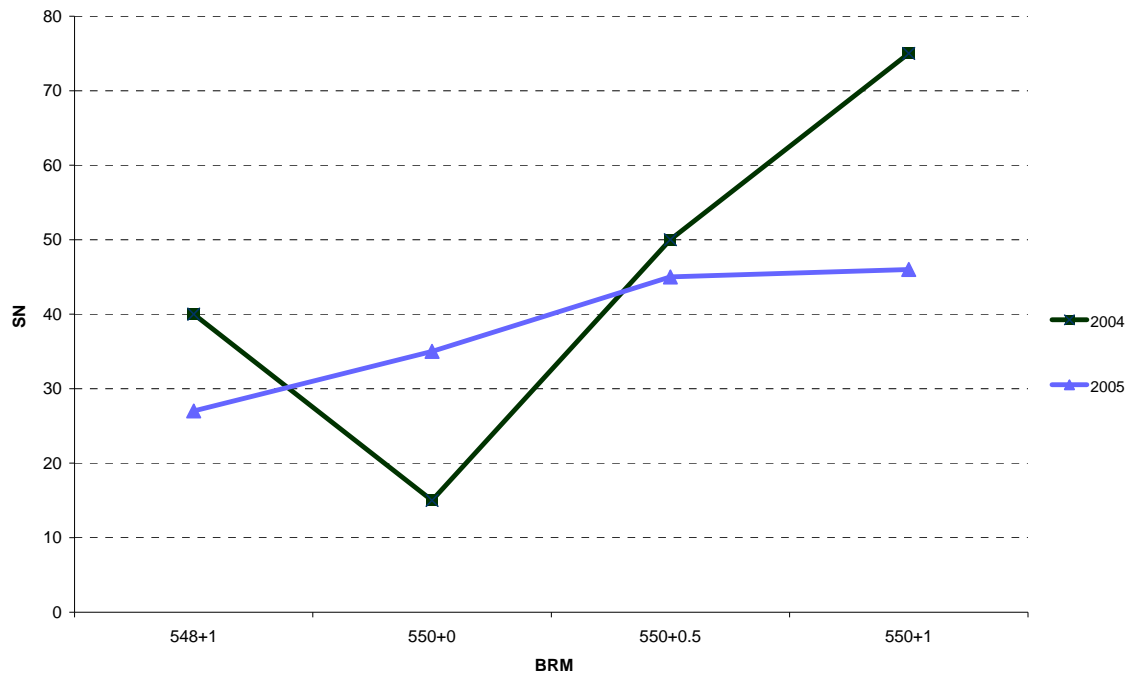
US0067 R



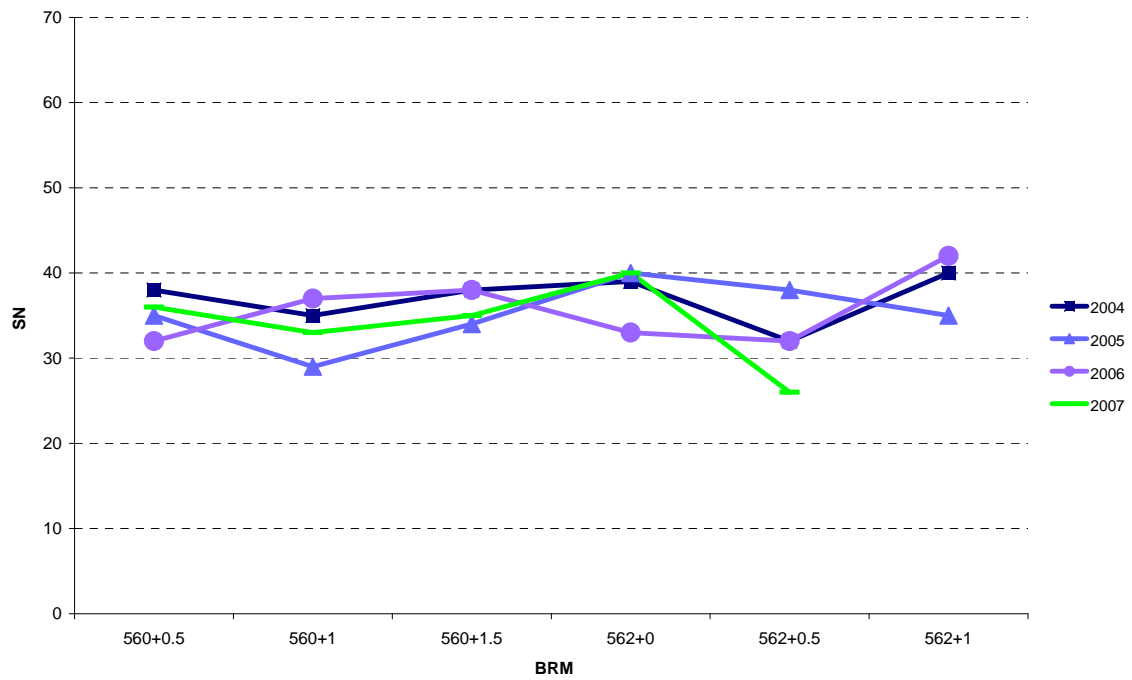
US0084 K



US0087 K

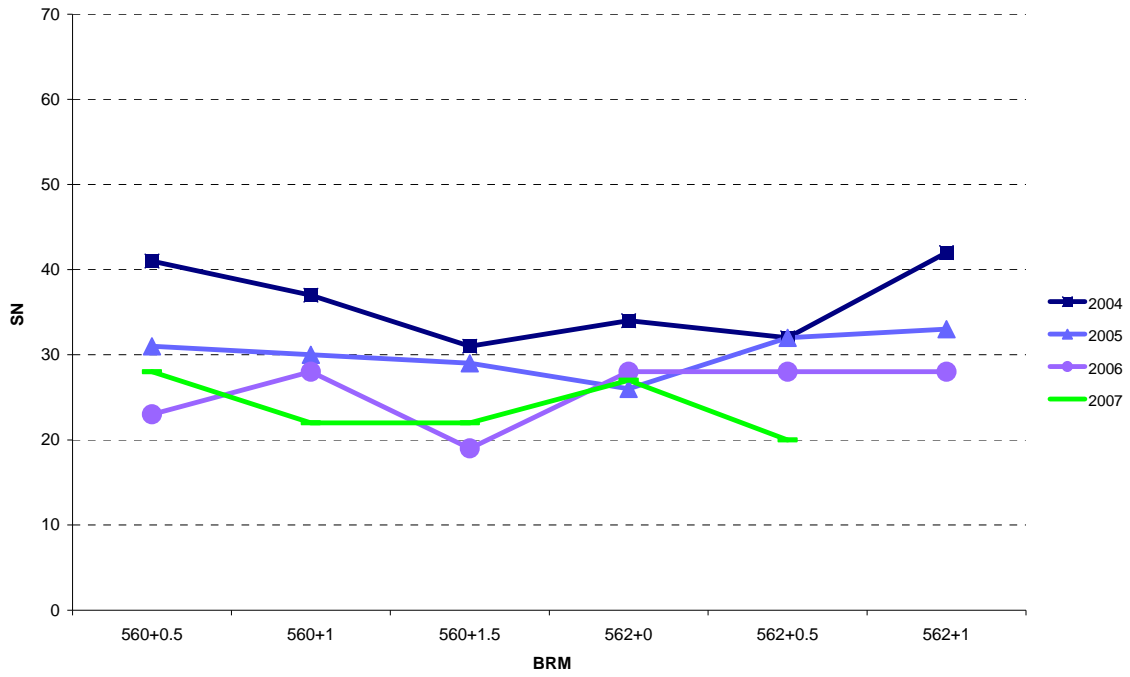


US0090 L

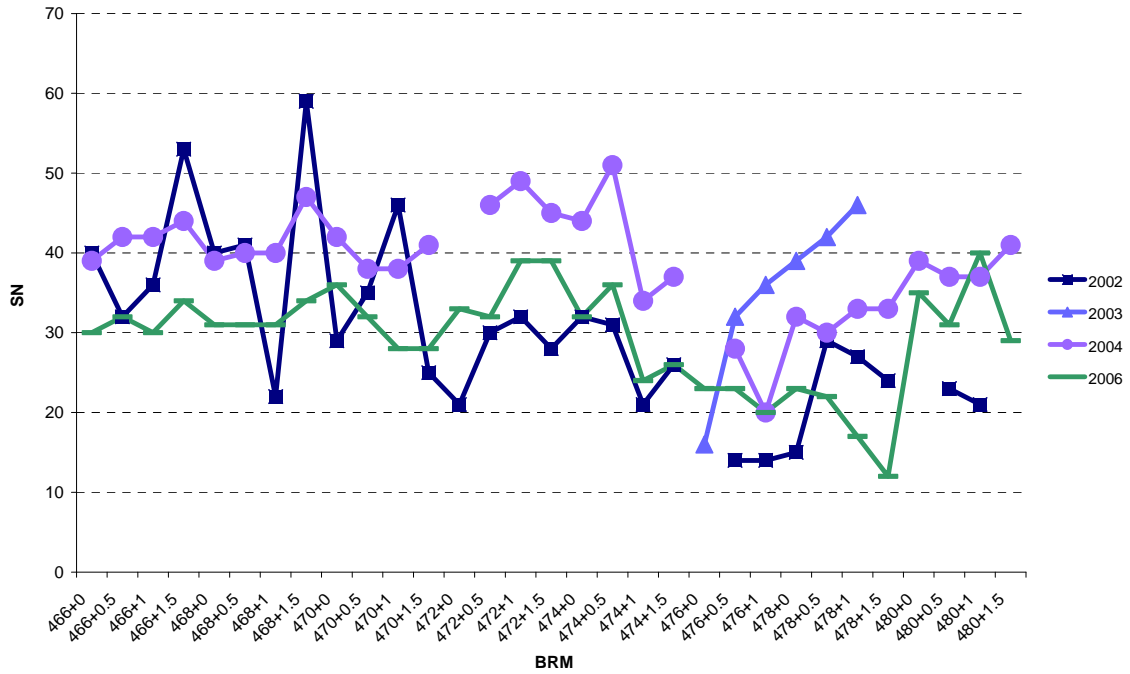




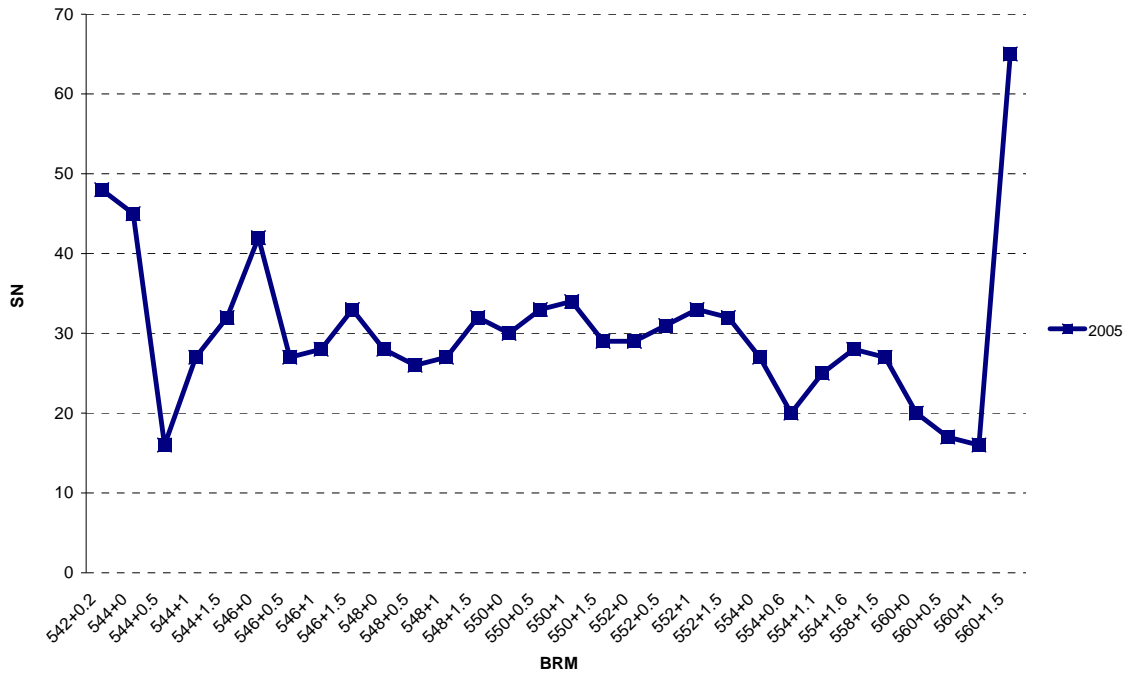
US0090 R



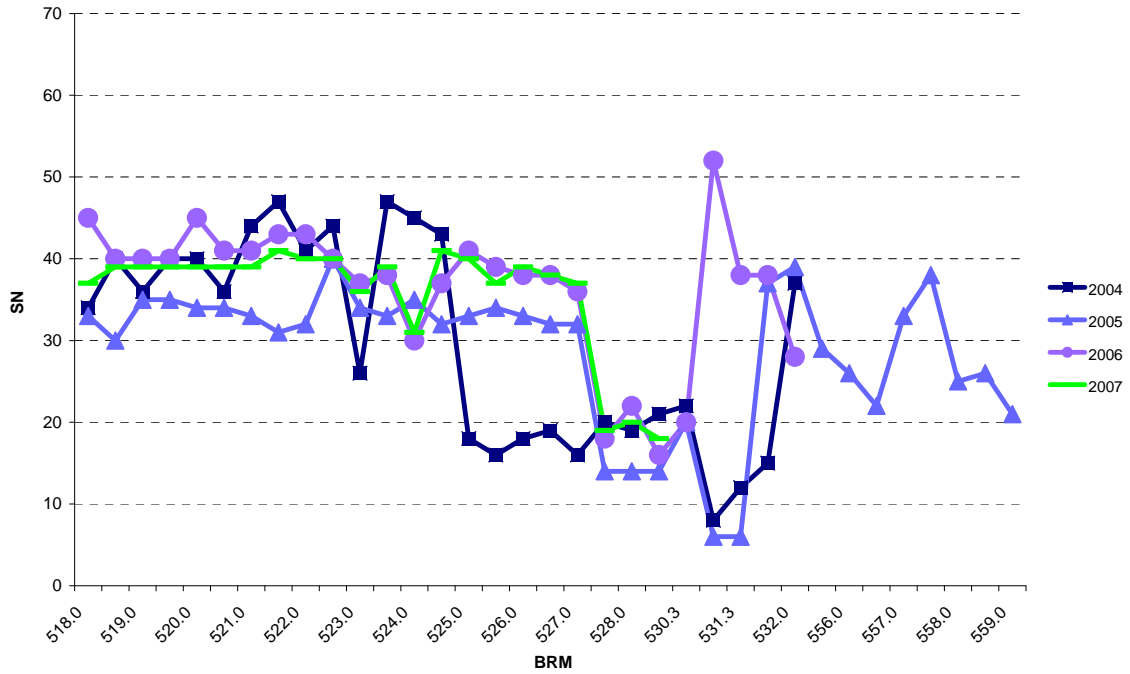
US0180 K



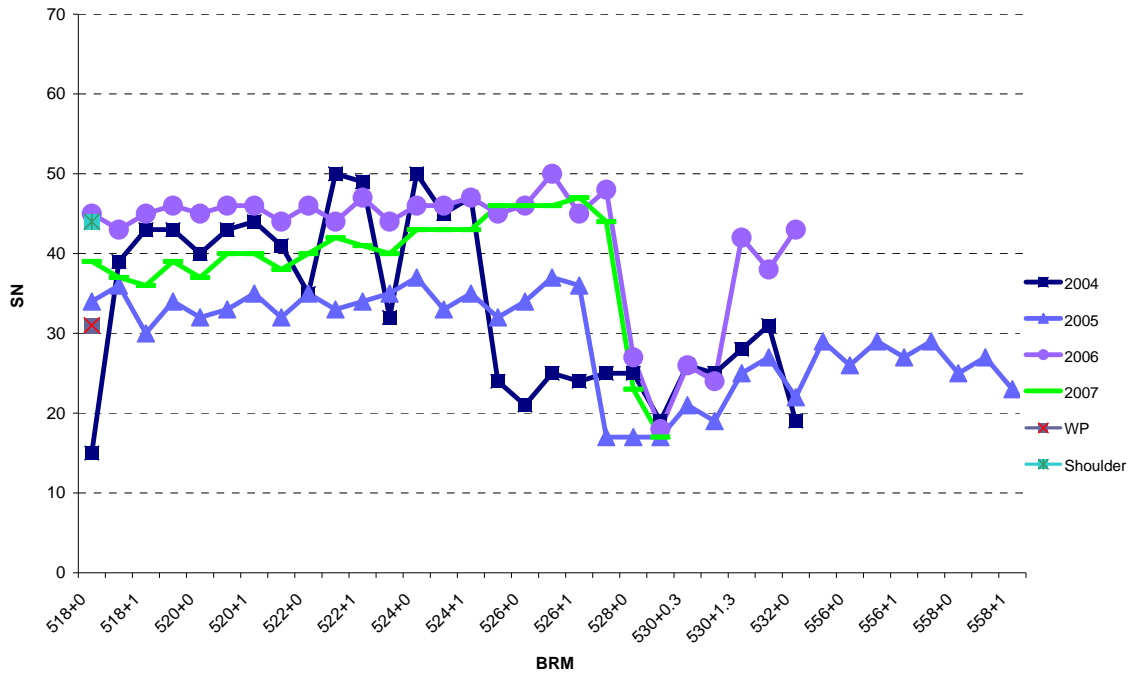
US0181 K



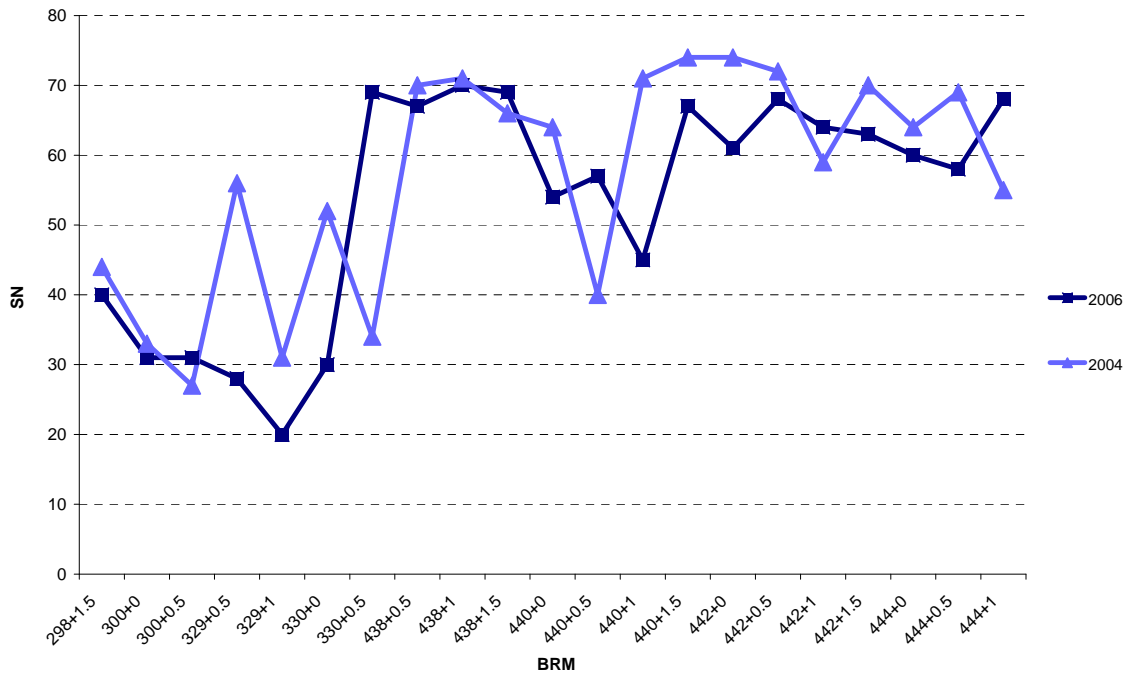
US0181 L



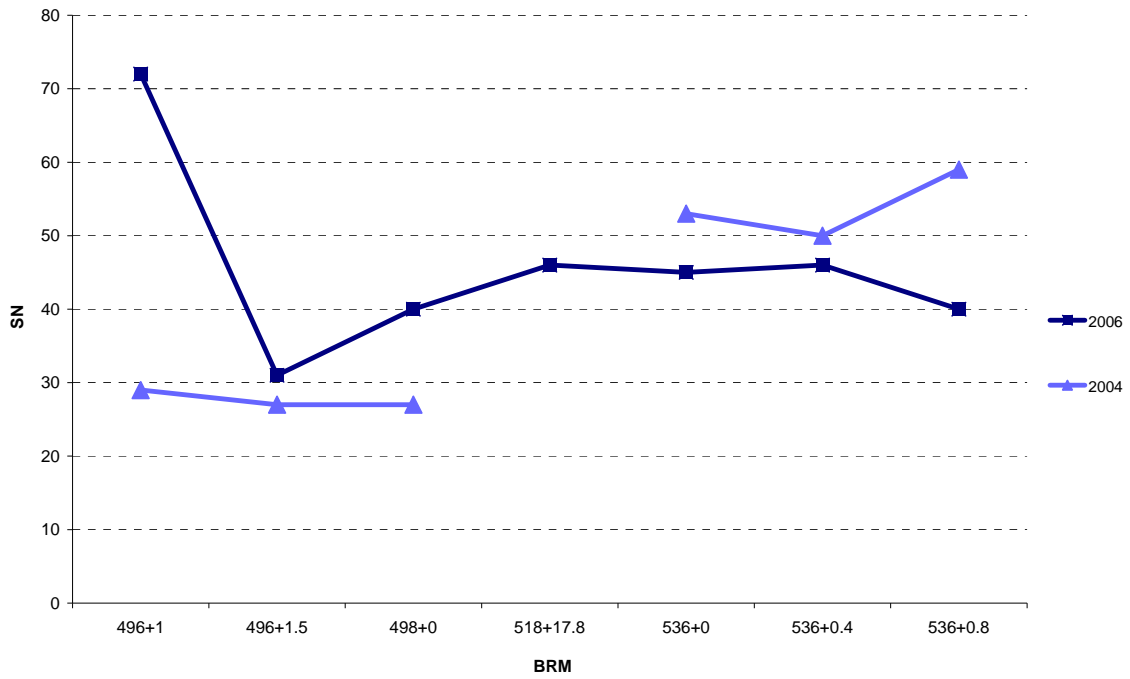
US0181 R



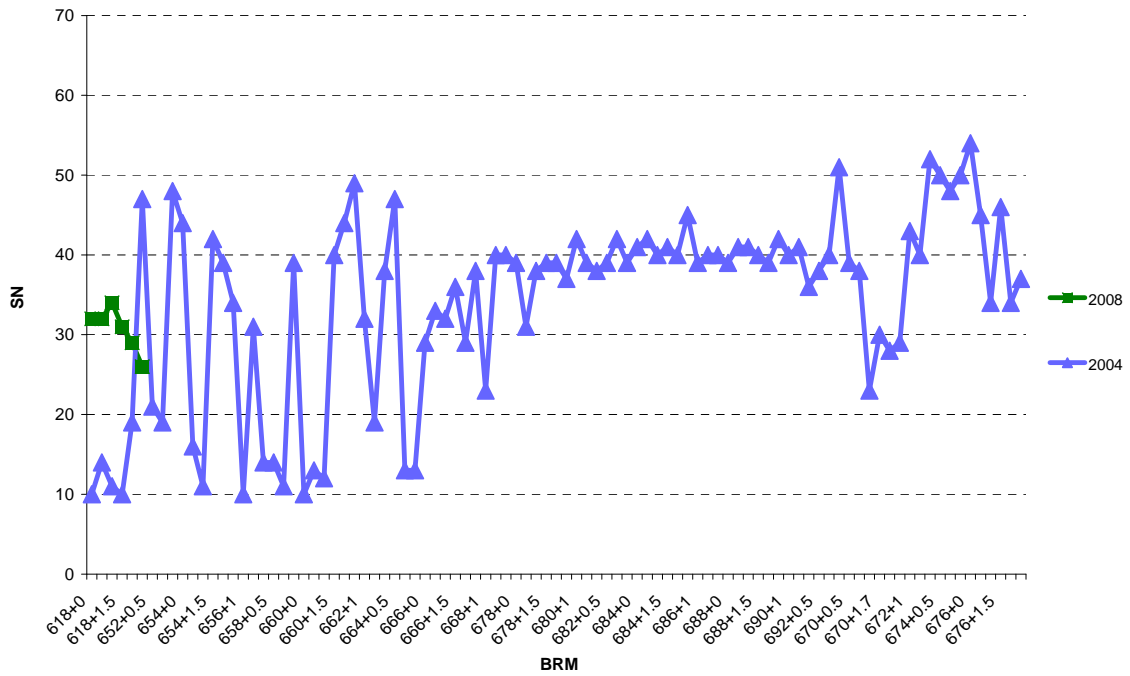
US0183 K



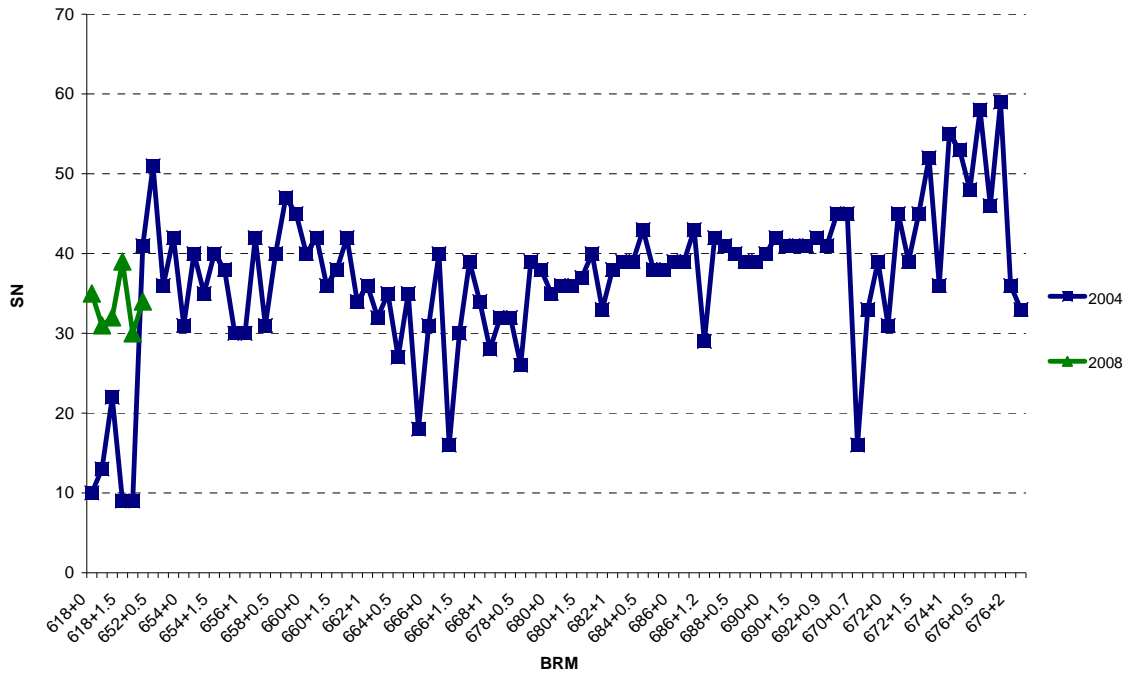
### US0190 K



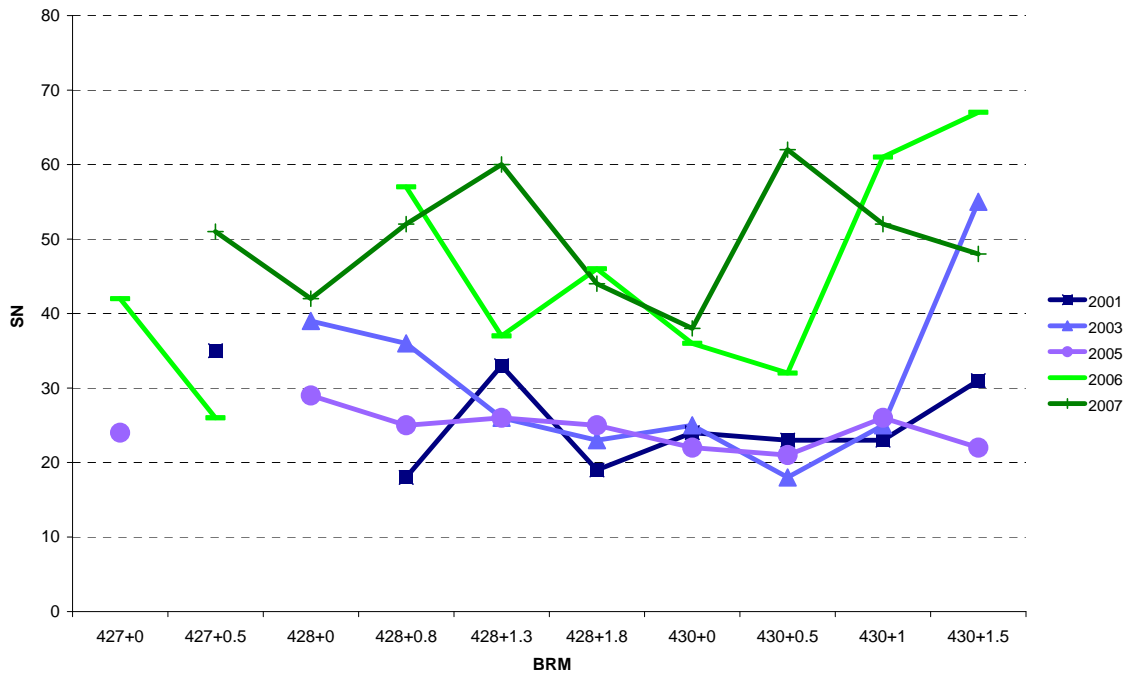
### US0281 L



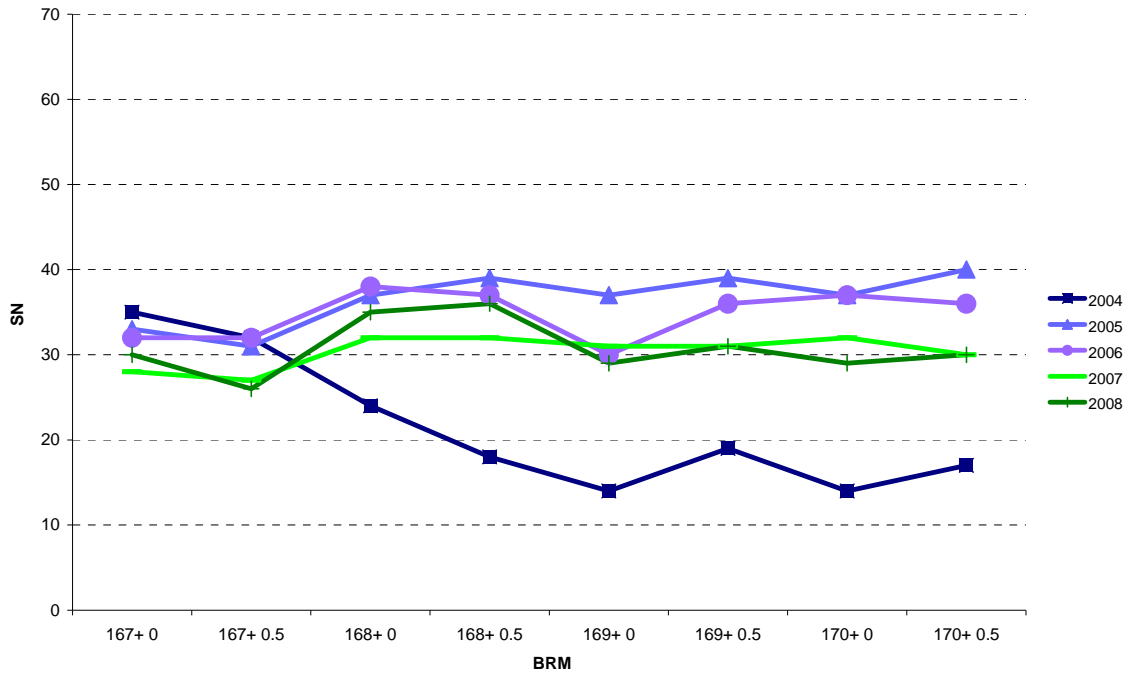
US0281 R



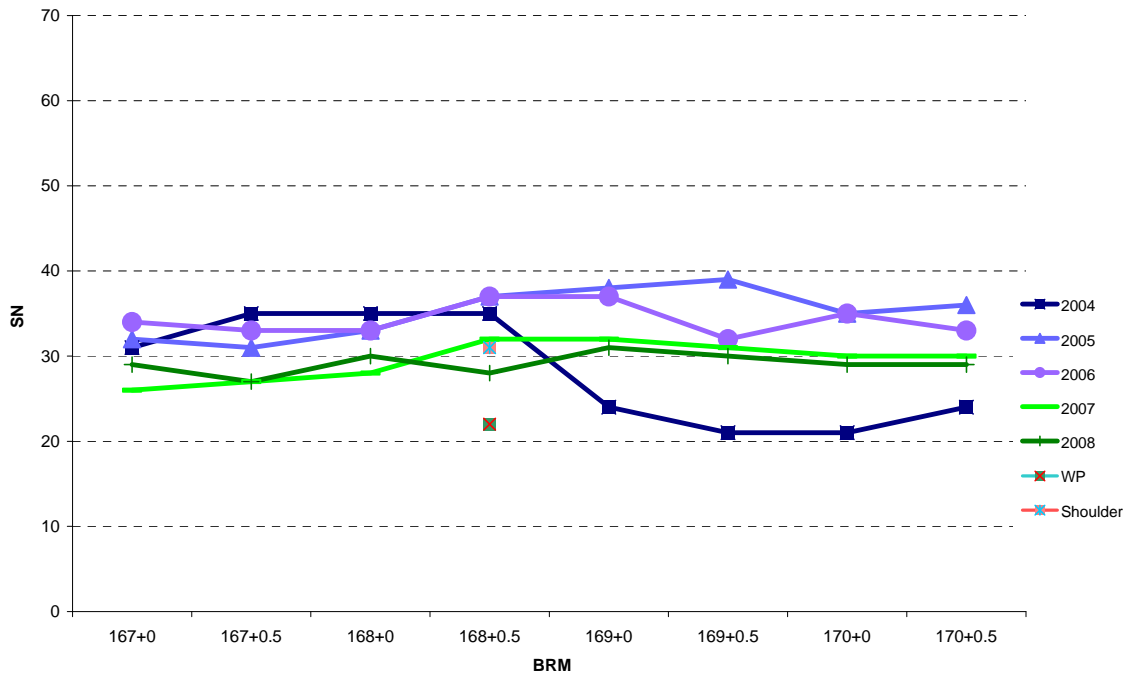
US0377 K



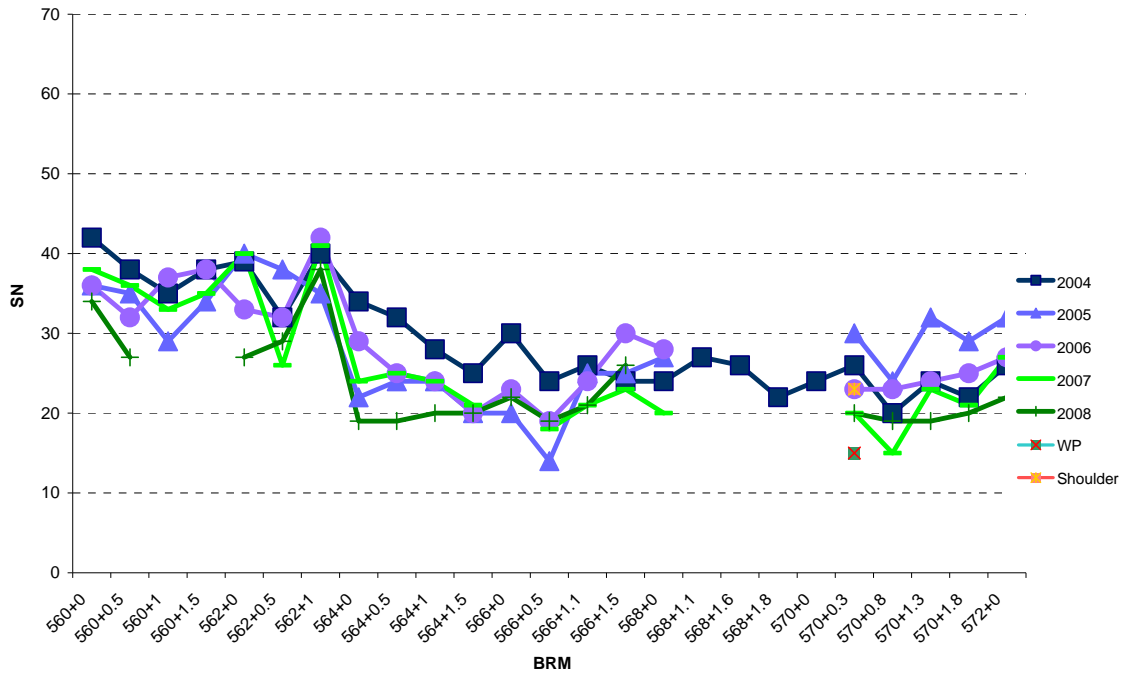
IH0035 L



IH0035 R



US0090 L1



US0090 R1

